

Dissertation

GALERKIN SIMULATION OF HYDRODYNAMIC DISPERSION

Submitted by

Anand Prakash

In partial fulfillment of the requirements

for the Degree of Doctor of Philosophy

Colorado State University

Fort Collins, Colorado 80521

April, 1974

CED73-74AP17

To my parents.

## ABSTRACT

The problem of predicting salt-content of waters pumped by fully or partially penetrating wells in an aquifer, contaminated by salt-water intrusion on sea-coasts, indiscriminate pumping of deep saline aquifers or waste-water recharge over prolonged periods of time, has demanded the attention of hydraulic engineers and geohydrologists for the last two decades or so. This investigation is an attempt to develop a new approach for modeling such situations.

A numerical simulator has been developed to represent the problem of salt-water movement induced by pumping from a saturated elastic aquifer. This simulator is based upon the Galerkin-finite-element formulations of the flow and convective-dispersion equations in cylindrical polar coordinates. Appropriate flow and convective-dispersion equations have been derived from first principles in tensorial form, taking the tensorial nature of dispersion and molecular diffusion into account. Finite-element-formulations have been developed for both the equations following the Galerkin-weighted-residual process both for the space and time domains. The flow equation formulation results in a system of symmetric matrices and that for the convective-dispersion equation in a system of non-symmetric matrices. Both these systems have been solved by Gauss-elimination. The flow and convective-dispersion equations are solved in sequence following the leap-frog-technique.

The numerical simulator consists of three computer programs; MESH, FLOW and DISPER. Program MESH is an automatic generation scheme for a suitable mesh layout with triangular elements, given the geometry of the flow region. This program incorporates an optimization scheme for

band-width reduction. The other two programs, FLOW and DISPER, operate in tandem. Program FLOW solves the flow equation and computes new pressures at the end of the time interval. These pressures and velocities computed from them, are used as input for program DISPER, which solves the convective-dispersion equation and calculates new concentrations. For operational simplicity program FLOW and DISPER are combined into a single program FFLOW.

The validity of the simulator has been tested with known exact and approximate analytical solutions for simplified cases. Program FLOW gives comparable results with the Theis equation and Program DISPER yields values reasonably matching the solutions for radial dispersion obtained by earlier investigators. Practical application of the simulator is demonstrated by applying it to hypothetical field problems.

The simulator could be used to analyze groundwater quality resulting from pumping or recharging of water from an aquifer having increased salt concentration with depth.

Anand Prakash  
Civil Engineering Department  
Colorado State University  
Fort Collins, Colorado 80521  
April, 1974



## ACKNOWLEDGEMENTS

The author wishes to thank his advisors, Professor R. A. Longenbaugh and Dr. J. W. N. Fead, for their encouragement, guidance and constructive comments. Thanks are also due to Dr. E. G. Thompson, Dr. D. W. Zachmann and Dr. D. B. McWhorter for the sound counsel, guidance and motivation provided by them during the period of development of this subject matter. The advice of Dr. D. K. Sunada, Dr. A. T. Corey, Dr. John Raich and Dr. A. Klute at different stages of this investigation is sincerely appreciated.

Sincere thanks are extended to Mrs. Diane English and Mr. John A. Brookman for their kind cooperation and effort in preparing the typed draft of this dissertation and to Mr. Shariatmadar Mahmood, Mr. V. P. Singh and Robert A. Chandler for day to day constructive discussions on the various aspects of this study.

The financial support provided by Colorado State University Experiment Station Project 110 and the computer money received from the Civil Engineering Department through unsponsored research funds, are thankfully acknowledged.

Last but not least, thanks are due to the author's family, Mrs. Chandrakanta, Manju and Ajay for the unlimited inspiration, exemplary cooperation and immense forbearance displayed by them through the periods of pessimism and optimism experienced in the process of accomplishment of this dissertation.

## TABLE OF CONTENTS

<u>CHAPTER</u>	<u>PAGE</u>
I. INTRODUCTION . . . . .	1
1.1 Description of the Problem . . . . .	1
1.2 Purposes and Objectives . . . . .	3
II. REVIEW OF LITERATURE . . . . .	5
2.1 Introduction . . . . .	5
2.2 Conceptual and Analytical Developments . . . . .	6
2.3 Development of Numerical Techniques . . . . .	17
2.4 Applications of the Finite-Element Technique . . . . .	23
2.5 Summary . . . . .	28
2.6 Further Definition of the Problem . . . . .	30
III. MATHEMATICAL MODEL AND NUMERICAL SIMULATOR . . . . .	32
3.1 Development of the Flow Equation . . . . .	32
3.2 Development of the Convective-Dispersion Equation . . . . .	36
3.3 The Finite-Element Method . . . . .	38
3.4 Mesh Layout . . . . .	41
3.5 Finite-Element Formulation of the Flow Equation . . . . .	44
3.6 Time-Domain Formulation of the Flow Equation . . . . .	48
3.7 Treatment of Boundary and Initial Conditions for the Flow Equation . . . . .	50
3.8 Finite-Element Formulation of the Convective-Disper- sion Equation . . . . .	52
3.9 Time-Domain Formulation of the Convective-Dispersion Equation . . . . .	58
3.10 Treatment of Boundary and Initial Conditions for the Convective-Dispersion Equation . . . . .	59

TABLE OF CONTENTS (cont'd)

<u>CHAPTER</u>	<u>PAGE</u>
III. MATHEMATICAL MODEL AND NUMERICAL SIMULATOR (cont'd) . . . .	60
3.11 The Implicit Leap-Frog Technique . . . . .	60
IV. DISCUSSION AND APPLICATION OF THE NUMERICAL SIMULATOR . . .	63
4.1 Description . . . . .	63
4.2 Leap-Frog Technique and Program FLOW . . . . .	68
4.3 Tests for the Performance of the Numerical Simulator .	69
4.4 Application of the Simulator to Field Problems . . . .	83
4.5 Galerkin and Rayleigh-Ritz Simulators . . . . .	88
4.6 Stability and Convergence . . . . .	90
V. CONCLUSIONS AND RECOMMENDATIONS . . . . .	94
5.1 Summary . . . . .	94
5.2 Evaluation and Practical Applications of the Simulator	95
5.3 Limitations and Suggestions for Future Work . . . . .	97
REFERENCES . . . . .	100
LIST OF SYMBOLS . . . . .	114
APPENDICES . . . . .	119
A. Derivation of the Flow Equation . . . . .	119
B. Derivation of the Convective-Dispersion Equation . . .	127
C. Finite-Element Formulation for the Flow Equation . . .	136
D. Finite-Element Formulation for the Convective-Disper- sion Equation . . . . .	146
E. Rayleigh-Ritz Formulation for the Convective-Dispersion Equation . . . . .	153
F. Flow Charts . . . . .	160
G. Program MESH . . . . .	165

TABLE OF CONTENTS (cont'd)

<u>CHAPTER</u>	<u>PAGE</u>
APPENDICES (cont'd) . . . . .	
H. Program Listings . . . . .	169

LIST OF TABLES

<u>TABLE</u>	<u>Page</u>
4.1 Comparison of Program FLOW and DISPER . . . . .	74
4.2 Data for Hypothetical Problems . . . . .	84
4.3 H-values at the Well Face After Prolonged Pumping . . . . .	85
4.4 H-values After 55.5 Seconds of Pumping . . . . .	91
4.5 H-values at Well Face With Different Values of DT . . . . .	92
4.6 H-values at Well Face With Different Values of DT . . . . .	93
G.1 JOIN (I,J,K) Array . . . . .	168

LIST OF FIGURES

<u>FIGURE</u>	<u>PAGE</u>
4.1 Typical Loop Subdivision . . . . .	64
4.2a Typical Element-Layout . . . . .	70
4.2b Alternative Element Layout with Diagonals Reversed . . . . .	70
4.3 Analytical and Numerical Solutions of Flow Equation . . . . .	73
4.4 Steady-State Solutions of Convective-Dispersion Equation . . . . .	76
4.5 Analytical and Numerical Solutions of Convective-Dispersion Equation, $a_I = 1.0$ foot . . . . .	79
4.6 Analytical and Numerical Solutions of Convective-Dispersion Equation, $a_I = 0.1$ foot . . . . .	81
4.7 Propagation of Concentration with Different Geometric Dis- persivities . . . . .	82
4.8 Propagation of Concentration for a Fully Penetrating Well . . . . .	86
4.9 Propagation of Concentration for a Partially Penetrating Well . . . . .	87
C.1 Schematic of Flow Boundaries . . . . .	137
G.1 Boundary Subdivisions for Program MESH . . . . .	166

CHAPTER I  
INTRODUCTION

1.1 Description of the Problem

The ever expanding population of the world has placed greater-than-ever emphasis on the exploitation and utilization of ground water resources for the enhancement of agricultural production on one hand and for the extensive development of industrial and domestic water-supply systems on the other. Directly related to the development of ground water resources, is the common geological occurrence of fresh water aquifers underlain by salt water zones of varying depths. Due to indiscriminate ground water development, mostly through partially penetrating wells in such aquifers, during the last fifty years or so, their capacities to yield fresh water have been greatly impaired. As most of the aquifers of this type underlie highly developed urban and agricultural regions, their waters are subject to quality deterioration induced by the infiltration of liquid industrial wastes, irrigation return flows and incompletely treated domestic waste water.

Such situations are frequently encountered in aquifers extending along sea coasts of almost all the continents of the world, where salt water intrusion commences as a result of excessive pumping in the adjoining connected aquifers, but, the same are, by no means, confined to coastal aquifers alone. One of the largest and perhaps the most important non-coastal aquifer in the world viz. the Indus Basin in Pakistan falls under this category. Detailed accounts of the existence, nature, shape, slope and depths of fresh water - saline water interfaces for various types of aquifers have been given by Todd (1959), Davis and DeWeist (1966), Walton (1970), Feth (1970) and others.



Such aquifers are characterized by a vast number of special problems concerning the hydraulic engineer; the most important being the prediction of the rate of pumping at which a well of given penetration depth will discharge water having a salt concentration within the permissible limit for agricultural, industrial or domestic use. Intimately connected with the above is the assessment of the rate and extent of recouplement of fresh water or mixed quality of water when the pumping is stopped for a certain period and continued intermittently thereafter.

A problem somewhat analogous to the above, involving an oil-saturated region overlying a brine-saturated zone in a confined aquifer has been analyzed by Muskat (1949) who suggested a graphical procedure to solve the water coning problem beneath a partially penetrating oil well. This method has been adapted by Bennett et al. (1968) to study the upconing of saline water beneath a fresh water well. The problem of salt water - fresh water interface beneath a well has been studied by Wang (1965). This study purported to relate the discharge of a partially penetrating well to the well spacing, well penetration, well radius, aquifer thickness and fluid densities and to determine the optimum rate of fresh water production without entrainment of saline water, as a function of well geometry and aquifer characteristics. Experimental and numerical models for the movement of salt water cone in response to pumping by a partially penetrating well in a situation similar to the above have been constructed and studied by Sahni (1972) and Chandler (1973).

All these investigations assume the existence and persistence of a sharp interface between the fresh and salt water zones, as if the two were immiscible. Besides, the problem is treated as a steady-state case



of three-dimensional flow of incompressible fresh water over a static brine phase in radial coordinates, through non-deformable, isotropic and homogeneous porous media.

### 1.2 Purposes and Objectives.

In an actual field situation, the problem indicated in section 1.1 involves analysis of the non-uniform, non-steady movement of two miscible fluids of varying densities, viscosities and concentrations. The drawdown in the partially penetrating well causes radially symmetrical, three-dimensional, non-steady, non-uniform flow towards the well, which is governed by the mass-balance equation for water, hereafter called the 'flow equation' and the concentration gradient coupled with convection induces a transport of the solute towards the well governed by the convective-dispersion equation in radial coordinates.

The broad objective of this investigation is to find a solution to the above situation which will involve:

(i) Development of the appropriate flow equation for three-dimensional, non-steady, non-uniform flow of a compressible non-homogeneous fluid through elastic formations in a general system of coordinates.

(ii) Development of the appropriate convective-dispersion equation in tensorial form taking into account the tensorial nature of the dispersion coefficient. This will mean a combination of the mass-balance equation for the solute, Fick's law and an equation of state connecting the mass-density of the fluid at any point with the pressure and concentration at that point.

(iii) Development of a digital computer model simulator (taking advantage of radial symmetry to reduce the problem to a two

dimensional one) which seeks to solve the flow and convective-dispersion equations over the region of influence of the partially penetrating well.

(iv) Testing the validity of the simulator by comparison with available analytical, experimental or approximate solutions of simple cases.

## CHAPTER II

### REVIEW OF LITERATURE

#### 2.1 Introduction.

As outlined in the previous chapter, this investigation involves the derivation and solution of the flow and convective-dispersion equations for a porous medium by the leap-frog technique. The flow equation, being an enunciation of the Eulerian mass-conservation principle coupled with Darcy's law for the unsteady flow of a non-homogeneous, compressible fluid through a non-reactive, isotropic and elastic porous medium, is one of the most well discussed topics in the literature connected with ground water movement; Jacob (1950), Hantush (1964), Davis and DeWeist (1966), Kochina (1949), Walton (1970), Bear (1972), Todd (1959), Harr (1962), Muskat (1946). Different forms of the flow equation suitable for different conditions have been arrived at by different investigators. As this principle of continuity has been in use in varied forms in almost all branches of science from the very early stages of development it is difficult to assign the credit for its development to any one individual. The flow equation appropriate to this study has been derived from first principles in Appendix A.

Unlike the flow equation, the convective-dispersion equation based on the concept of hydrodynamic dispersion through porous media is of a comparatively recent origin. Attempts made by investigators to explain the phenomenon of hydrodynamic dispersion have been multi-directional, varying from a purely theoretical analysis (mathematical or statistical) to experimental verifications and computer simulations. A chronological review of some of the important developments of this concept leading to the derivation and solutions of the convective-dispersion equation in

different forms is presented in the following paragraphs.

## 2.2 Conceptual and Analytical Developments.

According to Bear (1968), hydrodynamic dispersion is the macroscopic outcome of the actual movements of the individual tracer particles through the pores and the various physical and chemical phenomena that take place within the pores. Normally, two basic transport phenomena are involved in the process, a convective mass transport where the liquid moves along definite paths that may be averaged to yield streamlines and a process of molecular diffusion resulting from variations in tracer concentration within the liquid phase. Thus hydrodynamic dispersion is due to the combined action of both a purely mechanical phenomenon on a macroscopic scale (dispersion) and a physio-chemical phenomenon on a microscopic scale (molecular diffusion). The mathematical model of the phenomenon of hydrodynamic dispersion is a partial differential equation which is an expression for the mass-conservation of a tracer.

Fried and Combarous (1971) define a tracer as a chemical compound dissolved in a fluid phase. The displacement of two miscible fluids may be considered as a tracer case when the fluids have the same densities and viscosities and there is no volume contraction by mixing. The terms coefficient of hydrodynamic dispersion, coefficient of dispersion, and coefficient of diffusion which are often used as measures of hydrodynamic dispersion may be defined as follows:

Let  $F_{t_i}$  = Total mass flux of the tracer carried by the fluid in direction  $i$  [ $ML^{-2}T^{-1}$ ].

$F_{c_i}$  = Convective component of the mass flux of the tracer in direction  $i$  [ $ML^{-2}T^{-1}$ ].

$J_i$  = Diffusive component of the mass flux of the tracer in direction  $i$  [ $ML^{-2}T^{-1}$ ].

$$F_{t_i} = F_{c_i} + J_i \quad . \quad (2.1)$$

On a macroscopic scale,

$$F_{c_i} = c\bar{v}_i + cv_{oi} \quad (2.2)$$

where,

$\bar{v}_i$  = Average seepage velocity in direction  $i$  [ $LT^{-1}$ ].

$v_{oi}$  = Fluctuations of the seepage velocity about the average in direction  $i$  [ $LT^{-1}$ ].

$c$  = Concentration of the tracer in the fluid [ $ML^{-3}$ ].

$c\bar{v}_i$  = Flux carried by the average fluid motion.

$cv_{oi}$  = Dispersive flux resulting from the velocity fluctuations about the mean.

Also by Fick's law of diffusion,

$$J_i = - D_d \cdot T_{ij} \cdot \nabla c \quad (2.3)$$

where;  $\nabla c$  = Gradient of concentration.

$D_d$  = Coefficient of molecular diffusion.

$\bar{T}_{ij}$  = Correction factor applied to the coefficient of molecular diffusion due to the tortuosity of the medium. It is a second rank tensor and is reciprocal of the tortuosity tensor as usually defined.

Therefore,

$$F_{t_i} = c\bar{v}_i + cv_{oi} - D_d \cdot T_{ij} \cdot \nabla c \quad . \quad (2.4)$$

In analogy to Fick's law, it can be shown, Bear and Bachmat (1965, 1967),

that,

$$c v_{oi} = - D_{ij} \nabla c \quad , \quad (2.5)$$

where,

$D_{ij}$  = Dispersion coefficient and is a second rank tensor.

Therefore,

$$\begin{aligned} F_{ti} &= c v_i - (D_{ij} + D_d T_{ij}) \cdot \nabla c \\ &= c v_i - D_{ij}^* \nabla c \quad , \end{aligned} \quad (2.6)$$

where,

$$\begin{aligned} D_{ij}^* &= D_{ij} + D_d T_{ij} \quad (2.7) \\ &= \text{Coefficient of hydrodynamic dispersion.} \end{aligned}$$

One of the earliest observations of the phenomenon of hydrodynamic dispersion was made by Slichter (1905), who discovered that even in a uniform flow field the tracer advances in the direction of the flow in a pear-like shape that becomes longer and wider as it advances. He explained this by noting that the soil complex is composed of a large number of capillary tubes in each of which there is a velocity variation across the cross-section, which was responsible for the phenomenon he observed. Subsequently, around 1930, a zone of diffusion was observed at the salt water - fresh water interface in coastal aquifers which could not be explained by the prevalent immiscible fluid theory. This prompted the recognition of the dispersion process as a possible cause for the above phenomenon. This aspect was investigated both experimentally and theoretically by Kitagawa (1934) and later by Wentworth (1948) who postulated a 'rinsing theory' based on the hypothesis that the pores of the medium act as mixing cells filled alternately with salt and fresh water by the ocean waves. Danel (1952) used the capillary tube model and concluded

that dispersion was due to and depended upon the parabolic velocity distribution inside the capillaries. Following a similar approach, Taylor (1953, 1954) also came to the same conclusion and observed that in a capillary tube model, fluid particles initially on a plane perpendicular to the tube's axis, lie on a paraboloidal surface at any subsequent time and that the coefficient of dispersion for one-dimensional flow was proportional to the square of the average velocity.

With increasing research and interest in the phenomenon of dispersion, a notion developed among some investigators, that because of the discrepancy between the idealized medium of the mathematical models and the real medium, the mathematical models could not adequately describe the dispersion phenomenon. Accordingly, they focussed their attention towards the development of statistical models. Scheidegger (1954) employed the statistical theory of random walk in three dimensions and obtained a normal probability distribution for the displacement of a fluid particle in an isotropic porous medium. He neglected molecular diffusion and assumed an isotropic spread of the tracer with the result that his coefficient of dispersion turned out to be scalar with no distinction between the longitudinal and transversal directions. Further work on the scalar form of the coefficient of dispersion was done by Van Deamter, Brader and Lauweir (1955) who obtained a generalized solution of the dispersion equation for the capillary tube model.

For uni-directional flow and with a scalar coefficient of dispersion, Ebach and White (1958) presented an analytical solution to the simplified equation,

$$\frac{\partial c}{\partial t} + u \frac{\partial c}{\partial x} = D_L \frac{\partial^2 c}{\partial x^2} \quad (2.8)$$



where the input concentration is a periodic function of time,  $u$  is the component of seepage velocity in the  $x$ -direction and  $D_L$  is the coefficient of longitudinal dispersion.

Scheidegger's finding of a scalar dispersion coefficient was, however, not supported by laboratory experiments which indicated a definite difference between the magnitudes of longitudinal and lateral dispersion. De Josselin de Jong (1958, 1958a) was perhaps the first to show by a statistical approach that the coefficient of the longitudinal dispersion  $D_L$  is about 5 to 7 times greater than the coefficient of lateral dispersion  $D_T$  and that both  $D_L$  and  $D_T$  are directly proportional to  $\bar{v}$ .

Rifai, Kaufman and Todd (1956) made a very comprehensive laboratory study to verify their theoretical work which was based on the capillary-tube and the disordered medium models and concluded that the dispersion coefficient in the direction of flow was nearly proportional to the first power of the average velocity. They derived the following equation for a three-dimensional case, assuming dispersion to be basically due to molecular diffusion and velocity convection, and neglecting the difference between the longitudinal and lateral dispersion coefficients:

$$\frac{\partial c}{\partial t} = D \nabla^2 c - \text{div} (vc) \quad . \quad (2.9)$$

where,

$D$  = coefficient of dispersion, and

$v$  = component of seepage velocity.

Aris (1956) extended Taylor's analysis to straight tubes of any cross-section and showed that the effective coefficient of dispersion



could be obtained from the variance of the average concentration distribution caused by the phenomenon of dispersion. This was experimentally verified by Blackwell (1957). Following Wentworth's approach, Aris and Amundson (1957) also analyzed dispersion as a process of mixing in cells.

Based on further analysis of the dispersion coefficient, Scheidegger (1957, 1958) suggested two possible relationships:

$$(i) \quad D \sim a' \bar{v}^2 \quad , \quad (2.10)$$

where  $a'$  is the dynamic dispersivity of the porous medium which is derived by a dynamic procedure applicable when there is enough time in each flow channel for appreciable mixing to take place by molecular transverse diffusion and  $\bar{v}$  is the average seepage velocity.

$$(ii) \quad D \sim a'' \bar{v} \quad , \quad (2.11)$$

where  $a''$  is the geometric dispersivity of the porous medium and is derived by a geometric procedure applicable where there is no appreciable molecular transverse diffusion from one stream line to another.

Further work on the dependence of dispersion coefficients on the mean velocity of flow was done by Ebach and White (1958) who suggested the following expression for the longitudinal dispersion coefficient

$$D_L \quad , \quad \frac{D_L}{v} = \alpha \left( \frac{vd}{v} \right)^\beta \quad (2.12)$$

where,

$v$  = seepage velocity,

$d$  = particle size of the medium,

$v$  = kinematic viscosity,

$\alpha$  = experimentally determined coefficient dependent on the properties of the porous medium

$\beta$  = experimentally determined coefficient dependent on the flow regime.

Following a statistical approach similar to De Josselin de Jong, Saffman (1959) obtained the following expressions for  $D_L$  and  $D_T$  including the effect of molecular diffusion:

$$D_L = 1/2 \bar{V} \ell s^2 \quad , \quad (2.13)$$

$$D_T = 2/16 \bar{V} \ell \quad , \quad (2.14)$$

where,

$$s^2 = \text{Ln} \frac{3 \bar{V} \tau_o}{\ell} - \frac{1}{12}$$

$$\tau_o = \ell^2 / 2 D_d$$

$\ell$  = a characteristic length which is of the order of the grain size and depends on grain size distribution,

$D_d$  = coefficient of molecular diffusion,

$\bar{V}$  = average Darcy velocity.

Another attempt in the same direction was by Blackwell, Rayne and Terry (1959) who obtained the following relationship between  $D_L$  and  $D_d$  ;

$$D_L/D_d = 8.8 \cdot P_e^{1.17} \quad \text{valid when} \quad P_e > 0.5 \quad , \quad (2.15)$$

where,

$$P_e = \text{Peclet number} = \frac{\ell \bar{V}}{D_d}$$

In a bid to obtain a more accurate inter-relation between the coefficient of molecular diffusion, and the longitudinal and lateral dispersion coefficients, Saffman (1960) extended his earlier work to cases where the Peclet number was of order unity, i.e. where molecular diffusion and macroscopic mixing were of the same order of magnitude.

Experimental and theoretical investigations on the dispersion phenomenon conducted prior to 1960, confirmed that the mere existence

of the porous medium and flow gives rise to a multi-component dispersion phenomenon. This tensorial character of the dispersion coefficient was experimentally verified by Bear (1961a). By theoretical analysis, he (1961b) showed that the dispersivity of a porous medium is a fourth rank tensor, which, in three dimensions, has 81 components (16 in two dimensions), out of which only 21 components (8 in two dimensions) are non-zero if the medium is isotropic. For an isotropic case, all these components depend on two essential constants which are the longitudinal and lateral constants of dispersion  $a_I$  and  $a_{II}$  respectively. Thus he deduced the following form for the dispersivity tensor  $a_{ijkl}$  for an isotropic porous medium:

$$a_{ijkl} = \begin{bmatrix} a_I & a_{II} & 0 & 0 \\ a_{II} & a_I & 0 & 0 \\ 0 & 0 & (a_I - a_{II})/2 & (a_I - a_{II})/2 \\ 0 & 0 & (a_I - a_{II})/2 & (a_I - a_{II})/2 \end{bmatrix} \quad (2.16)$$

Extending this analysis to uniform flow in an isotropic medium, De Josselin de Jong and Bossen (1961) obtained the following expression for the coefficient of dispersion,

$$D_{kl} = a_{ijkl} \frac{v_i v_j}{v} \quad , \quad (2.17)$$

where,  $v_i$  and  $v_j$  are the components of the average velocity  $v$  in the  $i$  and  $j$  directions respectively.

Based on Bear's hypothesis that only that part of the velocity component was of significance, which was either parallel or normal to the mean flow direction, Scheidegger (1961) deduced a general form of

the dispersivity tensor in three dimensions having 36 independent non-zero components, which, for an isotropic case and for complete symmetry of the whole group of rotations, could be expressed by the following matrix:

$$a_{\alpha\beta} = \begin{bmatrix} a_{1111} & a_{1122} & a_{1122} & 0 & 0 & 0 \\ a_{1122} & a_{1111} & a_{1122} & 0 & 0 & 0 \\ a_{1122} & a_{1122} & a_{1111} & 0 & 0 & 0 \\ 0 & 0 & 0 & a_{1212} & 0 & 0 \\ 0 & 0 & 0 & 0 & a_{1212} & 0 \\ 0 & 0 & 0 & 0 & 0 & a_{1212} \end{bmatrix} \quad (2.18)$$

where,

$$a_{1212} = \frac{1}{2} (a_{1111} - a_{1122}) \quad (2.19)$$

$$a_{1111} = a_I \quad \text{and} \quad a_{1122} = a_{II} ,$$

$\alpha$  represents the indices  $ij$  and  $\beta$  represents  $kl$ .

Thus he concluded that the dispersivity tensor given by Bear was a special case of this general dispersivity tensor. Writing in general form, Scheidegger's equation for geometric dispersivity of an isotropic medium becomes,

$$a_{ijkl} = a_{II} \delta_{ij} \delta_{kl} + \frac{a_I - a_{II}}{2} (\delta_{ik} \delta_{jl} + \delta_{il} \delta_{jk}) \quad (2.20)$$

where  $\delta$  stands for Kronecker delta.

Thus,

$$D_{ij} = a_{II} v \delta_{ij} + (a_I - a_{II}) v_i v_j / v \quad (2.21)$$

Bachmat and Bear (1964) generalized these expressions for the curvilinear coordinate system as;

$$a_{ijkl} = \lambda g_{ij} g_{kl} + 2\mu g_{ik} g_{jl} \quad (2.22)$$

and,

$$D_{ij} = \lambda g_{ij} v + 2\mu v_i v_j / v \quad (2.23)$$

Also, they derived a general partial differential equation of hydrodynamic dispersion in a homogeneous, isotropic, porous medium in curvilinear coordinates as,

$$\frac{\partial c}{\partial t} = \frac{\partial}{\partial y^i} \left[ |g|^{\frac{1}{2}} g^{ik} \left( \lambda v \frac{\partial c}{\partial y^k} + 2 \mu \frac{v_k v^l}{v} \frac{\partial c}{\partial y^l} \right) \right] - g^{ik} v_k \frac{\partial c}{\partial y^i} \quad (2.24)$$

which for an orthogonal system reduced to,

$$\frac{\partial c}{\partial t} = \frac{1}{h_1 h_2 h_3} \frac{\partial}{\partial y^i} \left[ \frac{h_1 h_2 h_3}{h_i^2} \left( \lambda v \frac{\partial c}{\partial y^i} + 2 \mu \frac{v_i v_k}{v h_k^2} \frac{\partial c}{\partial x^k} \right) \right] - \frac{v_i}{h_i^2} \frac{\partial c}{\partial y^i} \quad (2.25)$$

where,

$g_{ij}$  = the fundamental tensor of the Riemannian space (a symmetric tensor of second rank) and the subscripts denote covariant components, such that,

$g^{jk}$  = conjugate or reciprocal of  $g_{ij}$ , a second rank symmetric contra-variant tensor,

$h_i$  = scale factors for the coordinate system, and,

$\lambda$  and  $\mu$  are invariants.

They derived general dispersion equations for plane two-dimensional flow in terms of  $\Phi$ - $\Psi$  coordinates from which equations for different particular cases could be easily obtained. Poreh (1965) obtained a similar expression for isotropic media as:

$$D_{ij} = A_1 \delta_{ij} + A_2 v_i v_j \quad (2.26)$$

where  $A_1$  and  $A_2$  are arbitrary functions of  $v^2$  and the properties of the medium, fluid and tracer. From physical considerations he obtained different equations in dimensionless forms for low and high Reynolds numbers. Later, List and Brooks (1967) conducted a series of lateral

dispersion experiments and showed that for a given medium, the dynamic Peclet number  $vd/D_T$  is a function of any two of the following:

- (i) Molecular Peclet number  $vd/D_d$ ,
- (ii) Schmidt number  $v/D_d$ ,
- (iii) Reynold's number  $vd/\nu$ .

They observed that for low Reynold's numbers, the lateral dispersion coefficient is independent of viscosity, i.e.,

$$D_T/vd = f(vd/D_d) \quad (2.27)$$

Further analytical work on the tensorial concept of dispersion was done by Whitaker (1967) who volume averaged the fundamental transport equation and obtained the following form for the coefficient of hydrodynamic dispersion  $D_{jk}^*$  for anisotropic media,

$$D_{jk}^* = D_{\alpha\beta} (\delta_{jk} + R B_{jk}^I) + A_{jik}^I v_i + A_{jilk}^{II} v_i v_l \quad (2.28)$$

where,

$D_{\alpha\beta}$  = average molecular diffusivity,

$A^I$  and  $A^{II}$  = symmetrical tensors bearing some functional

relationship with the transport properties of the fluid,

$R$  = a coefficient,

$B_{jk}^I$  = tortuosity tensor.

For isotropic media, the third rank tensor term would be dropped and the expression becomes essentially the same as obtained by Bachmat and Bear.

Recently, Hunt (1973) analyzed the dispersion problem in a different manner and obtained the same expression for the coefficient of dispersion as was obtained by Bachmat and Bear (1964). A novel feature of his development was that he made only one assumption that the principal



directions of the dispersion tensor were respectively tangential and normal to the flow stream lines as against three assumptions used by Bachmat and Bear in their analysis (viz.  $D_{k\ell} = a_{ijkl} \cdot v_i v_j / v$ ,  $a_{ijkl} = a_{jikl}$ , and  $a_{ijkl}$  are invariant with respect to all coordinate rotations and reflections). Even this assumption has been verified by experiments.

With a view to analyze the effect of medium porosity on the longitudinal dispersion coefficient, Dagan (1967) used a Fourier Transform and perturbation analysis to conclude that  $D_L$  computed from the concentration profile decreased along a column of decreasing porosity in the direction of flow and vice-versa. Analytical solutions of some simplified idealized cases of the dispersion equation were developed by Ogata and Banks (1961), Ogata (1961), Harleman and Rumer (1962), Ogata (1964) and others. The same were later summarized and reviewed by Ogata (1970). But, since these cases have little, if any, practical importance, greater and greater attention has been given by investigators towards the development of numerical solutions of the generalized dispersion equation during the last few years.

### 2.3 Development of Numerical Techniques.

One of the first important works in this direction was by Douglas, Peaceman and Rachford (1959) who solved the problem of miscible displacement in a two-dimensional flow field using an alternating-direction implicit scheme. Later, Peaceman and Rachford (1962) used a weighting scheme for the convective terms at adjacent grid points in a centered-in-time finite difference analogue of the convective-dispersion equation and adopted the leap-frog technique of computing the pressure distribution at each time step from the flow equation, calculating the velocity

at each point from this pressure distribution and using these velocities to obtain the new concentration distribution at the next time step from the convective-dispersion equation. They demonstrated that the method worked well in one dimension. But, subsequent calculations with the method for two-dimensional miscible displacement with zero dispersivity produced the same results as were presented by them with non-zero dispersivities. This indicated that their method involved a numerical dispersion of the same order as the physical dispersion. Blair and Peaceman (1963) extended the work to include the effects of aquifer compressibility, but one of two difficulties was usually encountered: either the solution developed severe oscillations specially in the regions where the concentration changed rapidly or became smeared with numerical dispersion.

In a bid to tide over this difficulty, Stone and Brian (1963) developed a more sophisticated method which consisted of writing a general finite-difference equation for the one-dimensional convective-dispersion equation, containing arbitrary weightings of all the possible approximations to  $\partial c/\partial x$  (space derivative of the concentration) and  $\partial c/\partial t$  (time derivative of the concentration). This scheme involved six points for three adjacent space locations at two time levels and utilized the Crank-Nicolson (1947) approximation for the second space derivative  $\partial^2 c/\partial x^2$ . They also proposed an iterative scheme with three cycles per time step to improve the accuracy of the solution. With proper choice of weighting coefficients, this method did reduce oscillations and numerical dispersion but could not handle two- and three-dimensional problems and did not take the variations in density and viscosity into account.



With the primary object of reducing numerical dispersion, Garder, Peaceman and Pozzi (1964) successfully employed the method of characteristics (particle-in-cell method) for the solution of the convective-dispersion equation in two dimensions. The numerical procedure involved a stationary grid and a set of moving points to solve the characteristic equations of the convective-dispersion equation. Extensive testing in one dimension indicated that the method was accurate over a wide range of values of the dispersion coefficient, including zero and that increasing the number of moving points beyond two per grid did not significantly improve the accuracy of the solution. For a two-dimensional model, the method provided good agreement with observed values for low oil-solvent viscosity ratios, but failed to do so for high viscosity ratios. The method also did not take into account the tensorial nature of dispersion. According to Shamir and Harleman (1966) this method took much more computer time and storage than the Stone and Brian scheme for the same order of accuracy, except for the case where the coefficient of longitudinal dispersion was zero. However, the method was general and could be adapted to take the density and viscosity variations into account in a two-dimensional case.

Shamir and Harleman (1966) developed a very efficient method which took advantage of the Stone and Brian scheme by transforming the dispersion equation into  $\phi$ - $\psi$  (i.e., equipotential and stream lines) coordinates as,

$$\frac{\partial c}{\partial t} + q^2 \frac{\partial c}{\partial \phi} = q^2 \frac{\partial}{\partial \phi} [ (a_I q + D_d) \frac{\partial c}{\partial \phi} ] + q^2 \frac{\partial}{\partial \psi} [ (a_{II} q + D_d) \frac{\partial c}{\partial \psi} ] \quad (2.29)$$

where,

$q$  = seepage velocity along the stream line,

$a_I$  = longitudinal dispersivity,

$a_{II}$  = lateral dispersivity.

As the velocity was tangential to the  $\Psi = \text{constant}$  lines, there was only one convective term in this equation. This enabled the use of the Stone and Brian's weighting scheme for the convective and time terms without any modification. The dispersion at right angles to the direction of the velocity could be treated by the alternating-direction method. Once the convective term was treated correctly, superposition of the longitudinal and lateral dispersion on the convective solution yielded correct results. This method was found to be unconditionally stable and could be extended to three-dimensional problems without much difficulty. If the major axis of the dispersion tensor coincided with the velocity vector, the technique took into account the tensorial nature of the dispersion coefficient. For the case when the longitudinal dispersion was zero, the scheme displayed oscillations and it did not account for the variations in density and viscosity. For unsteady cases, its use was limited to only those situations where the stream lines and equipotentials did not shift position with time.

Hoppes and Harleman (1967a) developed the mass conservation equation for the tracer in a two-dimensional case and obtained an approximate analytical solution for a homogeneous, confined, isotropic aquifer under steady-state flow from a recharge well. The solution was verified with a numerical one and tested with experimental data. In extension of the above, Hoopes and Harleman (1967b) dealt with the problem of predicting temporal and spatial distributions of a tracer injected into

the steady flow between recharging and discharging wells of equal strength in an infinite, horizontal, confined aquifer. Approximate analytical solutions were obtained for various cases of the two-dimensional equation for mass conservation of the tracer in the  $\phi$ - $\psi$  coordinates and tested by comparisons with numerical solutions and experimental values.

Bruch and Street (1967) obtained a theoretical solution for two-dimensional, unsteady dispersion of a miscible fluid in an idealized, steady, one-dimensional flow through an isotropic porous medium. The results have been presented in terms of complementary error functions. The lateral and longitudinal dispersion coefficients were determined from a pair of steady-state dispersion experiments applied to two simplified mathematical models. With these values of the dispersion coefficients, the equations derived for the unsteady-state case were experimentally verified. It has been suggested that by transformation of the equation to  $\phi$ - $\psi$  coordinates, their results could be used for two-dimensional practical problems even with slightly converging or diverging stream lines.

Pinder and Cooper (1970) used the method of characteristics for the solution of the convective-dispersion equation and the iterative alternating-direction implicit scheme for the flow equation for numerical solution of the two-dimensional problem of transient salt water front. However, they assumed that the porosity, viscosity and dispersion coefficient were constant in time and space and that the dispersion coefficient was a scalar. Almost simultaneously, but independently, Reddell and Sunada (1970) developed flow and convective-dispersion equations for three-dimensional, non-homogeneous, unsteady flow fields

with density and viscosity variations between the two fluids, considering the tensorial nature of the dispersion coefficient in the Cartesian coordinate system. An implicit numerical technique was used to solve the flow equation and the method of characteristics with a tensor transformation was used to solve the convective-dispersion equation. The results from the flow equation were used in solving the dispersion equation and the results of the convective-dispersion equation were then used to solve the flow equation. This procedure was repeated over and over again following the so-called leap-frog technique. Because of the excessive storage required for information concerning each moving point, they used auxiliary storage in the form of a scratch tape. The results obtained displayed no over-shoot, under-shoot, or numerical dispersion. They, however, observed an erratic behaviour of the error when their model was tested for known solutions of one-dimensional cases, in as much as the error did not necessarily get smaller with smaller grid sizes. They proposed the trouble was due to the rough representation of straight boundary conditions by a series of rectangular or square grids. Another significant observation was a lag in the concentration profile resulting in a jerky frontal movement, when the same moving points remained inside a grid throughout a time step. This indicated that the method was sensitive to the number and relative position of the moving points in a particular grid at a given time level. These difficulties call for a better method for determining the average concentration in a grid.

Kraeger (1972) applied the method of Reddell and Sunada to a field problem and observed an artificial dispersion inherent in the method of characteristics which did not show up in Reddell and Sunada's analysis

due to the very small size of grids used by them. In the latter case, the effects of artificial dispersion were partially absorbed by the physical dispersion. Another difficulty encountered by her was a trial and error process to arrive at a time increment which produced a concentration distribution resembling the field situation. This rendered the method incapable of predicting reliable future concentration distributions. By hand calculations, she observed that use of distorted grids or different spacing of points in the  $x$  and  $y$  directions produced distorted concentration distributions, which further limited the use of the method for predictive purposes.

Bredehoeft and Pinder (1973) applied the method of characteristics and the iterative alternating-direction implicit technique, neglecting molecular diffusion and changes in density and viscosity, to the problem of aquifer contamination at Brunswick, Georgia with moderate success. Konikov and Bredehoeft (1973) applied the same technique to predict changes in dissolved solids concentration in response to spatially and temporally varying stresses in the Arkansas River Valley of south-eastern Colorado. They observed that the calculated changes in the concentration of dissolved solids were consistently less than the observed changes but that the relative increases from month to month tended to agree. These differences were attributed to either inaccurate or inadequate representation of the field situation by the numerical model. The scope of all these investigations was limited to uniform rectilinear flow of homogeneous fluids in a region which had no sources or sinks within it.

#### 2.4 Applications of the Finite-Element Technique.

As seen from the preceding discussion of the various numerical methods, either the computer time or storage required for them becomes



prohibitive or else numerical or artificial dispersion tends to vitiate the results and at certain other times, the solution becomes severely oscillatory. These limitations, among others outlined above, focussed the attention of investigators towards the application of the finite element method to the solution of miscible displacement problems. The first attempt to apply this method to the solution of problems related to steady flow through anisotropic porous media was by Zienkiewicz, Mayer and Cheung (1966) followed by Taylor and Brown (1967) who extended the method to the solution of problems involving free surface. Price, Cavendish and Varga (1968) used the Galerkin method for solution of the one-dimensional diffusion-convection equation and showed that this method produced results of higher order accuracy and required less computer time than the central difference or non-central difference approximations as also the method of characteristics. They extended the finite-element method to the solution of two-dimensional problems.

Javandel and Witherspoon (1969) extended the use of the finite element method to the treatment of the flow equation for multi-layered aquifers of finite radial extent being pumped at constant rate through completely penetrating wells, using an iterative procedure to satisfy the constant discharge condition at the well boundary. They applied the method to flow towards partially penetrating wells also in multi-layered systems. Volker (1969) applied the method to the solution of steady free surface seepage problems through earth dams. Neuman and Witherspoon (1970) extended the technique further and successfully applied it to the problems of axi-symmetric flow from a circular pond in isotropic, homogeneous porous medium, axi-symmetric flow to a well in an unconfined aquifer, plane flow through a homogeneous dam, plane flow through a

homogeneous dam with a toe drain and the complex problem of a dam with a sloping core and a horizontal drain resting on a slightly permeable foundation whose bedding planes were inclined to the horizontal. They also devised a new iterative approach to obtain rapid convergence. Their method could handle cases where the free surface is discontinuous or where portions of the free surface are vertical or nearly vertical.

Guymon (1970a) applied the finite element method to the solution of the unsteady-state one-dimensional diffusion-convection equation and extended it (1970b) to the two-dimensional case taking both the longitudinal and lateral coefficients of dispersion into account but neglecting molecular diffusion. He indicated that the method could further be extended to the three-dimensional case as well. He, however, pointed out that the method is not, in general, applicable to problems defined by differential equations involving mixed partials and therefore neglected such terms in his solution.

Nalluswami (1971) improved upon the method followed by Guymon and included the mixed partial terms and the molecular diffusion component in his analysis. Hurr (1971) developed a finite-element ground water model that could solve problems connected with confined and unconfined flows for transient as well as steady-state conditions. Guymon (1972) suggested an improvement over his previous solution of the convective-dispersion equation, which displayed numerical dispersion and gave erratic results for small values of the dispersion parameters. This new approach did not make use of the exponential transformation developed in his earlier work. However, even this method did introduce slight errors for non-uniform flow cases and was not applicable to convection-dominated mass transport.

The scope of Guymon and Nalluswami's work was limited only to the solution of the two-dimensional simplified convective-dispersion equation in Cartesian coordinates. Simultaneous solution of the flow equation was not attempted by them. A serious limitation of the method was that it could not be applied to convection-dominant transports, which is the case for most field situations. The time-domain solution comprised of inherently explicit schemes and so exhibited convergence and stability problems. Although the need and criteria for an efficient element layout were indicated, yet they did not provide any scheme for automatic generation of such an element layout so as to give minimum band-width for the finite-element solution of the convective-dispersion equation. Such a scheme for efficient mesh generation, though quite important in the case of equal size element layout like the one used by Nalluswami and Guymon, is still more important in cases where the number of elements to be used is large and where due to substantial differences in concentration and potential gradients in different parts of the flow-domain, adoption of variable size elements becomes inevitable.

Another notable advancement towards the application of finite element method to solve three-dimensional steady-state and transient seepage problems was made by France, Parekh, Peters, and Taylor (1971) who introduced the concept of isoparametric elements to ensure higher orders of accuracy in the solution. Later, Pinder and Frind (1972) applied the Galerkin method with curved isoparametric quadrilateral elements to the case of transient flow towards a well in an infinite aquifer and also to the case of flow towards a well in a leaky confined aquifer and compared the results so obtained with those available for the finite-difference method. Although, both the methods yielded results



of almost the same accuracy, the Galerkin procedure had more flexibility of application to a wide range of deterministic problems. Solution of the convective-dispersion equation was not attempted by these investigators.

Smith, Farraday and O'Connor (1973) compared the finite-element solutions of the two-dimensional diffusion-convection equation by the Rayleigh-Ritz and Galerkin methods and showed that the latter is more versatile in handling different types of boundary conditions and in solving problems like salt intrusion in long estuaries where the magnitude of the exponent used for transformation of the partial differential equation to a self-adjoint form is of the order of a few hundreds or more. The analysis was, however, limited to uniform rectilinear flow of homogeneous fluids in a region which had no sources or sinks within it.

Recently, Pinder (1973) used the Galerkin method, with curved isoparametric quadrilateral elements, to solve the two-dimensional groundwater flow and dispersion equations in cartesian coordinates and applied this mathematical model to simulate the movement of a plume of contaminated ground water on Long Island, New York. His results indicated that reasonably accurate simulation of the movement of contamination in the subsoil water can be obtained by the Galerkin-finite-element method. Solution in a radial flow field with well boundary was not attempted by him.

Desai (1973) developed a simplified and approximate finite-element solution of a linearized equation governing one-dimensional transient fluid flow such as occurs in the case of flow in and out of earthen banks with vertical faces. But, this method was limited only to situations that could be approximated as one-dimensional flow problems.

Neuman (1973) applied the Galerkin-finite-element formulation to the solution of saturated and unsaturated seepage problems and demonstrated that due to convenience in the treatment of prescribed flux boundary conditions in this method, handling of the seepage face is considerably simpler than the finite-difference techniques. This investigation did not cover miscible displacement problems.

### 2.5 Summary.

A review of the available literature on the subjects related to the present study indicates that finite difference and other numerical techniques developed by various investigators require prohibitive amounts of computer time and storage to solve the transient convective-dispersion equation with reasonable accuracy. Further, almost all the solutions exhibit numerical dispersion, artificial dispersion or severe oscillations in the results, or else require a not too well defined process of trial and error to arrive at the appropriate time increment for the solution to be reasonably good. Applications of the finite-element method have mostly been directed to the solution of the steady or unsteady flow equation with or without the free surface except the works of Guymon, Nalluswami, Smith et al., and Pinder. As stated before, the Rayleigh-Ritz approach of Guymon and Nalluswami is restrictive in practical applications.

The Galerkin approach of Smith et al. and Pinder does not have any such limitations. The latter, however, yields non-symmetric matrices, thus requiring larger computer time and storage. Both the approaches have been found to be comparatively free of numerical dispersion and oscillations and do not involve any uncertain trial and error procedures.

Besides these, the finite-element technique has the following additional advantages over other numerical methods:

(i) It can handle any irregular boundary configuration which may be discretized to triangular, quadrilateral or other isoparametric elements of any shape and size.

(ii) The method not only accommodates complex geometry and boundary conditions, but has also proved successful in representing various types of complicated material properties that are difficult to incorporate into other numerical methods. It is even possible to vary the properties within an element according to some preselected polynomial pattern.

(iii) Specified gradient boundary conditions are introduced naturally and with a better accuracy than in standardized finite difference procedures. This reduces the number of boundary conditions to be subsequently introduced into the matrices before solving them.

(iv) Higher order elements can also be conveniently used to improve accuracy without complicating the boundary conditions - a difficulty always arising with finite difference approximations of a higher order.

(v) As the finite-element formulation quite often results in a system of symmetric banded matrices, there is great ease and time-saving in solving them on a computer.

(vi) It can be conveniently extended to problems in higher dimensions.

(vii) Situations where the principal axes of the transmissibility or dispersivity tensors change in orientation may be conveniently handled by simple coordinate transformations in the finite-element

technique (Smith, et al. 1973). The same can not be easily modeled in a finite-difference approximation.

For self-adjoint problems, both the Rayleigh-Ritz and Galerkin finite-element formulations lead to identical systems of symmetric matrices. For non-self-adjoint problems, the latter results in non-symmetric matrices, whereas the former, almost always, yields symmetric matrices, provided the corresponding variational functional exists. In certain cases, like the one analyzed by Guymon and Nalluswami with the Rayleigh-Ritz formulation, the transformation variable required to transform the system to a self-adjoint form may pose computational problems. For certain other situations, the presence of higher order derivatives in the weighted-residual of the Galerkin approach may create insurmountable difficulties with regard to higher order continuities. A judicious choice between the two approaches has, therefore, to be made depending upon the problem under investigation.

#### 2.6 Further Definition of Problem.

With this background about the performance of the various solution techniques, it is proposed to use the finite-element method for the simultaneous solution of the flow and convective-dispersion equations applicable to the situation under study. This investigation would, thus, include the following:

1. Development of the general flow equation for an isothermal, three-dimensional flow field where the porous medium is deformable and isotropic and the fluid is compressible and non-homogeneous with regard to density and reduction of such a flow equation to the case of an axisymmetric flow towards a well.

2. Development of the general convective-dispersion equation for an isothermal three-dimensional case in an isotropic medium taking molecular diffusion and the tensorial form of the dispersion coefficient into account assuming isotropic dispersivity and a non-reactive tracer and reduction of such an equation to the case of an axisymmetric flow towards a well.
3. Finite-element formulations for the transient flow and convective-dispersion equations.
4. Development of an efficient scheme for automatic mesh generation for the simultaneous solution of the flow and convective-dispersion equations by the finite-element method for the field situation of axisymmetric flow towards a partially penetrating well.
5. Development of a scheme for handling the different boundary conditions for the flow and convective dispersion equations for the case of confined, axisymmetric, unsteady flow towards a partially penetrating well.
6. Development of a computer program for simultaneous solution of the flow and convective-dispersion equations by an implicit leap-frog technique, testing the program by comparison with other known solutions and finally applying the same towards the solution of field problems.

## CHAPTER III

### MATHEMATICAL MODEL AND NUMERICAL SIMULATOR

#### 3.1 Development of the flow equation.

As explained earlier, the flow equation is a combination of the principle of conservation of mass expressed from the Eulerian viewpoint of fluid motion and the generalized form of Darcy's law for non-homogeneous fluids. The principle of conservation of mass as explained in Appendix A is based on the following assumptions:

(i) The size of the volume-element over which the mass-balance is considered does not vary with time.

(ii) There are no chemical reactions going on in the system and there are no sources or sinks.

(iii) There is only one non-reactive tracer present in the system.

(iv) The relationship between the fluid-density, pressure and concentration can be expressed by a first order equation of state and the proportionality factors are independent of pressure and fluid-composition.

(v) There is no change in volume upon mixing of fluids of different ionic concentrations.

With these limitations, the mass-balance may be expressed in compact tensorial notation as follows:

$$(\phi S)_t + \frac{1}{\sqrt{g}} \left( \sqrt{g} \frac{q_i}{h_i^2} \right)_{,i} = - \frac{\phi S}{\rho} \rho_t - \frac{q_i}{\rho h_i^2} \rho_{,i} \quad (3-1)$$

where,

$\phi$  = Porosity of the porous medium.

S = Saturation of the porous medium.



$q_i$  = Macroscopic flow velocity in  $i$  direction.

$\rho$  = Mass density of the fluid.

$g$  = Absolute value of the determinant of the metric tensor.

$h_i$  = Scales of coordinate transformation.  $i=1,2,3$ .

For the general case of an anisotropic, non-homogeneous porous medium and for a fluid, non-homogeneous with respect to density, Darcy's law may be stated as, Happen and Brenner (1965); Yih (1961):

$$q_i = v_i \phi S = - \frac{k_i k_r}{\mu} \left( \frac{1}{h_i} P_{x_i} + \rho g z_{x_i} \right) \quad (3-2)$$

where, the subscript  $x_i$  denotes derivative with respect to  $x_i$ .

$v_i$  = Seepage velocity component in  $i$  direction.

$k_i$  = Absolute permeability in  $i$  direction at complete saturation.

$k_r$  = Relative permeability at saturation  $S$ .

$P$  = Fluid pressure.

Assuming that,

- (i) Darcy's law holds for the flow situation under study,
  - (ii) there is no contribution to flow due to thermo-dynamic and adsorptive force gradients or due to electric charges carried by wet soil particles,
  - (iii)  $k_i$  and  $k_r$  are independent of pressure, temperature and concentration,
  - (iv) a linear relationship exists between the porosity and pressure,
  - (v) the medium is isotropic,
- and combining equations 3-1 and 3-2 as elaborated in Appendix A,

$$\frac{1}{\sqrt{g}} \left[ \frac{\sqrt{g}}{h_i^2} \left\{ \frac{k_i k_r}{\mu} \left( \frac{1}{h_i} P_{x_i} + \frac{\rho g}{h_i} z_{x_i} \right) \right\} \right]_{,i} + \frac{1}{\rho h_i^2} \rho_{,i} \cdot$$

$$\left\{ \frac{k_i k_r}{\mu} \left( \frac{1}{h_i} P_{x_i} + \frac{\rho g}{h_i} z_{x_i} \right) \right\} = \left[ \rho_o \phi_o^S (\beta + C_F) P_t + \alpha \phi_o S C_t \right] \cdot \frac{1}{\rho} \quad (3-3)$$

For radial flow towards a partially penetrating well in a saturated medium, equation 3-3 reduces to the following approximate relationship,

$$\frac{1}{r} \left[ \left\{ \frac{\rho r k}{\mu} (P_r + \rho g z_r) \right\}_r + \left\{ \frac{\rho r k}{\mu} (P_z + \rho g) \right\}_z \right] =$$

$$\rho_o \phi_o (\beta + C_F) P_t + \alpha \phi_o C_t \quad (3-4)$$

For the problem under investigation, the assumption of the validity of Darcy's law is as much justified as it is for any other problem in well-hydraulics. No doubt, there will often be a small zone of non-linear flow in close proximity to the well where refinements to Darcy's law are warranted Ahmad (1967); Ahmad and Sunada (1969). However, such refinements are not considered necessary in the present investigation in view of the fact that minor approximations, thus introduced in a very small portion of the flow region, will not appreciably affect the total salt transport due to hydrodynamic dispersion and convection. The assumption that the contribution to flow due to thermodynamic gradient is small, is justified by the fact that temperature variations of the subsoil in any particular saturated region are generally small and past researchers have indicated that the quantum of thermal-gradient-actuated flow in a saturated soil is rather small as compared to that actuated by the mechanical gradient; Gurr, Marshall and Hutton (1952); Hadley and Eisenstadt (1955); Habib and Soerio (1957); Kuzmak and Serada (1958);

Rollins, Spangler and Kirkham (1954). The effect of electrical charges carried by wet soil particles and adsorptive force gradients is even less, Hillel (1971).

The assumption regarding the invariance of absolute and relative permeabilities with changes in pressure and concentration is justified by the observation that in naturally occurring saturated aquifers under isothermal conditions, there is hardly any effect of pressure or concentration on permeability so long as the fluid behaves as a continuum and the concentration remains small. The linear relationships between porosity and pressure and between the density, pressure and concentration used in the derivation of flow-equation in Appendix A, though not rigorously true, have often been used with success by earlier investigators Reddell and Sunada (1970); Breittenbach (1968). Under isothermal conditions, contribution to flow due to reactions between soil, water and ordinary salts is very small and so the reaction, production or consumption terms in the flow-equation may be omitted without introducing appreciable errors. By observations in physical chemistry, it is also known that there is little change in the volume of a solution upon mixing of fluids of different ionic concentration, Bredehoeft and Pinder (1973).

The only assumption made in Appendix A, that is questionable for a field situation, is that of the isotropy of the medium. This has been introduced in this study to avoid complex tensorial expressions for the coefficients of dispersion as explained in Chapter II. This analysis, based on the assumption of an isotropic medium, will, however, not apply to a flow region which is highly anisotropic.

### 3.2 Development of the Convective Dispersion Equation.

As discussed in Appendix B, the convective-dispersion equation is a combination of the mass-balance equation for the tracer and Fick's law of diffusion. The resulting equation in tensorial form is reproduced below.

$$C_t = \frac{\rho}{\rho - \alpha C} \cdot \frac{1}{\phi \sqrt{g}} \left[ \frac{\sqrt{g} \phi}{h_i^2} \left\{ \lambda V C_{,i} + \frac{2\mu v_i v_j}{V h_j^2} C_{,j} + D_d T C_{,i} \right\} \right]_{,i} - \frac{v_i}{h_i^2} C_{,i} \quad (3-5)$$

where,  $_{,i}$  = covariant derivative,

$C$  = concentration,

$\alpha$  = proportionality factor as defined in Appendix A,

$\lambda$  =  $a_{II}$  = lateral dispersivity of the medium,

$V$  = absolute velocity of the fluid,

$\mu$  =  $(a_I - a_{II})/2$ ,

$a_I$  = longitudinal dispersivity of the medium,

$D_d$  = coefficient of molecular diffusion,

$T$  = tortuosity.

For axi-symmetric flow towards a partially penetrating well, equation 3.5 reduces to,

$$C_t = \frac{\rho}{\rho - \alpha C} \left[ \frac{1}{\phi r} \left\{ \phi r (D_{11}^* C_r + D_{12}^* C_z) \right\}_r + \frac{1}{\phi} \left\{ \phi (D_{22}^* C_z + D_{12}^* C_r) \right\}_z \right] - u C_r - v C_z \quad (3.6)$$

where,

$$\begin{aligned} D_{11}^* &= \lambda V + 2\mu \frac{u^2}{V^2} + D_d T \quad , \\ &= D_T + (D_L - D_T) \frac{u^2}{V^2} + D_d T \quad , \end{aligned}$$

$$\begin{aligned} D_{22}^* &= \lambda V + 2\mu \frac{v^2}{V^2} + D_d T \quad , \\ &= D_T + (D_L - D_T) \frac{v^2}{V^2} + D_d T \quad , \end{aligned}$$

$$\begin{aligned} D_{12}^* &= D_{21}^* = 2\mu \frac{uv}{V^2} + D_d T \quad , \\ &= (D_L - D_T) \frac{uv}{V^2} \quad , \end{aligned}$$

$D_T = a_{II} V$  = coefficient of lateral dispersion,

$D_L = a_I V$  = coefficient of longitudinal dispersion,

$u$  and  $v$  are radial and vertical components of velocity.

The various assumptions inherent in the development of the above equation are:

- (i) Fick's law is applicable.
- (ii) There is no production or consumption of the tracer due to chemical reactions.
- (iii) The medium is isotropic so that dispersion coefficients  $D_T$  and  $D_L$  could be defined as above and the tortuosity tensor  $T$  is a scalar.

All these assumptions are reasonable for a dilute solution of an inert tracer under isothermal state, Crank (1956), which is the case for the situation under study. Limitations of the assumption of isotropy have already been indicated in the previous section. The main advantage of this assumption is that the dispersivity tensor  $a_{ijlm}$ , which is of rank four, reduces to only two terms,  $a_I$  and  $a_{II}$  (longitudinal and lateral dispersivities) for an isotropic porous medium.

### 3.3 The Finite-Element Method.

As outlined in Chapter II, finite-element approximation for any tractable problem could be obtained either by an adaptation of the Rayleigh-Ritz technique of variational calculus, which requires a variational functional, physically representing the rate at which energy is being dissipated per unit volume or weight of the fluid, to be minimized over the entire flow domain; or by using weighted residual techniques like the Galerkin method, which preclude the necessity of developing a variational functional for the problem. The Rayleigh-Ritz method is the most widely accepted means of arriving at the finite element representation of a problem. In addition to the numerous merits pointed out by Guymon (1970b), it admits less restrictive approximating functions and the conditions of convergence for this method have been well established, Tottehnem and Brebbia (1970).

The fact that a variational functional may not exist for a wide variety of problems or may be too complicated to handle by readily available numerical schemes, does impose a limitation on its use. On the other hand, owing to the direct occurrence of the differential operators of the governing equation of the problem into the integrals involved in the Galerkin method, a higher order of continuity may have to be guaranteed by the shape function in order to avoid inter-element contributions. This restriction on the choice of shape functions may sometimes pose insurmountable difficulties, Zienkiewicz (1971).

In the formulation presented in this chapter both the approaches have been discussed in relation to the problem under study. Both these formulations are based on the inherent assumption that within each



element, the variables  $H$  (defined in section 3.5) and  $C$  are uniquely represented by a polynomial, continuous at the element boundaries. This assumption is justified within the limits of accuracy of the Weierstrass approximation theorem, Courant and Hilbert (1963) which states that a function  $H(x_1, x_2, x_3, \dots, x_n)$  or  $C(x_1, x_2, x_3, \dots, x_n)$ , which, along with its derivatives up to the  $k^{\text{th}}$  order, is continuous in the closed region  $a_{i-1} < x_i < b_i$ , may be uniformly approximated by polynomials in this interval in such a way that the derivatives of  $H$  or  $C$  up to the  $k^{\text{th}}$  order are also approximated uniformly by the corresponding derivatives of the polynomials.

Rigorous criteria for selecting the order of the polynomial representing these variables  $H$  or  $C$  are completeness, compatibility and independence of the pattern from the orientation of the local coordinate system. The requirement of completeness implies that over the region of application of the polynomial, there should exist combinations of values of the generalized coordinates that cause all points on an element to experience the same pressure or concentration. A polynomial with a constant term in it might take care of this requirement. The compatibility requirement implies that there should be no discontinuities of pressure or concentration within an element and between adjacent elements. Since polynomial models are inherently continuous, continuity within the element is ensured by the choice of any polynomial.

The condition of interfacial compatibility is satisfied if;

- (i) the same polynomial model is used for all the elements,
- (ii) the pressure or concentration values along any interface

depend on the nodal-point values pertaining to that interface only, (iii) inter-element nodal compatibility is ensured.

It may be shown, Desai and Abel (1972), that polynomial models do satisfy requirements (i) and (ii) and that requirement (iii) is implied in the usual assembly procedure of the finite-element method.

As the differential operators in the governing equations 3.4 and 3.6 happen to be of the second order, prima facie, it appears that second order continuity has to be guaranteed by the shape function for the Galerkin method, but as has been shown later, use of the divergence theorem reduces the order of these differentials to one and thus obviates the requirement of second order continuity. For both the approaches in this study, although higher order shape functions might add to accuracy, only linear polynomials have been considered, on the presumption that other approximations implicit in the analysis would far offset the improved accuracy attained by adopting more complex polynomial representations of the functions  $H$  or  $C$ . Following a similar reasoning, although, as indicated in Chapter II, isoparametric elements could be used, yet, in this investigation, where the scope is limited to simpler boundary configurations, triangular elements have been considered adequate.

Since, as explained above, the pressure or concentration varies linearly along any side of a triangular element, the same pressure or concentration is bound to exist all along an interface, if identical pressures or concentrations are imposed at the nodes. Thus the pressure or concentration distribution functions automatically guarantee continuity of pressure or concentration with adjacent elements. However, there may be discontinuities in the first derivative of the pressure or

concentration parameters between adjacent elements. To minimize the effects of such discontinuities, it is necessary to use smaller elements in areas of rapid changes in the first derivatives of pressure or concentration, while larger elements may be adequate for comparatively insensitive regions.

Once continuity between adjacent elements is ensured, the Galerkin method would consist of choosing a continuous weighting function which might be the shape function itself, and equating the element by element weighted residuals to zero. On the other hand, the Rayleigh-Ritz method would consist of minimization of the variational functional over the entire flow region. That this is a true minimizing or stationarity principle can be mathematically proved, Kantorovich and Krylov (1958) and that this minimization process implies solution of the flow or convective-dispersion equation can be shown by using the fundamental lemma of calculus of variations.

The linear models discussed above, satisfy the last criterion of independence of the pattern from the orientation of the local coordinate system also. This aspect has been elaborated in detail by Desai and Abel (1972) and Dune (1948). This property of the model is known as geometric isotropy, spatial isotropy or geometric invariance.

#### 3.4 Mesh Layout.

Once the element shape and degree of polynomial approximating the function  $H$  or  $C$  has been finalized, the next step is to figure out an element layout covering the flow domain. Taking advantage of radial symmetry and assuming that the contribution of the nearly spherical and non-radial flow towards the bottom of a partially penetrating well, Muskat (1946) is negligible, the three-dimensional flow problem may be

reduced to one that could be studied on a two-dimensional region in the  $r$ - $z$  plane typified by a vertical cross-section of the aquifer passing through the axis of the well. Even on this cross-section, only one-half portion lying towards any one side of the well-axis would be adequately representative of the flow system as far as this investigation is concerned. Therefore, it is this two-dimensional region, that has been sub-divided into a mesh of triangular finite elements, not necessarily congruent or symmetric. For a general case, the triangular elements would comprise an assortment of acute angle, right angle and obtuse angle triangles with few, if any, of their sides parallel or perpendicular to the coordinate axes. For such cases, closed form expressions for higher moments over the elemental area, although possible to derive, would become rather complex and tedious. It is, therefore, desirable to use the Gauss-quadrature approximation as suggested by Zienkiewicz (1971).

As explained in Section 3.3, the element layout is to be arranged in such a way that the regions of maximum pressure or concentration gradients are covered by smaller size elements. Thus, smaller elements have to be provided in the vicinity of the well, with the sizes gradually increasing with distances from the well both in  $r$  and  $z$  directions, so that abrupt changes in element sizes are avoided. Another important requisite for the mesh layout stems from the point of view of computational efficiency. It is well known that finite element formulation of the flow or dispersion equation would result in the formation of banded matrices, with the band-width given by the following rules:

- (i) For symmetric matrices, band-width = IBAND = Maximum of the differences in the numbers assigned to any two adjacent nodal points in the entire mesh layout plus one.

(ii) For unsymmetric matrices, band-width = twice the maximum of the differences in the numbers assigned to any two adjacent nodal points in the entire mesh layout plus one.

Thus, there is a certain mesh layout with a certain numbering scheme for the nodal points and elements that will give the smallest possible band width.

An indication of the boundary orientation for an efficient element layout for simple flow regions has been given by Guymon (1970b). However, he did not develop any mesh-generation scheme for a suitable element layout. In this investigation, a computer program has been developed<sup>1</sup> for automatic mesh-generation, based on the algorithm of Zienkiewicz and Phillips (1971). As discussed in Chapter IV, this program requires the flow region to be divided into one or more loops depending upon the variations in element sizes. Each loop is divided into a number of quadrilaterals and the shorter diagonal of each quadrilateral is joined to produce a triangular element layout. For multi-loop regions, this program incorporates an optimization scheme, Collins (1973), to renumber all the nodes in the mesh so as to yield a minimum band-width. Data requirement for this program consists of the coordinates of eight points delineating the boundary geometry of each loop taken in an anti-clockwise sense, the number of divisions into which each side is to be divided and the maximum and minimum values of the  $r$  and  $z$  coordinates for each loop. In addition, information regarding the common sides between any two loops has also to be provided as input in the form of an array as

---

<sup>1</sup>With the cooperation of Dr. E. G. Thompson, Civil Engineering Dept., Colorado State University.

explained in Appendix G. The output comprises a film plot of the layout and a deck of punched cards giving the coordinates of all the nodes and assigned numbers of all the nodes and elements.

### 3.5 Finite Element Formulation for the Flow Equation.

With a view to transform equation 3.4 to a tractable form, it is expedient to introduce two terms of negligibly small magnitudes viz.  $gz \rho_r$  and  $gz \rho_z$  and modify it as follows:

$$\rho_o \phi_o (\beta + C_F) P_t + \alpha \phi_o C_t \cong \frac{1}{r} \cdot \frac{\rho k}{\mu} \{ P_r + \rho g z_r + g z \rho_r \} \\ + \left\{ \frac{\rho k}{\mu} (P_r + \rho g z_r + g z \rho_r) \right\}_r + \left\{ \frac{\rho k}{\mu} (P_z + \rho g + g z \rho_z) \right\}_z$$

where the subscripts  $r$ ,  $z$  and  $t$  denote derivatives with respect to them. Setting, (3.7)

$$\begin{aligned} \rho_o \phi_o (\beta + C_F) &= E \\ \alpha \phi_o &= F \\ P + \rho g z &= H \\ \frac{\rho k}{\mu} &= S \\ EP + FC &= Y \end{aligned}$$

equation 3.7 reduces to,

$$Y_t = \frac{1}{r} (r S H_r)_r + (S H_z)_z \quad (3.8)$$

The Galerkin Approach. Following the Galerkin technique as discussed in Appendix C with an arbitrary weighting function  $W_p$  where  $p=i,j,k$  and applying divergence theorem to the weighted residual, with a view to reduce the order of differentials occurring in it, the following equation is obtained:



$$\iint_V [S H_r (W_p)_r + S H_z (W_p)_z + W_p Y_t] r dr dz = \int_S W_p S H_r n^1 dS$$

$$+ \int_S W_p S H_z n^3 dS \quad (3.9)$$

Using the boundary conditions discussed in Section 3.7, the R.H.S. of equation 3.9 reduces to zero except for the well face and the constant head boundaries. For the well boundary, value of the expression on the R.H.S. is known in terms of the flow rate  $q$  and for the constant head boundaries, this expression may be set equal to some unknown value  $[R]$ . It is shown in Section 3.7 that, in view of the known values of  $H$  on the constant head boundaries, the value of  $[R]$  is not required to be computed for the solution of the resulting system of simultaneous equations.

Substituting the above values on the R.H.S. of equation 3.9 and transforming it to a local coordinate system referred to the centroid of the element as the origin, the following system of equations is obtained,

$$\iint_{R^m} [S H_\xi (W_p)_\xi + S H_\eta (W_p)_\eta + W_p Y_t] (\bar{r}^m + \xi) d\xi d\eta =$$

$$\int_{S_2^m} W_p \rho q r_w d\eta + [R] \quad (3.10)$$

where, the subscripts  $\xi$ ,  $\eta$  and  $t$  denote derivatives with respect to  $\xi$ ,  $\eta$  and  $t$ ,

$$\xi = r - \bar{r}^m$$

$$\eta = z - \bar{z}^m$$

$\bar{r}^m$  and  $\bar{z}^m$  are the global coordinates of the centroid and  $\bar{R}^m$  and  $\bar{S}_2^m$  respectively refer to the area and the portion of the well-face, if any, covered by the boundary of the  $m^{\text{th}}$  element.

Defining a continuous shape function  $[A]$  as explained in Appendix C, such that,

$$H = [A] \{H\}^m$$

where the matrix  $\{H\}^m$  refers to nodal point values of  $H$  for the  $m^{\text{th}}$  element and assuming that this shape function itself is the weighting function, equation 3.10 yields,

$$\iint_{R^m} ([S [A]_{\xi} (A_p)_{\xi} + S [A]_{\eta} (A_p)_{\eta}] \{H\}^m + A_p [A] \{Y_t\}^m) (\bar{r}^m + \xi) d\xi d\eta = \int_{S_2^m} A_p \rho q r_w d\eta + [R] \quad (3.11)$$

Evaluating the differentials and integrals and writing the system in the symbolic form defined in Appendix C, equation 3.11 may be written as,

$$[FSL] \{H\}^m + [FPLE] \{Y_t\}^m = [Q]^m + [R]^m \quad (3.12)$$

Following the general process of assembly applicable to finite element formulations for combining equations similar to 3.12 for all the elements in the layout, the following system of simultaneous equations is obtained,

$$[SK] \{H\} + [PK] \{Y_t\} = [QK] + [R] \quad (3.13)$$

The Rayleigh-Ritz Approach. Following the alternative Rayleigh-Ritz technique, the variational principle for equation 3.8 may be verified to be, Hildebrand (1965),

$$J = \iint_R \left[ \frac{S}{2} (H_r)^2 + \frac{S}{2} (H_z)^2 + H Y_t \right] r dr dz - \int_{S_2} \rho q r_w H dz \quad . \quad (3.14)$$

Equating the first variation of  $J$  to zero, it may be shown that the natural, geometric and well boundary conditions are included in this variational principle. Its transformed form written for the  $m^{\text{th}}$  element in terms of local coordinates is,

$$J^m = \iint_{R^m} \left[ \frac{S}{2} \{ (H_\xi)^2 + (H_\eta)^2 \} + H Y_t \right] (\bar{r}^m + \xi) d\xi d\eta - \int_{S_2^m} \rho q r_w H d\eta \quad (3.15)$$

The minimization process for this functional,  $J$ , consists of evaluating the contributions from all the nodes in the layout to the differentials  $J_{H_p}^m$  ( $p=i,j,k$ ) for each element, summing the relevant contributions for each node and equating the sum to zero for stationarity. This process for the  $m^{\text{th}}$  element yields,

$$J_{H_p}^m = \iint_{R^m} \left[ S H_\xi (H_\xi)_{H_p} + S H_\eta (H_\eta)_{H_p} + Y_t H_{H_p} \right] (\bar{r}^m + \xi) d\xi d\eta - \int_{S^m} (r_w \rho q H)_{H_p} d\eta = 0 \quad , \quad (3.16)$$

where the subscript  $H_p$  denotes a derivative with respect to  $H_p$ . Equation 3.16 may be verified to be the same as equation 3.11 except for the unknown terms  $[R]$  which do not affect the solution at all. Thus, so far as the flow equation 3.8 is concerned, which is already in the self-adjoint form, Hildebrand (1965), both the Galerkin and Rayleigh-Ritz techniques lead exactly to the same system of simultaneous equations 3.13.

### 3.6 Time Domain Formulation of the Flow Equation.

As discussed in Section 3.5, the finite element formulation of equation 3.8 yields,

$$[PK] \{Y_t\} = [QK] + [R] - [SK] \{H\} \quad .$$

Time domain solution of this system may be obtained in several ways, viz. by the methods of undetermined parameters (collocation, subdomain, Galerkin or least squares) as outlined by Crandall (1956) or by combining the usual integration schemes Runge-Kutta and Adams-Moulton, etc., Nalluswami (1971), Guymon (1970b). The latter approach is time consuming, requires extra computer storage and has been found to cause stability and convergence problems unless the time step chosen is very small. The shortcuts suggested, Robert G. Baca (1973)<sup>1</sup>, to expedite convergence of the scheme are not applicable to a general system of equations. Unlike the case of a single first order equation, Gerald Curtis (1970), it is extremely difficult to develop criteria for the convergence of successive recorrections by the Adams-Bashford corrector for a system of equations. It is even more difficult, in any particular case, to know whether such criteria, if available, are actually satisfied or not. Therefore, most authors, Conte (1965), Peter Henrici (1965), caution against the use of the corrector more than once and recommend to restart from the Runge-Kutta onwards at every change of the time-step, which is a time consuming process. In the present study both the undetermined parameters and Adams-Moulton methods were tried and finally, to retain simplicity without substantial loss of accuracy, the Galerkin method of weighted residuals has been adopted. For the Galerkin method developed in Appendix C, the equation residual for the time-domain solution gives,

<sup>1</sup>By personal communication with Robert G. Baca, 1973, Pac. NW Labs..

$$\int_0^{\Delta t} N_1 [ [PK] \{Y_t\} + [SK] \{H\} - [QK] - [R] ] dt = 0 \quad . \quad (3.17)$$

In similarity to the finite-element discretization in space, assuming a linear interpolation of  $H$  in the time-domain for a small time interval  $\Delta t$ ,

$$\{H\} = [N] \begin{Bmatrix} \{H\}_0 \\ \{H\}_1 \end{Bmatrix} \quad (3.18)$$

where,

$$[N] = [ N_0 \quad N_1 ] = [ 1 - \frac{t}{\Delta t} \quad \frac{t}{\Delta t} ]$$

$$\{H\}_0 = \text{nodal point values of } H \text{ at } t=0 .$$

$$\{H\}_1 = \text{nodal point values of } H \text{ at } t=\Delta t .$$

As for the formulation in space, higher order polynomials with more elaborate elements may be tried for the time domain solution if the accuracy desired warrants, Zienkiewicz (1971). For the present study, results obtained by the linear relationship of equation 3.18 are considered adequate and therefore, the time-domain formulation is based on this linear relationship.

Since,

$$Y_0 = E (H_0 - \rho_0 g z) + F C_0 \quad , \quad (3.19)$$

it follows that within the approximation inherent in the leap-frog technique,

$$Y_1 \approx E (H_1 - \rho_0 g z) + F C_0 \quad , \quad (3.20)$$

and,

$$Y_t \approx E \cdot H_t \quad (3.21)$$

where the subscripts 0 and 1 refer to the time levels  $t=0$  and  $t=\Delta t$  respectively.

Substitution of equation 3.21 into 3.17 and integration of the latter yields,

$$\left[ [PK] \frac{E}{\Delta t} + \frac{2}{3} [SK] \right] \{H\}_1 = [QK] + [R] + \left[ [PK] \frac{E}{\Delta t} - \frac{1}{3} [SK] \right] \{H\}_0 \quad (3.22)$$

which is the required recurrence relation for the time-domain solution. A similar recurrence relation may be obtained by following the subdomain method as explained in Appendix C.

### 3.7 Treatment of Boundary and Initial Conditions for the Flow Equation.

To start with, values of  $\phi$ ,  $\rho$ ,  $C$  and  $H$  for each node are prescribed as initial conditions, say,

$$\phi_0(r,z), \rho_0(r,z), C_0(r,z), H_0(r,z) \quad \text{at } t=0.$$

Besides these initial conditions, there will, in general, be three types of boundary conditions:

(i) Natural or reflective boundary conditions which specify that  $H_n = 0$ , on a portion of the exterior boundary,  $n$  being normal to the boundary surface drawn in an outward sense. The subscript  $n$  denotes a derivative with respect to  $n$ . Such boundary conditions apply to all impermeable or no-flow boundaries. As shown in Appendix C, the finite element formulation, in itself, implies satisfaction of such boundary conditions.

(ii) Geometric boundary conditions which specify the values of  $H$  on a portion of the boundary. At a section of the aquifer, beyond the radius of influence,  $r_0$  of the well, or at a large depth below the bottom of the well,  $H$  will remain unchanged for all time periods and so, will be represented by specified values such as,

$$H_1(r,z), H_2(r,z), \dots, H_n(r,z) \quad \forall \quad t \geq 0.$$



A convenient device that has been adopted in the computer program, to take such geometric boundary conditions into account is described below:

Let  $H(j)$  be the known value at node number  $j$  of the element layout. The coefficient associated with this value in the simplified matrix on the L.H.S. of equation 3.22 is, say,  $PK(j,j)$  and the corresponding element of the R.H.S. column matrix, obtained after simplifying the R.H.S. of equation 3.22 is, say,  $F(j)$ , which includes the unknown element of  $[R]$  also. These values of  $PK(j,j)$  and  $F(j)$  are replaced by the following new values,

$$PK(j,j)_{\text{new}} = PK(j,j)_{\text{old}} * 10^{50}$$

and,

$$F(j)_{\text{new}} = PK(j,j)_{\text{old}} * 10^{50} * H(j) \quad .$$

Solution of the system of equations 3.22, with the above replacements, would meet the requirements of the given boundary conditions. The multiplier  $10^{50}$  is an arbitrarily chosen large number used to force the given value of  $H(j)$  for the nodal point in question to come out as the final solution for that node. It is seen here that the solution procedure does not require  $[R]$  to be known.

(iii) A special boundary that has to be treated for the problem under study is the well face. At this boundary, a constant rate of pumping would imply that,

$$H_r \Big|_{r=r_w} = \text{constant, for each length segment.}$$

But, due to non-uniform distribution of discharge along the penetration depth of the well, this constant may not have the same value for all the length segments between adjacent nodes along the well face, Muskat (1946). Therefore, a prerequisite to properly account for the

well-boundary is to estimate the values of this constant applicable to the various nodal points on the well-face. Assuming that the flow at the well-face is purely radial and also assuming that the potential inside the well is the same at every point along the penetration depth, Hantush (1964), an iterative procedure suggested by Muskat (1932) was devised, but it proved to be very time consuming. Further, prior investigations, Hantush (1964) indicated that the gain in accuracy achieved by adopting such an elaborate procedure, is not worth the effort and that in most cases, it is reasonable to assume a uniform distribution of discharge over the penetration depth. Accordingly, for the present investigation, an average value of  $q_i$  given by the following equation has been used,

$$q_i = Q_w / 2\pi r_w \times \text{PENETR}$$

where,

$$Q_w = \text{well discharge,}$$

$$\text{PENETR} = \text{depth of well penetration,}$$

The subscript  $i$  denotes the  $i^{\text{th}}$  node on the well face.

As explained in Appendix C, the elements of matrix  $[QK]$  on the R.H.S. of equation 3.22 may be computed with this known value of  $q_i$  for the well-face. It is also known that the unknown  $[R]$  contributes nothing on the well-boundary. Thus the R.H.S. of equation 3.22 is completely known for all the nodes along the well face.

### 3.8 Finite-Element Formulation for the Convective-Dispersion Equation.

Assuming that the velocities  $u$  and  $v$ , the porosity  $\phi$ , the fluid density  $\rho$  and the coefficients of dispersion  $D_{11}^*$ ,  $D_{22}^*$  and  $D_{12}^*$  are invariants within an element for a particular time step, the

convective-dispersion equation 3.6 may be expressed in the following form,

$$\frac{1}{r} (r D_{rr} C_r + r D_{rz} C_z)_r + (D_{zz} C_z + D_{rz} C_r)_z - uC_r - vC_z - C_t = 0 \quad (3.23)$$

where,

$$\begin{aligned} D_{rr} &= D_{11}^* \frac{\rho}{\rho - \alpha C} \\ D_{rz} &= D_{12}^* \frac{\rho}{\rho - \alpha C} \\ D_{zz} &= D_{22}^* \frac{\rho}{\rho - \alpha C} \end{aligned}$$

and  $D_{11}^*$ ,  $D_{12}^*$  and  $D_{22}^*$  are as defined in Section 3.2.

The Galerkin Approach. Following the Galerkin approach as discussed in Appendix D, with an arbitrary weighting function  $W_p$  and applying the divergence theorem to the weighted residual, as was done for the flow equation, the following equations are obtained,

$$\begin{aligned} \iint_R [ (W_p)_r (D_{rr} C_r + D_{rz} C_z) + (W_p)_z (D_{zz} C_z + D_{rz} C_r) + W_p (uC_r \\ + vC_z + C_t) ] r dr dz = \int_S W_p (D_{rr} C_r + D_{rz} C_z) n^1 dS \\ + \int_S W_p (D_{zz} C_z + D_{rz} C_r) n^3 dS \quad \cdot \text{Where } p=i,j,k \quad (3.24) \end{aligned}$$

Using the boundary conditions discussed in Section 3.9, the R.H.S. of equation 3.24 reduces to zero except for the well-face and the boundaries where concentration is invariant with time. For the well-boundary, value of the R.H.S. expression of equation 3.24 is known in terms of the flow rate  $q$  and for the boundary where concentration is invariant with time, the expression on the R.H.S. of equation 3.24 may be set equal to some unknown value  $[R]$ . It is shown in Section 3.9 that, as

for the flow equation, the value of  $[R]$  is not required to be computed for the solution of the resulting system of equations. Substituting these values in equation 3.24 and transforming it to a local coordinate system, the following equations are obtained for the  $m^{\text{th}}$  element of the layout,

$$\begin{aligned} \iint_{R^m} [ (W_p)_\xi (D_{rr} C_\xi + D_{rz} C_\eta) + (W_p)_\eta (D_{zz} C_\eta + D_{rz} C_\xi) \\ + W_p (uC_\xi + vC_\eta + C_t) ] (\bar{r}^m + \xi) d\xi d\eta = \\ - \int_{S_2^m} W_p qC \left( \frac{1}{\phi} - 1 \right) r_w d\eta + [R] \quad . \end{aligned} \quad (3.25)$$

Defining a continuous shape function  $[A]$  as explained in Appendix D, such that,

$$C = [A] \{C\}^m \quad , \quad (3.26)$$

and assuming that this shape function itself is the weighting function, equation 3.25 transforms as follows:

$$\begin{aligned} \iint_{R^m} \{ ( (A_p)_\xi [D_{rr} [A]_\xi + D_{rz} [A]_\eta] + (A_p)_\eta [D_{zz} [A]_\eta + D_{rz} [A]_\xi] \\ + u [A]_\xi A_p + v [A]_\eta A_p ) (\bar{r}^m + \xi) d\xi d\eta \} \{C\}^m \\ + \iint_{R^m} \{ A_p [A] (\bar{r}^m + \xi) d\xi d\eta \} \{C_t\}^m = - \int_{S_2^m} A_p [A] q \left( \frac{1}{\phi} - 1 \right) r_w \\ \{C\}^m d\eta + [R] \quad . \end{aligned} \quad (3.27)$$

Evaluating the differentials and integrals and writing the resulting system of equations in the symbolic form defined in Appendix D, the

following relationship is obtained for the  $m^{\text{th}}$  element,

$$[\text{SL}] \{C\}^m + [\text{PL}] \{C_t\}^m = - [Q]^m + [R]^m \quad . \quad (3.28)$$

Following the usual assembly procedure for combining contributions of all the elements to the various nodes in the layout, the following system of simultaneous equations results,

$$[\text{SK}] \{C\} + [\text{PK}] \{C_t\} = - [Q] + [R] \quad . \quad (3.29)$$

An important point to be noted here is that the very fact that the convective-dispersion equation (3.23) is not in a self-adjoint form, causes the matrices  $[\text{SL}]$  and  $[\text{PL}]$  and, hence, the matrices  $[\text{SK}]$  and  $[\text{PK}]$  to be unsymmetric, which is a disadvantage for numerical solutions.

The Rayleigh-Ritz Approach. Since equation 3.6, as such, is not in a self-adjoint form, a reducing factor has to be developed for it.

Following Hildebrand (1965), it may be seen (Appendix E) that the required reducing factor is,

$$r \cdot \exp(\beta) \quad (3.30)$$

where,

$$\begin{aligned} \beta &= \frac{v D_{rz} - u D_{zz}}{D_{zz} D_{rr} - D_{rz}^2} \cdot r + \frac{u D_{rz} - v D_{rr}}{D_{zz} D_{rr} - D_{rz}^2} \cdot z \\ &= - \frac{\rho - \alpha C}{\rho} \cdot \frac{ur + vz}{D_L + D_d T} \quad . \end{aligned}$$

Multiplying equation 3.6 by this reducing factor and for convenience of numerical computation, transforming it in terms of a new variable  $\psi$ , such that,

$$\psi = C e^{\beta/2} \quad , \quad (3.31)$$

the following equation is obtained,

$$\frac{1}{r} (r D_{rr} \psi_r)_r + (D_{zz} \psi_z)_z + \frac{1}{r} (r D_{rz} \psi_z)_r + \frac{1}{r} (r D_{rz} \psi_r)_z =$$

$$\psi_t + (f(r, z) - \frac{u}{2r}) \psi \quad , \quad (3.32)$$

where,

$$f(r, z) = \frac{u^2 D_{zz} + v^2 D_{rr} - 2D_{rz} u v}{4 (D_{rr} D_{zz} - D_{rz}^2)}$$

The variational functional for this equation, Hildebrand (1965) reduced to the local coordinate system, with reference to the centroid of the  $m^{\text{th}}$  element as the origin, as shown in Appendix E is:

$$J = \iint_{R^m} \left[ \frac{D_{rr}}{2} (\psi_\xi)^2 + D_{rz} \psi_\xi \psi_\eta + \frac{D_{zz}}{2} (\psi_\eta)^2 + \psi \left( \frac{u}{2} \psi_\xi + \frac{v}{2} \psi_\eta \right) \right. \\ \left. + \frac{\psi^2}{2} f(r, z) + \psi \cdot \psi_t \right] (\xi + \bar{r}^m) d\xi d\eta + \int_{S_2^m} r_w q \left( \frac{1}{\phi} - 1 \right) \frac{\psi^2}{2} dS \quad , \quad (3.33)$$

where  $S_2^m$  refers to the portion of the well-boundary, if any, common with the boundary of the  $m^{\text{th}}$  element.

The boundary conditions in terms of the new variable  $\psi$  are,

- (i)  $\left. \begin{aligned} D_{rr} \psi_r + D_{rz} \psi_z + \frac{u\psi}{2} &= 0 \\ D_{rz} \psi_r + D_{zz} \psi_z + \frac{v\psi}{2} &= 0 \end{aligned} \right\}$  along natural boundaries,
- (ii)  $\delta\psi = 0$  along geometric boundaries
- (iii)  $D_{rr} \psi_r + D_{rz} \psi_z + \frac{u\psi}{2} - q \left( \frac{1}{\phi} - 1 \right) \psi = 0$  along the well face.

It may be shown by equating the first variation of  $J$  to zero and by substituting the above boundary conditions in the resulting equation, that equation 3.6 in its transformed form as equation 3.32 is the Euler's equation for the above variational functional. Adopting the



same shape function for  $\psi$ , as was assumed for  $C$  in the Galerkin approach, so that,

$$\psi = [A] \{\psi\}^m \quad (3.34)$$

and computing the contribution of the  $m^{\text{th}}$  element to the differentials  $J_{\psi_p}^m$  ( $p=i,j,k$ ), the following equations are obtained,

$$\begin{aligned} J_{\psi_p}^m = & \iint_{R^m} [ D_{rr} \psi_{\xi} (\psi_{\xi})_{\psi_p} + D_{rz} \{ \psi_{\xi} (\psi_{\eta})_{\psi_p} + \psi_{\eta} (\psi_{\xi})_{\psi_p} \} \\ & + D_{zz} \psi_{\eta} (\psi_{\eta})_{\psi_p} + \psi \{ \frac{u}{2} (\psi_{\xi})_{\psi_p} + \frac{v}{2} (\psi_{\eta})_{\psi_p} \} \\ & + (\psi)_{\psi_p} \{ \frac{u}{2} \psi_{\xi} + \frac{v}{2} \psi_{\eta} \} + \psi \frac{\rho - \alpha C}{\rho} \cdot \frac{u^2 + v^2}{4(D_L + D_d T)} \cdot (\psi)_{\psi_p} \\ & + \psi_t (\psi)_{\psi_p} ] (\xi + \bar{r}^m) d\xi d\eta + \int_{S_2^m} r_w q \left( \frac{1}{\phi} - 1 \right) \psi (\psi)_{\psi_p} d\eta = 0 \end{aligned}$$

where the subscript  $\psi_p$  denotes a derivative with respect to  $\psi_p$ . (3.35)

This system, even if the transformation in terms of  $\psi$  was not affected, would not be identical to that obtained by the Galerkin method in equation 3.27. Evaluating the differentials and integrals occurring in equation 3.35 will also result in a system of equations of the form,

$$[SL] \{\psi\}^m + [PL] \{\psi_t\}^m + \{Q\}^m = 0 \quad (3.36)$$

The [SL] and [PL] matrices in this case, though more complicated than those obtained by the Galerkin method, happen to be symmetric (Appendix E). Following the usual assembly procedure, applicable to the finite-element formulation, the following system of simultaneous equations is obtained,

$$[SK] \{\psi\} + [PK] \{\psi_t\} + [QK] = 0 \quad (3.37)$$

This system is mathematically similar to that obtained in equation 3.29 except for the numerical values of the matrices [SK] and [PK]

and has the additional qualification that the matrices [SK] and [PK] are symmetric. However, the appearance of the variable  $\psi$  in place of  $C$ , makes it radically different as far as the difficulties in the numerical solution are concerned. The variable  $\psi$  involves the exponential of  $\beta$  and thus can not be evaluated by a CDC 6400 computer if the values of  $\beta$  exceed 1483.34 .

As discussed in Chapter IV, this limitation imposes a serious restriction on the practical application of the Rayleigh-Ritz formulation for the solution of the convective-dispersion equation and nullifies the computational advantage that it could have by way of generating symmetric matrices. Therefore, in this investigation the Galerkin method is used.

### 3.9 Time Domain Formulation of the Convective-Dispersion Equation.

As discussed in Section 3.6, the Galerkin approach may be adopted for the time domain solution of equation 3.29 in preference to the Runge-Kutta and Adams-Moulton schemes. Thus, as before, the equation for the weighted residual becomes,

$$\int_0^{\Delta t} N_1 [ [PK] \{C_t\} + [SK] \{C\} + [QK] - [R] ] dt = 0 \quad (3.38)$$

where,

$$\{C\} = [N] \begin{Bmatrix} \{C\}_0 \\ \{C\}_1 \end{Bmatrix}$$

and

$$[N] = [ N_0 \quad N_1 ] = [ 1 - \frac{t}{\Delta t} \quad \frac{t}{\Delta t} ] .$$

Evaluating the integrals in 3.38 and collecting terms in  $\{C\}_0$  and  $\{C\}_1$  separately, gives,

$$\left[ \frac{1}{\Delta t} \cdot [PK] + \frac{2}{3} \cdot [SK] \right] \{C\}_1 = - [QK] + [R] + \left[ \frac{1}{\Delta t} \cdot [PK] - \frac{1}{3} \cdot [SK] \right] \{C\}_0 \quad (3.39)$$

which is the required recurrence relation to get the values  $\{C\}_1$  at time step  $\Delta t$  from known values  $\{C\}_0$  at time step 0 in the convective-dispersion equation. An alternative relation obtained by the subdomain method is given in Appendix D.

### 3.10 Treatment of the Boundary and Initial Conditions for the Convective-Dispersion Equation.

Initial values of  $C$  for all the nodal points are specified as initial conditions, say  $C_i(r,z)$  etc.. As explained in Appendix D, the boundary conditions on the well-face are accounted for in the finite-element formulation through the matrix  $[QK]$  of equation 3.39. The unknown  $[R]$  contributes nothing for such boundaries and so the R.H.S. of equation 3.39 is fully known. Natural or reflective boundary conditions, specifying  $C_n=0$  on impervious boundaries are included in the formulation by setting the R.H.S. terms of equation 3.24 equal to zero. Obviously, both  $[QK]$  and  $[R]$  will contribute nothing to nodal points on such boundaries. This type of boundary condition applies to the top impermeable layer overlying the confined aquifer and to the vertical stream-line running from the center of the well-bottom down to the lower boundary of the aquifer, across which there is no flow. In this investigation where the well radius  $r_w$  is small compared to the element sizes and where the bottom of the well is treated as impermeable, this boundary is approximated to coincide with the vertical running at distance

$r_w$  from the well-center and extending from the well-bottom down to the lower boundary of the aquifer.

Along a section of the aquifer, beyond the radius of influence  $r_o$  of the well and at a large depth below the bottom of the well,  $C$  remains invariant with time and so may be represented by specified values  $C_1(r,z)$ ,  $C_2(r,z)$ , ...,  $C_n(r,z)$  etc.,. As explained in section 3.7, such boundary conditions, referred to as geometric boundary conditions, may be accounted for by multiplying the coefficients, say,  $PK(j,j)$  of the known values  $C(j)$  for the  $j^{\text{th}}$  node in equation 3.39, by an arbitrarily large number, say,  $10^{50}$  and replacing the original R.H.S. by the value  $C(j) * PK(j,j) * 10^{50}$ . This device makes it unnecessary to compute the value of the R.H.S. expression of equation (3.39) which includes the undetermined term  $[R]$  for such boundary conditions and at the same time ensures that the value  $C(j)$  is maintained on the  $j^{\text{th}}$  node through successive time steps.

### 3.11 The Implicit Leap-Frog Technique.

As discussed in the previous sections, given appropriate boundary and initial conditions, the R.H.S. of equation 3.22 is known at time level  $t_0$ , in terms of  $\{H\}_0$ ,  $\{C\}_0$ ,  $\{\phi\}_0$  and  $\{\rho\}_0$ , etc.. To start with  $\{C_t\}$  may either be specified or taken as zero. The corresponding values at time level  $t_0 + \Delta t$ , are then obtained by solving the system of equations 3.22 by the Gauss-elimination scheme for banded symmetric matrices. This gives the values of  $\{H\}_1$  for all the nodes at the next time-step. From these, values of the new pressures  $\{P\}_1$  and hence of the new densities  $\{\rho\}_1$  and aquifer porosity  $\{\phi\}_1$  are computed for all the nodes. Values of elemental velocities  $u$  and  $v$  at the new time-step are then computed from these known nodal point values  $\{H\}_1$ ,

by applying Darcy's law as follows,

$$u = - \frac{k}{\mu} \cdot H_{\xi}$$

$$v = - \frac{k}{\mu} \cdot H_{\eta}$$

where,

$$H = [A] \{H\}_1 \quad .$$

Therefore,

$$u = - \frac{k}{2\mu A^m} [ a_{2i} \quad a_{2j} \quad a_{2k} ] \{H\}_1$$

and

$$v = - \frac{k}{2\mu A^m} [ a_{3i} \quad a_{3j} \quad a_{3k} ] \{H\}_1$$

where the symbols  $A^m$ ,  $a_{2i}$  and  $a_{3i}$ , etc. are defined in Appendix C,  $u$ ,  $v$ ,  $k$  and  $\mu$  refer to the elemental values and  $\{H\}_1$  refer to the already computed nodal point values.

With these values of  $\{u\}_1$ ,  $\{v\}_1$  for all the elements and  $\{\rho\}_1$  and initially prescribed values of  $\{C\}_0$  for all the nodes, the system of equation 3.39 is solved by Gauss-elimination for banded matrices to obtain the values  $\{C\}_1$  at the next time-step. With these values of  $\{C\}_1$ , the density matrix  $\{\rho\}_1$  is updated again and values of  $\{\rho_t\}$  and  $\{C_t\}$  are computed. The values of  $\{\rho_t\}$  and  $\{C_t\}$  are then used to form a new system of equations, 3.13, which may be solved as before and the above sequence repeated over and over again.

For the purposes of this investigation, however, in order to save computer time without appreciable loss of accuracy, the values of  $\{\rho\}$  are updated only once after new values of  $\{C\}_1$  are obtained from the solution of the system 3.39 and not twice as indicated above. Further, values of  $\{C_t\}$  and  $\{\rho_t\}$  are not used to form new systems of equations 3.13 again and again. The changes in  $\{C\}$  and  $\{\rho\}$  with time being

very small, these simplifications are not expected to introduce appreciable errors. This premise has been corroborated by the results discussed in Section 4.4. For cases where these changes are likely to materially affect the results, the above simplifications may be avoided.

## CHAPTER IV

### DISCUSSION AND APPLICATION OF THE NUMERICAL SIMULATOR

#### 4.1 Description.

The numerical simulator developed in this study is comprised of three computer programs; MESH, FLOW and DISPER. Program MESH is a modified version of an existing one, Thompson<sup>1</sup> (1972) and programs FLOW and DISPER have been written exclusively for this investigation. A description of each of these programs follows:

(a) Program MESH - A listing of this program is given in Appendix H. It incorporates a scheme for generating a suitable element layout for the finite-element solution of any problem. For complex flow regions, the elements have to vary in size depending upon their distances from the well. For this purpose, the flow region is divided into different loops depending upon the nature of the problem, as illustrated in Fig. 4.1. With the input data explained in Appendix G, this program subdivides each loop into a number of quadrilaterals and joins the shorter diagonal of each, as illustrated by representative dashed lines in figure 4.1, to generate a triangular mesh, with specific numbers assigned to all the nodes and elements.

For situations, like the one described in Section 4.3, an alternative element layout with diagonals of the quadrilaterals reversed is also required. To take care of such cases, program MESH has been equipped with an algorithm to produce both the element layouts.

---

<sup>1</sup>With the cooperation of Dr. E. G. Thompson, Civil Engineering Department, Colorado State University, Fort Collins.



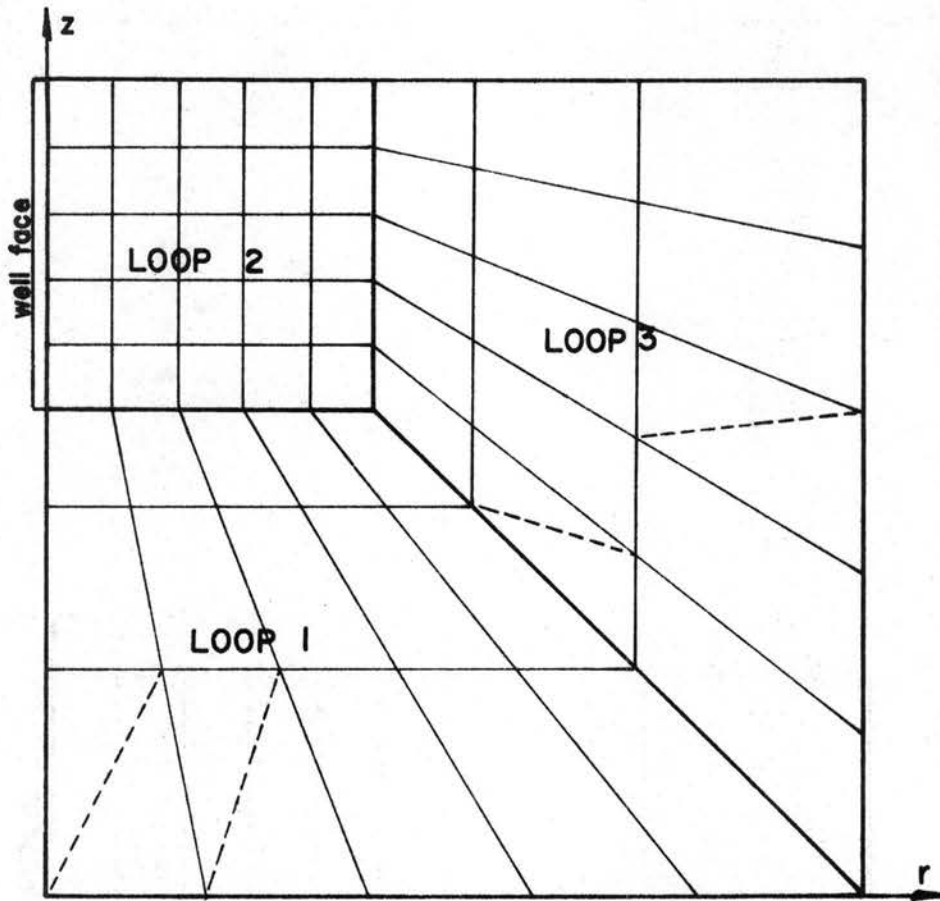


Fig. 4.1 Typical Loop Subdivision

For flow regions with more than two loops, program MESH gives an element layout which has a very large band-width. In order to reduce the band-width, two subroutines, viz. subroutine SETUP and subroutine OPTNUM (Collins, 1973) have been introduced into this version of program MESH. Subroutine SETUP arranges the data generated by repetitive application of the algorithm MESH in the following form:

N	JMEM(N)	MEMJT(N)
Original Node Number	Total number of nodes in the layout to which the Nth node is connected.	Assigned numbers of individual nodes to which the Nth node is connected.

With this information as input, subroutine OPTNUM treats each node as the origin of the new numbering scheme, in turn, so that the number of different renumbering schemes attempted is equal to the total number of nodes in the layout. At each trial, it checks the band-width obtained and finally yields a new numbering scheme that gives the smallest band-width with the initial and modified node numbers identified as follows:

N	JNT(N)
Old Node Number	New Node Number

This information along with the coordinates of each node and the new numbers assigned to the three nodes of each individual element is obtained as a deck of punched cards. This program turns out a microfilm plot of the element layout also.

For simpler flow regions, where the element sizes are not to be varied in both the  $r$  and  $z$  directions, a simpler version of this program is used, which treats the entire flow domain as one loop and

bypasses the optimization subroutines. Once the orientation of the boundaries is so arranged that node numbering starts in sequence along the side with smaller number of nodes or divisions, this version produces an element layout with a reasonably small band-width.

Program MESH gives the output in  $x$  and  $y$  coordinates which are read as  $r$  and  $z$  in programs FLOW and DISPER.

(b) PROGRAM FLOW - As explained in Chapter III, both the Rayleigh-Ritz and Galerkin formulations yield identical matrices for the flow equation. Because these matrices are banded and symmetric, only the upper diagonal elements within the band-width have to be stored, thus reducing the computer storage considerably. Program FLOW solves the flow equation and consists of various subroutines to perform the operations developed in Appendix C. A flow chart describing the various steps involved in this program is given in Appendix F. The subroutines CENTOD, CLOCAL and AREA evaluate respectively the global coordinates of the centroid, local coordinates of the nodal points and the area of each triangular element. Subroutine TEGRAL computes the various volume integrals (reduced to surface integrals due to radial symmetry) involved in the finite-element formulation discussed in Chapter III, using three integration points with Gauss-Radau coefficients for Gauss-quadrature. Subroutine RHOSEL evaluates the average values of the mass-density of the fluid and salt concentration applicable to an element, from given nodal point values. Subroutine FSLPL generates the elemental  $3 \times 3$  symmetric matrices [FSL] and [FPLE] in terms of the contributions received by each nodal point from the minimization process of the variational functional for the Rayleigh-Ritz formulation and from the weighted-residual process for the Galerkin formulation.

Subroutine FSLSK combines the 3x3 elemental matrices [FSL] and [FPLE] to form the large (NUMNP X IBAND) symmetric matrices [SK] and [PK] and the column vector [QK] representing the contribution of the well, in such a way that all the elemental contributions to any node common to two or more elements are added up and the diagonal elements (i,i) of the original (NUMNP X NUMNP) matrices are stored as the first elements (i,1) of each row in the rearranged (NUMNP X IBAND) matrices. The symbol NUMNP used herein signifies the total number of nodal points and IBAND stands for the band-width for symmetric matrices as defined in Chapter III. Subroutine FSKPSI multiplies the rearranged matrix SK(NUMNP, IBAND) with a column vector PSI(NUMNP). Subroutine GAUSS solves the above system of NUMNP simultaneous equations by Gauss-elimination in such a way that only the upper diagonal elements are used in the process. This yields values of H for all the nodes at the new time level, from where nodal point pressures are readily obtained and elemental velocities u and v are computed by applying Darcy's law as explained in Chapter III.

(c) PROGRAM DISPER - Unlike the flow equation, the convective-dispersion equation, as such, is not in a self-adjoint form, mainly because of the presence of first derivative and mixed partial terms. Therefore, the Rayleigh-Ritz and Galerkin formulations do not yield identical system of matrices. Whereas the former yields symmetric matrices, the latter leads to a system of unsymmetric matrices. For reasons discussed later, the Galerkin formulation has been adopted for this study, although programs were written and run for both. The program DISPER seeks to solve the convective-dispersion equation by the Galerkin-weighted-residual technique. A flow chart for this program is

given in Appendix F. This program consists of various subroutines accomplishing the operations described in Appendix D. Subroutines CENTOD, CLOCAL, AREA and TEGRAL are exactly the same as for FLOW. Subroutine ELVEL computes the average elemental velocities from known values of nodal point pressures. Subroutine SLPL generates the 3x3 nonsymmetric elemental matrices [SL] and [PL] pertaining to each element.

Subroutine SLSK combines the matrices [SL] and [PL] to form the large (NUMNP X IBAND) unsymmetric matrices [SK] and [PK] and the column vector [QK] having NUMNP elements to account for the contribution of the well. The symbol IBAND here refers to the band-width for unsymmetric matrices as defined in Chapter III. The elements of matrices [SK] and [PK] are so arranged that element (i,j) of the original (NUMNP X NUMNP) banded unsymmetric matrices becomes element [ i, (j-1 + (IBAND + 1)/2) ] of the contracted (NUMNP X IBAND) matrices. Subroutine SKPSI is a modified version of its counterpart in program FLOW, and multiplies the (NUMNP X IBAND) matrix [SK] with a column vector PSI(NUMNP). Subroutine BSOLVE solves this system of NUMNP simultaneous equations by Gauss-elimination with row interchanges. This yields nodal point values for the concentration at the new time step.

#### 4.2 Leap-Frog Technique and Program FFLOW.

As indicated in Chapter III, the two programs, FLOW and DISPER, work in tandem in the leap-frog technique and so have been merged together into a composite program, FFLOW. A flow chart for the leap-frog technique is given in Appendix F. With given initial values of  $\rho$ ,  $\phi$  and  $P$  for each nodal point, next time values of  $P$  are computed in program FLOW (incorporated within FFLOW). Knowing new time  $P$  values, the elemental velocities  $u$  and  $v$  are computed. With these values of  $u$  and  $v$

and given initial values of nodal point concentrations, next time values of the latter are computed in program DISPER (incorporated within FFLOW). At this stage, with the current values of nodal point  $P$  and  $C$ , values of nodal point density and porosity are updated. With these new values of  $\rho$ ,  $\phi$  and  $P$  as input, program FLOW operates again to yield the next time values of  $P$  and thus the process of iteration is continued until the required time period is completed. A listing of the combined program FFLOW is attached in Appendix H.

#### 4.3 Tests for the Performance of the Numerical Simulator.

In the absence of pertinent experimental or field data, the results of the combined program FFLOW can not be verified. However, programs FLOW and DISPER have been tested separately by comparison with known exact and approximate solutions for simplified radial flow cases. A description of these tests is given below.

(a) Program FLOW - In order to test the validity and accuracy of the finite element formulation for the flow equation, the well known case of unsteady radial flow towards a well in a confined aquifer was run as a test with the following data:

Radius of well -  $r_w = 0.5$  ft.

Well discharge -  $Q = 1.0$  ft<sup>3</sup>/sec.

Depth of well penetration = PENETR = 100 ft.

Aquifer thickness =  $B = 100$  ft.

Assumed radius of influence =  $r_e = 950.5$  ft..

The very nature of the finite-element formulation, specially for cases where the aquifer depth is divided into very few divisions, tends to yield unequal values of  $H$  for various nodal points along the same vertical in the vicinity of the well, even for cases of pure radial



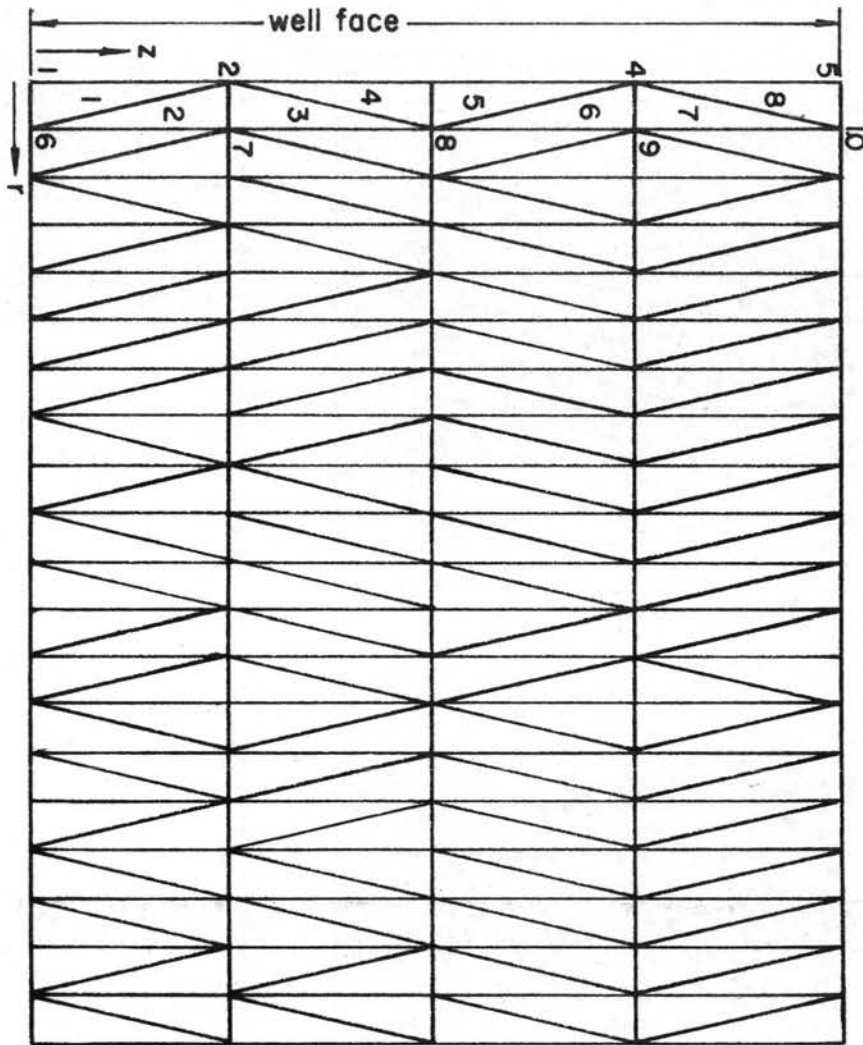


Fig. 4.2a Typical Element-Layout

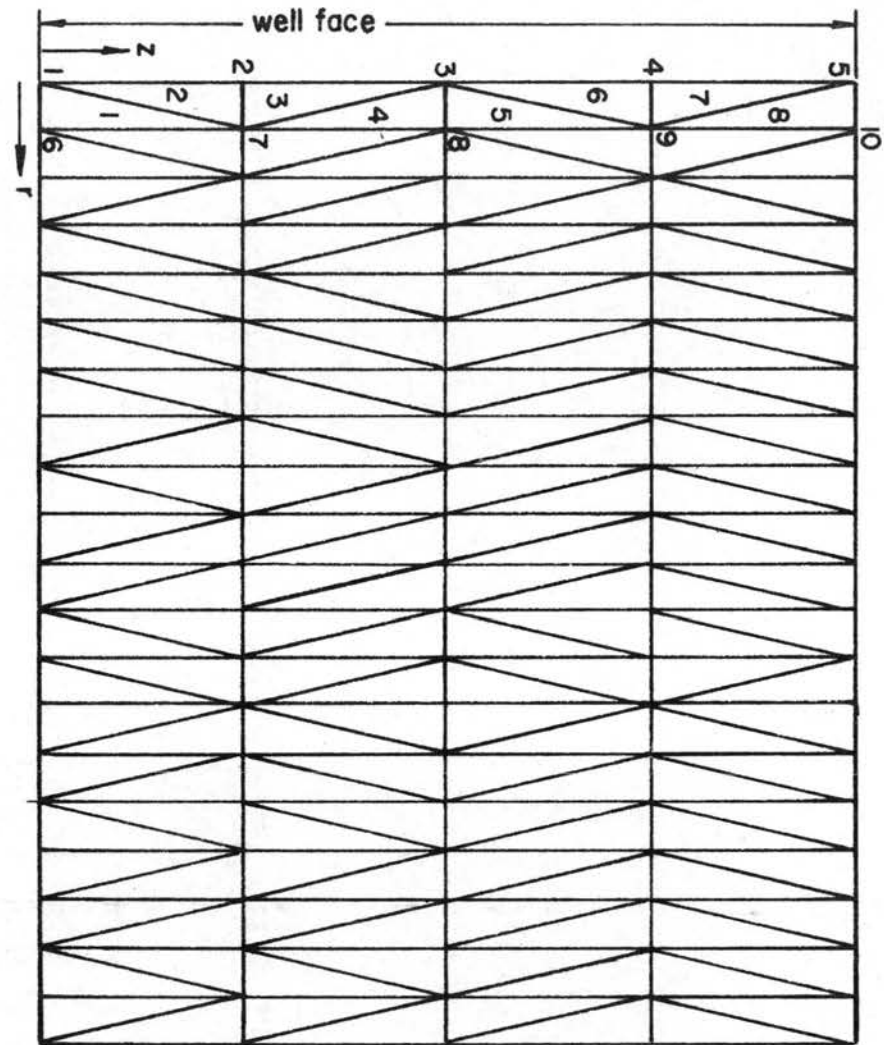


Fig. 4.2b Alternative Element Layout with Diagonals Reversed



flow. This occurs because of different weightages assumed by different nodes in a triangular layout due to their geometric placement. To resolve this, the [SK] and [PK] matrices are formed twice for each iteration, once for the original element layout as given by the program MESH and next for the alternative layout with the diagonals of quadrilaterals forming individual elements, reversed as shown in Figs. 4.2a and 4.2b. The averages of these two sets of [SK] and [PK] matrices are then taken as the final [SK] and [PK] matrices. This results in the allocation of equal weightage to all the nodal points on a vertical and thus yields equal values of H for such nodal points for purely radial flow.

The element layout was obtained from program MESH with the following data:

XMIN = 0.0 ft. (Minimum value of the x-coordinate).  
 XMAX = 100 ft. (Maximum value of the x-coordinate).  
 YMIN = 0.5 ft. (Minimum value of the y-coordinate).  
 YMAX = 950.5 ft. (Maximum value of the y-coordinate).  
 NDIVX = 2 (Number of divisions along the x-axis).  
 NDIVY = 95 (Number of divisions along the y-axis).

The output of the MESH program gave,

NUMNP = 288 (Number of nodal points).  
 NUMEL = 380 (Number of elements).  
 IBAND = 5 (Band-width for symmetric matrices).

Analytical solution for this case is available as follows, Walton (1970):

$$s = \frac{Q}{4\pi T} W(u) \quad (4.1)$$

where,

$s$  = drawn down in feet at time  $t$  and distance  $r$  from well center.

$T = kB$  = Aquifer transmissibility in  $\text{ft}^2/\text{sec}$ .

$k$  = Hydraulic conductivity in  $\text{ft}/\text{sec}$ .

$$u = \frac{Sr^2}{4Tt}$$

$S$  = Storage coefficient of the aquifer =  $\gamma B(\phi\beta + C_F)$ .

$\gamma$  = Unit weight of the fluid in  $\text{lbs}/\text{ft}^3$ .

$B$  = Aquifer thickness in feet.

$t$  = Time at which drawdown  $s$  occurs at distance  $r$  from the well center.

$$W(u) = \int_u^{\infty} \frac{e^{-u}}{u} du = \text{Well function.}$$

$\phi$  = Porosity, taken as 0.5 for this test.

$\beta$  = Fluid compressibility in  $\text{sq. ft.}/\text{lb}$ .

$C_F$  = Aquifer compressibility in  $\text{sq. ft.}/\text{lb}$ .

The results of the numerical and analytical solutions are shown in Fig. 4.3. It is seen that the results are in excellent agreement. The minor differences of about 4 to 10% in the drawdown at the well face may be attributed to two factors, viz. larger size of elements and smaller radius of influence used. The analytical solution assumes an infinite radius of influence against 950.5 ft. used in the numerical solution. Also accuracy demands that smaller size elements should be used in the vicinity of the well, whereas equal size elements have been used in the mesh layout for the above numerical solution. With smaller size of elements provided near the well and with larger radius of influence, the solution will become more and more accurate even at the well face.

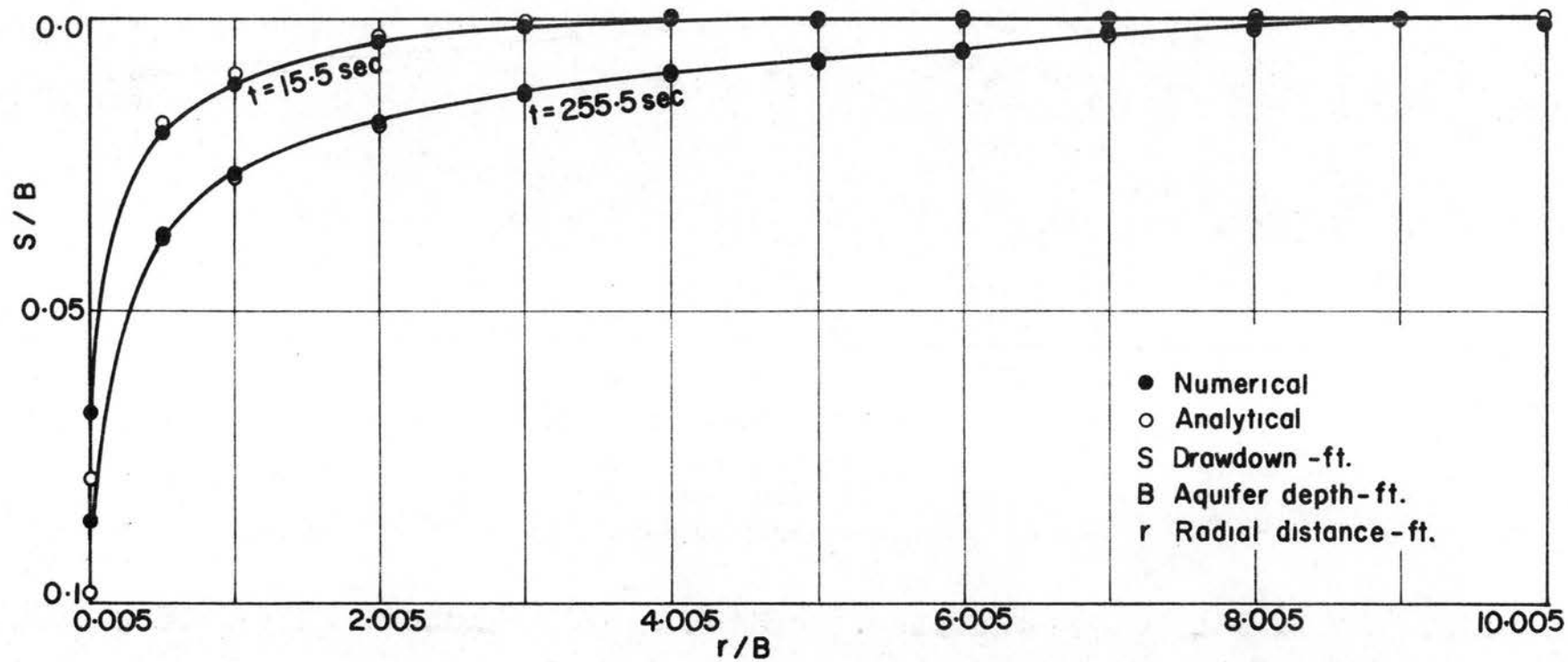


Fig. 4.3 Analytical and Numerical Solutions of Flow Equation

Since program DISPER constitutes different subroutines for matrix multiplication and Gauss-elimination, it was run on the same set of data as was used for program FLOW with a view to verify the validity of the formulation for unsymmetric matrices involved in program DISPER. The input data was modified so that the dispersion equation becomes identical to the flow equation, treating concentration  $C$  as synonymous with the variable  $H$ . The two runs of program FLOW and program DISPER on identical data yielded identical results up to 8 significant figures for all the 8 iterations for which comparison was made, thus establishing the equivalence, accuracy and correctness of the two programs. Representative values for the 7<sup>th</sup> iteration at time 2.5 seconds are reproduced in Table 4.1 for comparison.

TABLE 4.1  
COMPARISON OF PROGRAM FLOW AND DISPER

Radial Distance ft.	Values of H (lbs/ft <sup>2</sup> )	
r	PROGRAM FLOW	PROGRAM DISPER
0.5	7935.96014469	7935.960001
50.5	8075.27685378	8075.276814
100.5	8113.05940422	8113.059394
200.5	8124.93396647	8124.933966
300.5	8124.99956215	8124.999562

(b) PROGRAM DISPER - In order to test the accuracy of the program and formulation for the convective-dispersion equation, program DISPER was run for a dispersion-dominated transport until steady state. The numerical solution was assumed to have reached steady state when the change in concentration at any point between two time steps was less than 0.00001. For such a case, steady state solution may be analytically

obtained. Setting,

$$D_{rz} = D_{zz} = 0 \quad , \quad \text{and} \quad v=0$$

the convective-dispersion equation, 3.6, reduces to,

$$C_r = \frac{D_o}{A} C_{rr} \quad (4.2)$$

where,

$$A = \frac{Q}{2\pi X \text{ PENETR} X \phi}$$

$$D_o = a_I \cdot A$$

and the subscript rr denotes second derivative with respect to r .

For the boundary conditions,

$$C = C_o \quad \text{at} \quad r = r_w \quad \text{and,}$$

$$C = 0 \quad \text{at} \quad r = r_o \quad ,$$

equation 4.2 may be solved to yield,

$$\frac{C}{C_o} = \left[ \exp \left( \frac{Ar}{D_o} \right) - \exp \left( \frac{Ar_o}{D_o} \right) \right] / \left[ \exp \left( \frac{Ar_w}{D_o} \right) - \exp \left( \frac{Ar_o}{D_o} \right) \right] \quad (4.3)$$

Results of the analytical solution of equation 4.3 have been compared with the numerical solution run until steady state, in Fig. 4.4. For this case, steady state was reached after 830 seconds. The excellent agreement of the two solutions demonstrates the accuracy and convergence of the dispersion part of program DISPER.

To test the validity of the formulation for the convective-dispersion equation for a situation where the contributions of both dispersion and convection are equally dominant, program DISPER was run for the case of purely radial flow in a confined isotropic aquifer, for which an approximate analytical solution is available, Hoopes and Harleman (1965); Shamir and Harleman (1966). For such a case, assuming that

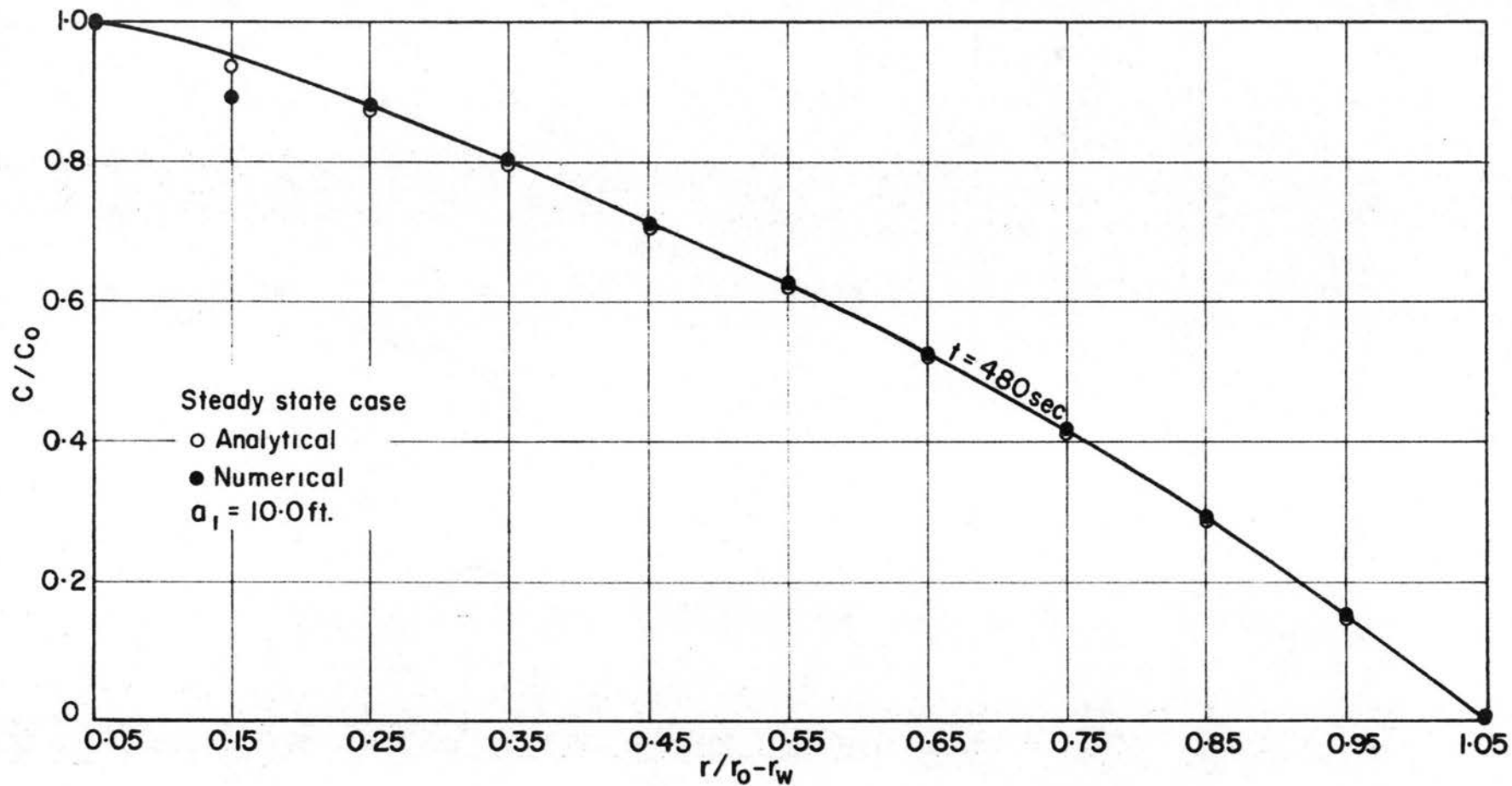


Fig. 4.4 Steady-State Solutions of Convective-Dispersion Equation

$$D_T = 0 \quad , \quad D_d = 0 \quad , \quad v = 0 \quad \text{and} \quad \rho = \text{constant},$$

the convective dispersion equation (3.6) reduces to the following form,

$$(D_L C_r)_r + \left( \frac{D_L}{r} - u \right) C_r = C_t \quad . \quad (4.4)$$

Recognizing that,

$$\begin{aligned} D_L = a_I u &= a_I \cdot \frac{Q}{2\pi x \text{PENETR} x \phi x r} \\ &= a_I \frac{A}{r} = \frac{D_o}{r} \quad , \end{aligned} \quad (4.5)$$

equation 4.4 may be written as,

$$C_t + \frac{A}{r} C_r = \frac{D_o}{r} C_{rr} \quad . \quad (4.6)$$

An approximate analytical solution to equation 4.6 has been given by Raimondi et al. (1959) for the case when a tracer is injected at  $r=0$  for a finite time period. The same has been modified by Hoopes and Harleman (1965) for the case of continuous injection of a tracer of constant concentration,  $C_o$  at  $r=0$ . Their solution is as follows:

$$\frac{C}{C_o} = \frac{1}{2} \operatorname{erfc} \left[ \frac{r^2/2 - At}{\sqrt{\frac{4}{3} a_I r^3}} \right] \quad . \quad (4.7)$$

It may be seen that this solution satisfies the two boundary conditions,

$$C (r=0, t>0) = C_o \quad \text{and}$$

$$C (r=\infty, t>0) = 0 \quad ;$$

but does not satisfy the initial condition,

$$C (r, t=0) = 0 \quad .$$



In obtaining this solution, it has been assumed that,

$$C_t = 0 \quad \text{at} \quad t = 0 \quad ,$$

which is not true in the immediate vicinity of the source. Thus the approximate solution of equation 4.7 holds only for points away from the source.

The element layout for this case was also obtained from program MESH, with the following input data:

$$\begin{aligned} XMIN &= 0.0 \text{ ft.} & , & & XMAX &= 1.0 \text{ ft.} & , \\ YMIN &= 0.5 \text{ ft.} & , & & YMAX &= 10.5 \text{ ft.} & , \\ NDIVX &= 4 & , & & NDIVY &= 20 & . \end{aligned}$$

The output of program MESH gave,

$$NUMNP = 105 \quad , \quad NUMEL = 160 \quad , \quad \text{and} \quad IBAND = 7 \quad .$$

Program DISPER was run with,

$$\begin{aligned} a_I &= 1.0 \text{ ft.} \\ Q &= .25 \text{ ft}^3/\text{sec.} \\ \phi &= 0.5 \quad . \end{aligned}$$

Results of the numerical and approximate analytical solutions are presented in Fig. 4.5 for two representative time periods. The agreement between the two solutions is reasonable for points away from the source for which the approximate analytical solution is applicable. Because of the assumption made to arrive at equation 4.7, the solution does not hold for steady state cases also. However, for a steady state case, equation 4.6 reduces to equation 4.2 and so the solution given by equation 4.3 holds. Comparison of this exact solution for steady state with the numerical solution has also been shown in Fig. 4.5. The steady state was reached after 2330 seconds. The two solutions are in excellent agreement.

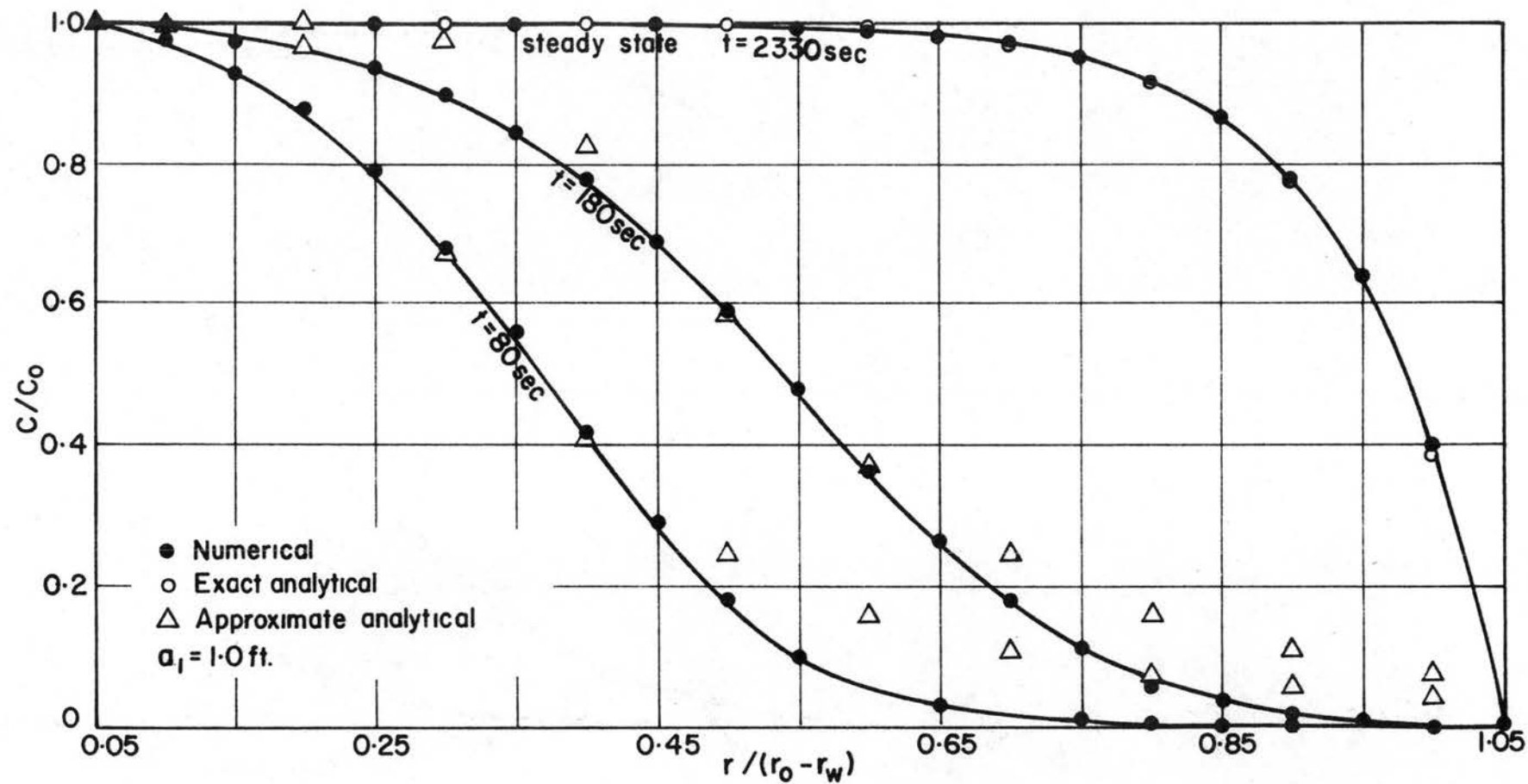


Fig. 4.5 Analytical and Numerical Solutions of Convective-Dispersion Equation,  $a_1 = 1.0$  foot

Program DISPER was run for a convection dominant transport also, using the same data as was used for the previous two runs except for the value of  $a_I$  which was taken as 0.1 ft. for this case. Results of the numerical and analytical solutions are depicted in Fig. 4.6 both for the transient and steady-state cases. The agreement between the two solutions is reasonable.

It is noted that the agreement improves as the distance from the source increases. This is due to the fact that the approximate solution holds only for points away from the source. In this case, steady-state reached after 730 seconds, whereafter no marked change was observed in the concentration distribution. As for the previous case, the numerical solution for steady-state has been compared with the exact solution and not with the approximate solution, which holds only in the transient state.

A comparative picture of the three types of transports with different geometric dispersivities, discussed above, has been presented in Fig. 4.7, where the propagation of concentration with time has been plotted for all the three cases for one and the same point in the flow-domain. Both the numerical and approximate analytical values have been indicated on the three plots.

For all the three cases, the numerical solution is in reasonable agreement with the approximate solution in the transient zone and with the exact solution after steady-state is reached. These plots corroborate the well known effect of dispersion to flatten out the break-through curve. The effect gets more and more pronounced with increasing values of the geometric dispersivity of the soil.

The various tests discussed in this section prove the validity and accuracy of the numerical finite-element models developed in this study.

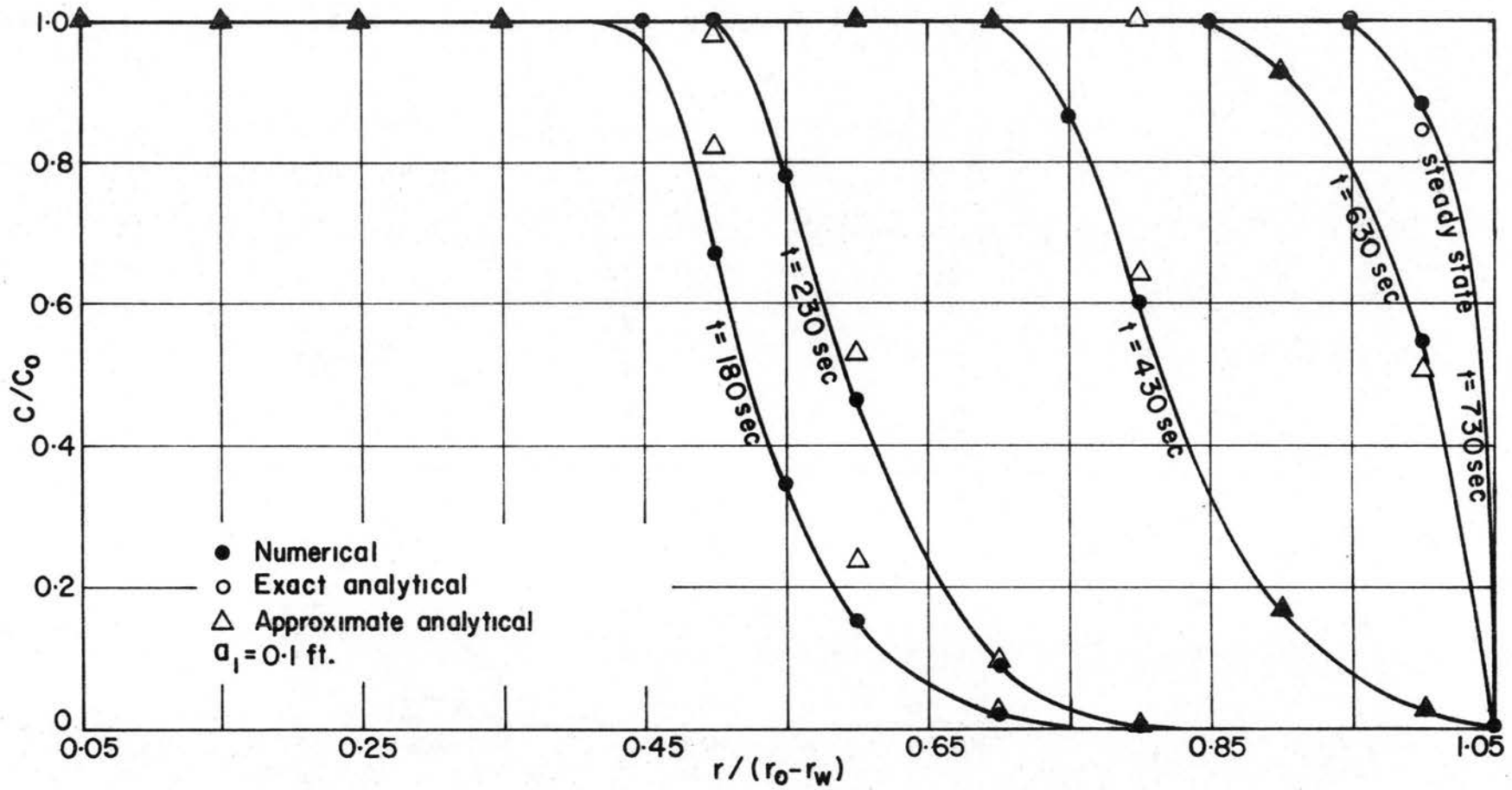


Fig. 4.6 Analytical and Numerical Solutions of Convective-Dispersion Equation,  $a_I = 0.1$  foot

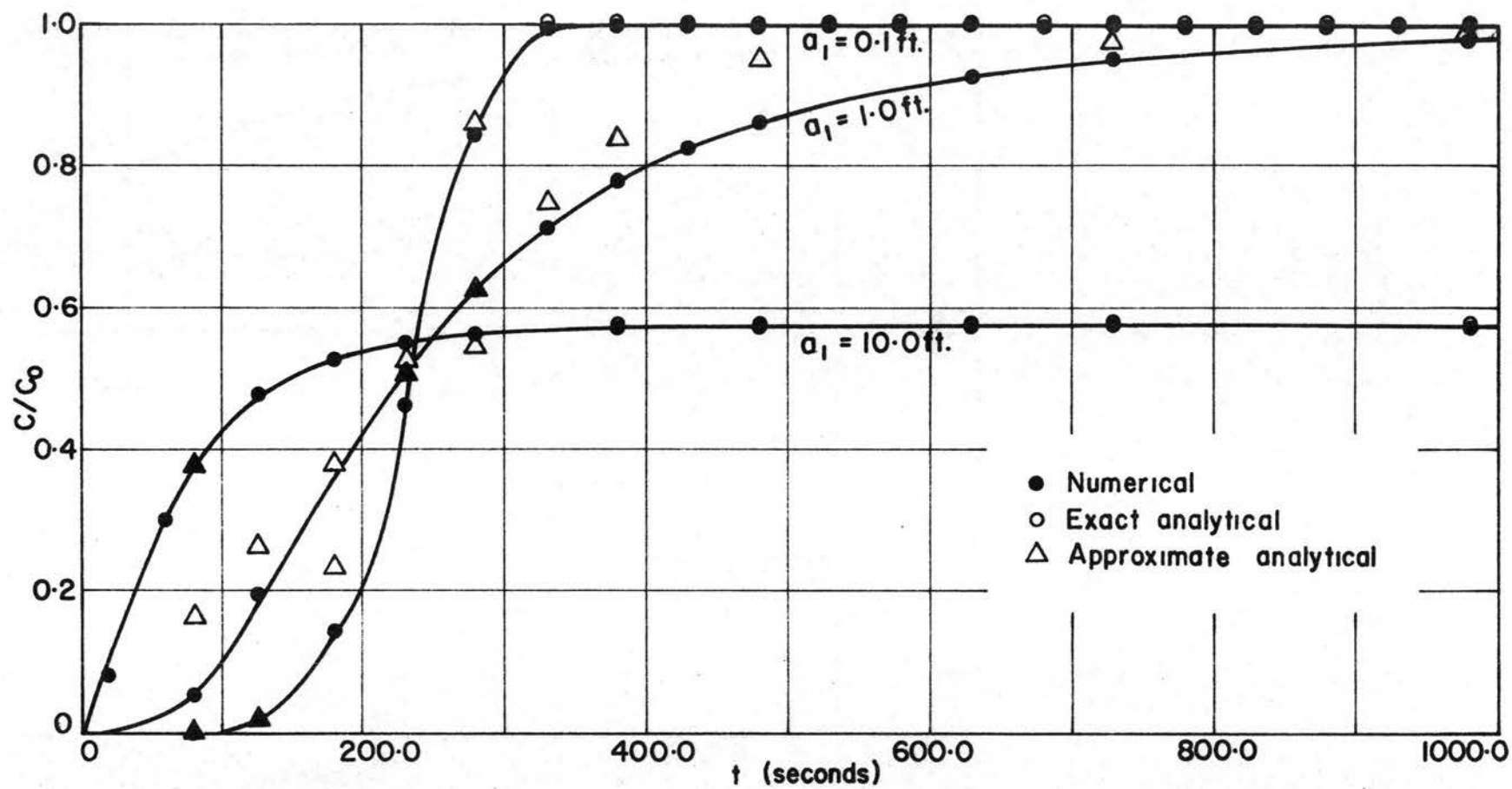


Fig. 4.7 Propagation of Concentration with Different Geometric Dispersivities

#### 4.4 Application of the Simulator to Field Problems.

In order to demonstrate the capability of the simulator to solve field problems, two hypothetical cases were run, one for a confined aquifer having a salt-water reservoir as its outer boundary and being pumped by a fully penetrating well, and the other for a very deep aquifer containing fresh water underlain by very deep belts of salt-water and being pumped by a partially penetrating well. Element layouts for both these cases were generated by using program MESH. The data used for these cases are tabulated on the following page.

The values 780.5 and 510.5 feet used for the radius of influence of the well in these cases are smaller than those expected for a field situation. This was done to save computer time and storage. Taking advantage of the dynamics of the problem, the convective-dispersion equation was solved only once with time step  $\Delta t$  for every ten solutions of the flow equation with time step  $\Delta t/10$ . Even with these expedients, the concentration propagated only 160 feet over a period of  $2.29 \times 10^8$  seconds (7.26 years) for the fully penetrating well case. This took 300 iterations and 2000 seconds of C. P. time on the CSU CDC 6400 computer. The compilation time was only 14.685 seconds. For these iterations, the time step was successively increased from 0.1 second at the first iteration to 1,000,000 seconds at the 80<sup>th</sup> iteration, whereafter, it was maintained at this value through the 300<sup>th</sup> iteration.

For the partially penetrating well case, it took  $2.2 \times 10^7$  seconds (255 days) for the concentration to propagate 90 feet involving 320 iterations and 3600 seconds of C. P. time. The compilation time was only 14.714 seconds. As in the previous case, the time step was successively increased from 0.1 second at the first iteration to 100,000

TABLE 4.2. DATA FOR HYPOTHETICAL PROBLEMS

DATA	Fully penetrating well with a salt water reservoir as the outer boundary.	Partially penetrating well with a salt water reservoir as the lower boundary.
(a) FOR PROGRAM MESH:		
XMIN	0.5 ft.	0.5 ft.
XMAX	780.5 ft.	510.5 ft.
YMIN	0.0 ft.	0.0 ft.
YMAX	100.0 ft.	300.0 ft.
(b) FOR PROGRAM FFLOW:		
NUMNP	200	198
NUMEL	312	340
Q	2.0 ft <sup>3</sup> /sec.	4.0 ft <sup>3</sup> /sec.
r <sub>w</sub>	0.5 ft.	0.5 ft.
PENETR	100.0 ft.	120.0 ft.
φ <sub>o</sub>	0.5	0.5
α	0.74	0.74
β	2.3x10 <sup>-8</sup> ft <sup>2</sup> /lb.	2.3x10 <sup>-8</sup> ft <sup>2</sup> /lb.
C <sub>F</sub>	0.6x10 <sup>-8</sup> ft <sup>2</sup> /lb.	0.6x10 <sup>-8</sup> ft <sup>2</sup> /lb.
μ	2.4x10 <sup>-5</sup> lb.sec./ft <sup>2</sup>	2.4x10 <sup>-5</sup> lb.sec./ft <sup>2</sup>
ρ	2.0 slugs/ft <sup>3</sup>	2.0 slugs/ft <sup>3</sup>
a <sub>I</sub>	0.1 ft.	1.0 ft.
a <sub>II</sub>	0.0 ft.	0.1 ft.
D <sub>d</sub>	0.0 ft <sup>2</sup> /sec.	0.0001 ft <sup>2</sup> /sec.
H	8125.0 ft.lbs.; r>780.5,t>0 8125.0 ft.lbs.; r<780.5,t=0	54,000.0 ft.lbs.; r>510.5,t>0 54,000.0 ft.lbs.; z<0,t>0 54,000.0 ft.lbs.; r<510.5,z>0,t=0
C/C <sub>o</sub>	1.0 ; r>780.5,t>0 0.0 ; r<780.5,t=0	1.0 ; z<0,t>0 0.0 ; z>0,t=0



seconds at the 110<sup>th</sup> iteration, whereafter, it was maintained at that value through the 320<sup>th</sup> iteration.

The propagation of concentration with time at two representative locations in the flow field for both these cases, has been shown in Figs. 4.8 and 4.9. Although these plots lack verification with experimental models or with actual field data, they do demonstrate the capability of the simulator to handle such field problems. The qualitative trends depicted by these runs indicate that for a normal size well, the computer time required for the concentration to appear in the well discharge might be of the order of 10,000 seconds or so and the actual time of travel might be in the range of a few years depending upon the aquifer properties.

In both these cases, the values of  $H$  tend to become almost steady after a certain time level as may be seen from the values tabulated below:

TABLE 4.3. H-VALUES AT THE WELL FACE AFTER PROLONGED PUMPING

Time (seconds)	Full Penetration Case	Time (seconds)	Partial Penetration Case
1.2x10 <sup>8</sup>	7168.4994	7.2x10 <sup>6</sup>	53973.1828
1.3x10 <sup>8</sup>	7168.5129	8.2x10 <sup>6</sup>	53973.1830
1.4x10 <sup>8</sup>	7168.5276	9.2x10 <sup>6</sup>	53973.1833
1.5x10 <sup>8</sup>	7168.5436	10.2x10 <sup>6</sup>	53973.1837

After prolonged pumping beyond the transient state, the only variables that change and affect the values of  $H$  are the fluid density and aquifer elasticity. Stationarity of the  $H$  values in the above table indicates that the effects of variable fluid density and aquifer elasticity on the transport process are very small.

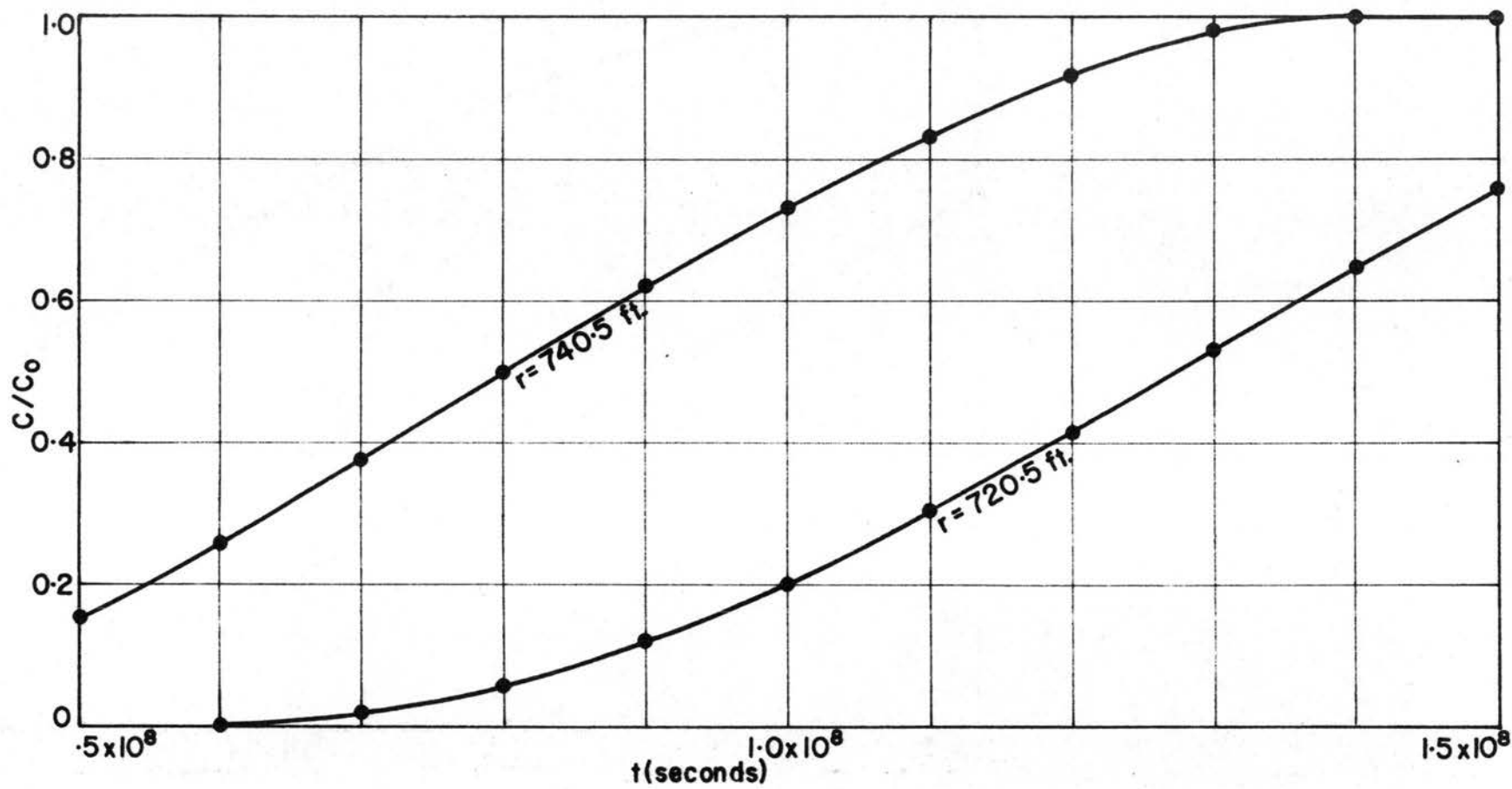


Fig. 4.8 Propagation of Concentration for a Fully Penetrating Well

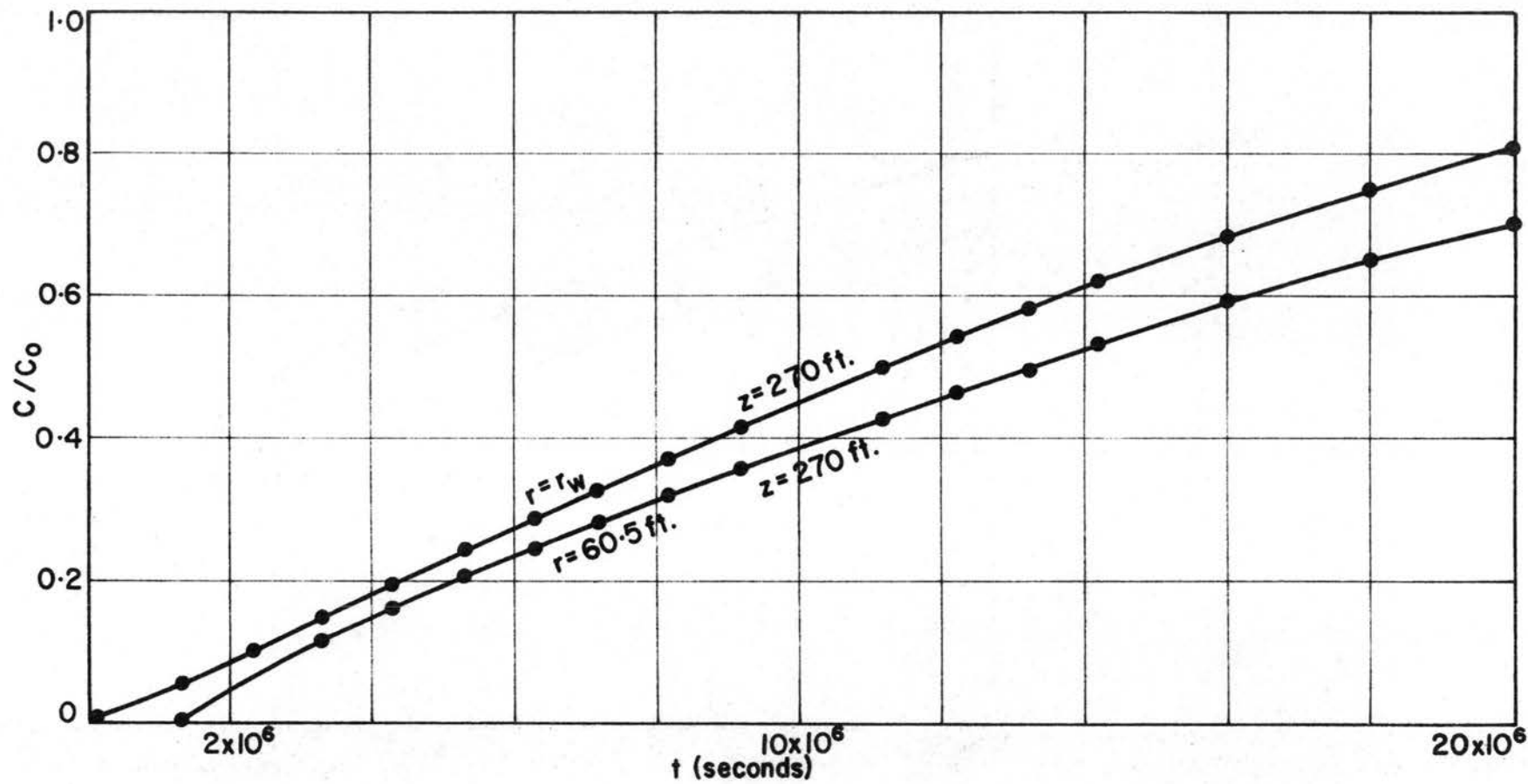


Fig. 4.9 Propagation of Concentration for a Partially Penetrating Well

#### 4.5 Galerkin and Rayleigh-Ritz Simulators.

As already stated the Rayleigh-Ritz formulation has a significant advantage over the Galerkin in so far as it, almost always, yields symmetric matrices. The Galerkin formulation, on the other hand, leads to unsymmetric matrices except for self-adjoint systems. Therefore, this study was initially started with the Rayleigh-Ritz formulation in view, but the exponential transformation function  $\beta$ , so essential for the Rayleigh-Ritz formulation of the convective-dispersion equation, 3.16, which is not in a self-adjoint form (Appendix E), makes it almost impossible to follow the method on a computer. The  $\beta$  transform function and the transformed variable  $\psi$  are defined as (Appendix E),

$$\beta = - \frac{ur + vz}{D_d T + D_L} \cdot \frac{\rho - \alpha C}{\rho}$$

and

$$\psi = C \cdot e^{\beta/2}$$

For large radii of influence or for deep aquifers, the values of  $\beta$  for the exterior nodes or elements may easily exceed the limit of 1483.34 for a CDC 6400 computer and so it may not be possible to evaluate  $\beta$  at nodes or elements far away from the origin, for normal values of the coefficient of hydrodynamic dispersion. For transports that are highly convection dominant, such a difficulty arises even for nodes or elements moderately away from the origin. Since, in most cases of salt-water dispersion and diffusion in saturated soils, the contribution of hydrodynamic dispersion is small and the transport is convection-dominant, the method, though mathematically elegant, has a serious limitation for practical problems in geohydrology.

In pursuance of this method for the solution of cases pertinent to this investigation, an attempt was made to extend the limits up to which this formulation could be handled by the CDC 6400 machine, by dividing the previous time values of  $\psi$  at all the nodes by a constant sufficiently large in value to bring the largest  $\psi$  value within the computer range without letting the smallest  $\psi$  value go below the lowest limit of the computer, viz.  $e^{-741.67}$ . Obviously, even this device could work only within twice the range of the original limits and therefore, the method still remained far from general. Besides, the vary nature of the  $\beta$  transform function, yields very widely different  $\psi$  values for nodes near and far from the origin, even though the corresponding concentration values may be more or less equal. Thus, the same order of truncation error in the Gauss-elimination at such nodes, manifests itself into largely vitiated results. These difficulties with the Rayleigh-Ritz formulation appear to be insurmountable at this stage. Therefore, this method was abandoned in favour of the Galerkin.

For practical well-flow problems, the regions to be simulated are of the order of 1000 feet or so in radial length and aquifer depths vary from 200 feet to 1000 feet. Following the mesh pattern discussed in section 4.1(a), with reasonable element sizes, the band-width for symmetric matrices for such regions might easily be as high as 16 even after band-width reduction; which for unsymmetric matrices obtained in the Galerkin formulation rises to 33. With such a large band-width, a moderate element layout even with 150 nodes, would yield [SK] and [PK] matrices of size (150x33). For larger number of nodes, the band-width will further rise and consequently, the storage requirement for the [SK], [PK] and their auxiliary matrices becomes prohibitive.

Besides, the diagonal inversion technique for developing an alternative element layout indicated in Section 4.3(a), if adopted, would produce such a large band-width that the storage requirement will become prohibitive. However, this plausibly insurmountable impediment of the Galerkin process may be overcome by a judicious use of auxiliary tape storage. This, in no way, is too great a disadvantage, in view of the versatility of the formulation for handling cases of any order of convection or dispersion dominated transports.

#### 4.6 Stability and Convergence.

By definition unstable methods are those in which growth of individual round off errors, inherent in the inexact arithmetical operations performed by the computer, causes a significant and unwarranted error in the computed solution. In such schemes, a decrease in step size may reduce the inherent error of the method but may increase round off errors by a much greater amount. A particular solution is said to be stable if the propagated errors are bounded. On the other hand, convergence is the property of a numerical solution to tend to the exact solution with finer and finer discretising functions. For the numerical simulator developed in this investigation, stability and convergence have to be studied from the following view-points:

- (i) Solution in the space domain.
- (ii) Solution in the time domain.
- (iii) Integration scheme.
- (iv) Data input.

The finite-element solution of the problem in the space-domain results in an implicit scheme, yielding a set of simultaneous equations to be solved by Gauss-elimination and so is inherently stable. However,

sometimes difficulties might arise with non-homogeneous problems, described by matrices which are not diagonally dominant for some particular element layout. For such cases the problem can be alleviated by changing the node numbering pattern by trial and error until non-singular diagonally dominant matrices with positive diagonal entries are obtained. As the properties of the [SK] and [PK] matrices generated for the space-domain solution are dependent upon the geometry and size of individual elements, it is important to be judicious in choosing a suitable mesh with almost equilateral triangles. With regard to the convergence, it has been observed that the finer the mesh the more accurate is the solution.

TABLE 4.4. H-VALUES AFTER 55.5 SECONDS OF PUMPING

r	Analytical Solution	Numerical Solution	
		380 Element Mesh	240 Element Mesh
.5	7558.60	7641.49	7795.97
50.5	7951.43	7945.48	7946.93
100.5	8012.18	8004.06	8004.24
200.5	8070.60	8059.60	8059.99
300.5	8082.46	8087.86	8088.12
400.5	8108.07	8104.11	8104.29
500.5	8124.88	8113.61	8113.76
950.5	8125.00	8125.00	8124.59

The above values demonstrate the convergence of the numerical solution to the analytical solution at the well face, as the mesh is made finer. Values at points away from the well are not appreciably affected.

For the time domain solution, the Galerkin or the Sub-domain method, which ever is employed, results in an implicit formulation and so is potentially stable. Yet, if the choice of time increment is large, the



accumulation of round off errors may render the solution unacceptably inaccurate. This type of divergence from the true solution is sometimes termed as induced instability. However, if higher order interpolation functions are used for the time dependence, greater stability of solution is obtained and larger time increments may be used. For the problem at hand, since both the flow and convective-dispersion equations are solved in sequence and since the former is a faster process than the latter, the flow equation is solved for a much smaller time interval than the convective-dispersion equation. For large initial time intervals, the flow equation tends to exhibit oscillations, which may be avoided by gradually increasing the time step as shown in the following table.

TABLE 4.5. H-VALUES AT WELL FACE WITH DIFFERENT VALUES OF DT.

DT(sec)	TIME(sec)	H	DT(sec)	TIME(sec)	H
5.0	5.0	7505.77	0.1	1.0	7639.59*
	10.0	7948.51	1.0	10.1	7434.39*
	15.0	7507.50	10.0	110.1	7227.94*
	20.0	7889.13	100.0	1110.1	7168.44*
	25.0	7508.71			

\* These values are the same as were used in Fig. 4.3.

Time intervals ranging from 0.1 to 100,000 seconds in successive iterations have been found sufficiently accurate and stable. The solution tends to converge to exact values with smaller and smaller time intervals.

Coming to the integration scheme, convergence of the finite-element process occurs if the integrals evaluated in subroutine TEGRAL are sufficiently accurate. Whereas, it is not possible to quantify the term 'sufficiently accurate', it may be stated qualitatively that if fewer

elements are used to represent the flow region, then larger number of integrating points are desirable in the Gauss-quadrature scheme, to ensure reasonably fast convergence. For the cases analyzed in this investigation, results obtained with three integrating points per triangle matched with those obtained with exact integrations up to eight decimal places. Representative values are tabulated below.

TABLE 4.6. CONCENTRATION DISTRIBUTION AFTER 146.0 SECONDS

$r$ ft.	Gauss Quadrature	Exact Integration
0.5	.99191130	.99191130
1.5	.99418559	.99418559
2.5	.98790338	.98790338
3.5	1.00063250	1.00063250

Trial runs with different data input displayed no convergence or stability problems. Unlike the method of Guymon and Nalluswami, the method has worked well with values of the geometric dispersivity of the aquifer ranging from 0.1 to 10.0 and can admit even smaller or higher values without blowing up and so there appears to be no need to define a convergence parameter like the one specified by Guymon (1970b) for the Rayleigh-Ritz formulation in cartesian coordinates for a uniform flow system.

## CHAPTER V

### CONCLUSIONS AND RECOMMENDATIONS

#### 5.1 Summary.

The complex problem of salt-water movement induced by pumping from an aquifer is not amenable to exact mathematical analysis. Numerical techniques developed by past investigators to analyze miscible displacement problems in general, have been limited to uniform rectilinear flow of homogeneous fluids. In this investigation, the flow equation governing the movement of a non-homogeneous, compressible fluid in an isotropic, elastic saturated aquifer, in response to well pumping has been developed in a general system of coordinates. The convective-dispersion equation describing the movement of an inert tracer in the above non-uniform flow field, under isothermal conditions, has also been derived. In this derivation, tensorial nature of dispersion and contribution of molecular diffusion have been taken into account, which were not included in earlier investigations.

A new version of the Galerkin-finite-element approach has been developed for both the space and time domain solutions of the flow equation in cylindrical coordinates. Using the flow parameters so obtained, velocity distribution in the non-uniform flow field is computed. This velocity distribution is used to develop the space and time domain Galerkin formulation for the convective-dispersion equation. To account for fluid non-homogeneity and aquifer compressibility, the variables fluid-density and aquifer porosity are updated at each time-step before passing on to the next iteration. These aspects were not considered in previous investigations.

Boundary conditions, which are of common occurrence in field problems, have been incorporated in the formulation. Natural or reflective boundary conditions are not required to be explicitly entered into the program. Geometric boundary conditions may be introduced as data and taken care of by simple devices provided in the program. Contribution of the well as a sink is evaluated separately and is distributed over all the points lying along the well face. Treatment of the well face boundary conditions has not been attempted by previous investigators.

An efficient scheme has been developed for generating a mesh layout which could represent the complex flow pattern around partially penetrating wells. This scheme incorporates an algorithm to minimize the band-width of the matrices obtained in the finite-element formulation.

Finally, a numerical simulator has been developed incorporating the scheme for automatic mesh generation and the Galerkin-finite-element formulations for the flow and convective-dispersion equations. The validity of this simulator has been tested for the flow and convective-dispersion parts separately. Results of the flow equation match the solution of Thisis equation for confined flow cases and those of the convective-dispersion equation compare well with the approximate solution given by Shamir and Harleman. Applicability of the simulator to practical problems has been demonstrated by analyzing two hypothetical field situations. The results of the hypothetical problems could not be verified in the absence of field or experimental data.

## 5.2 Evaluation and Practical Applications of the Simulator.

The simulator could be used for steady, unsteady, uniform or non-uniform flow and miscible displacement problems, with constant or

variable fluid density and with constant or variable aquifer porosity. Even variable viscosity may be taken care of with minor modifications. A wide range of values for the coefficients of dispersion, from zero to several hundreds or more, may be used without encountering computational problems such as those experienced by Guymon and Nalluswami.

The schemes used for the space and time domain solutions are implicit and inherently stable. For large initial time steps, the flow equation solution scheme tends to exhibit oscillations. This may be overcome by selecting a small initial time step followed by gradually increasing step size at successive iterations without experiencing instability or oscillations. A remarkable advantage of the simulator over the finite-difference model is that no approximation is involved in obtaining pressure and concentration values on the well-face.

The simulator is very versatile and can be applied to the following field situations with or without modifications:

(i) Movement of salt-water from a low lying bed of saline water towards a partially penetrating well. This type of situation exists in the Indus Basin, Pakistan.

(ii) Salt-water intrusion into a coastal aquifer due to pumping by a fully or partially penetrating well. The zigzag pattern of the constant head and constant concentration ocean boundary may easily be represented by triangular elements laid in a zigzag fashion.

(iii) Dispersion of liquid industrial or domestic wastes through recharge pits in an aquifer, induced by natural gradients or by discharging wells near by.

(iv) Movement of contaminants in an open channel and back flow of salt-water in an estuary due to tidal waves in an ocean. This type of

problems do not require the formulation in cylindrical polar coordinates and the well-face boundary conditions.

(v) Cooling of large cylindrical containers by cooler fluid injection through centrally located cylindrical sources. This problem is similar to the recharging well cases discussed in Chapter IV, except that the concentration is replaced by temperature.

### 5.3 Limitations and Suggestions for Future Work.

Although the simulator developed in this study is quite versatile, yet the various assumptions made at different stages, do warrant further research and study to evaluate the effect and validity of such simplifications. Some of the aspects not covered in this investigation, which require attention of future investigators are:

(i) The interpolation functions used for polynomial representation of the variables  $C$  and  $H$ , both in the space and time domains are linear. For more accuracy and stability even with coarser element layout and larger time-step size, it would be worthwhile to investigate how the results are affected, if parabolic or higher order interpolation functions with isoparametric elements are used. This investigation is especially important in view of the fact that for actual field aquifers, the number of elements required for reasonably accurate results with linear interpolation functions, has to be very large, requiring huge (sometimes prohibitive) amounts of computer storage. Also, the time required for the concentration to advance from the farthest or deepest point in the aquifer to the well, is so large, that with smaller time increments, inevitable for the linear interpolation function, the number of iterations to be performed becomes extremely large.



(ii) Although the mesh pattern generated can be optimized to yield a minimum band-width, if either the shorter or the larger of the two diagonals of every quadrilateral is joined to form triangular elements, nevertheless, sometimes, for finer meshes, even this minimized band-width turns out to be too large for unsymmetric matrices, causing formidable storage problems. To cope with such situations, the Gauss-elimination scheme needs to be reorganized in such a way that the moment the elements of [SK] and [PK] matrices corresponding to a particular node are generated, their elimination process is completed simultaneously and the result is stored on a tape. In this way, it may be possible to save a considerable amount of storage.

(iii) A thorough investigation needs to be carried out to develop criteria for arriving at an optimum time increment for a non-oscillatory behavior of program FLOW without unduly increasing the number of time steps required to reach a certain time level.

(vi) The simulator developed applies rigorously to a confined aquifer case. Possible extension and modification of the technique for solving unconfined flow problems needs to be investigated.

(v) In the development of flow and convective-dispersion equations in this study, the aquifer has been assumed to be fully saturated and the flow-field has been treated to be under isothermal state. It appears interesting to extend the work for unsaturated soils where thermal-gradient-actuated-flow is significant and needs to be taken into account.

(vi) A more complicated, though desirable, extension of the work is to study the effect of anisotropy and non-homogeneity of the aquifer on the movement of a tracer, induced by well-pumping. This will involve



consideration of the coefficient of dispersion as a fourth rank tensor with all the 36 components and the tortuosity and permeability to be treated as tensors and not scalars as assumed in the present investigation.

(vii) In this investigation, presence of only an inert tracer has been considered. The study needs to be extended to chemically active and radio-active tracers. This will require retention and quantification of the terms for chemical or radio-active reactions in the flow and convective-dispersion equations, which have been tacitly omitted in Appendices A and B.

(viii) In this investigation, it has been assumed that the discharge is uniformly distributed over the penetration depth. It is desirable to examine the difference in the results if the same potential is assumed to exist at every point inside the well, with non-uniform discharge distribution.

(ix) The simulator needs to be applied to and tested on an actual field situation for which observed concentration values at different spacings from the well for different periods of time and at different rates of pumping are available. Aquifer properties like permeability, porosity, tortuosity, geometric dispersivities and formation compressibility along with the coefficient of molecular diffusion, fluid compressibility, viscosity and density must be known with reasonable accuracy from reliable experimentation.

## REFERENCES

- Ahmad, Nazeer, 1967, Physical properties of porous medium affecting laminar and turbulent flow of water. Ph. D. Dissertation, Colorado State University, Fort Collins, June 1967, 102 p.
- Ahmad, Nazeer and D. K. Sunada, 1969, Nonlinear flow in porous media, Proceedings American Society of Civil Engineers (Hydraulics Div.), Vol. 95, No. HY 6, Nov. 1969, pp. 1847-1857.
- Aris, R., 1956, On the dispersion of a solute in a fluid flowing through a tube. Proc. Royal Society of London, Series A, Vol. 235, 1956, pp. 67-77.
- Aris, R. and N. R. Amundson, 1957, Some remarks on longitudinal mixing or diffusion in fixed beds. Am. Inst. of Chemical Engineers Journal, Vol. 3, No. 2, 1957, pp. 280-281.
- Bachmat, Y. and J. Bear, 1964, The general equations of hydrodynamic dispersion in homogeneous, isotropic porous mediums. Journal of Geophysical Research, Vol. 69, No. 12, June 1964, pp. 2561-2567.
- Bear, J., 1961a, On the tensor form of dispersion in porous media. Journal of Geophysical Research, Vol. 66, No. 4, April 1961, pp. 1185-1197.
- Bear, J., 1961b, Some experiments in dispersion. Journal of Geophysical Research, Vol. 66, No. 8, August 1961, pp. 2455-2467.
- Bear, J., 1972, Dynamics of fluids in porous media. American Elsevier, Environmental Science Series, 1972, 764 p.
- Bear, J. and Y. Bachmat, 1966, Hydrodynamic dispersion in non-uniform flow through porous media taking into account density and

- viscosity differences. (In Hebrew with English summary)  
Hydraulic Lab., Technion, Haifa, Israel, IASH, P.N. 4/66, 1966.
- Bear, J. and Y. Bachmat, 1967, A generalized theory on hydrodynamic dispersion in porous media. International Association of Scientific Hydrology, Publication No. 72, Symposium of Haifa, Israel on artificial recharge and management of aquifers, March 1967, pp. 7-16.
- Bear, J., D. Zaslavsky and S. Irmay, 1968, Physical principles of water percolation and seepage. UNESCO, Vol. XXIX in the series on Arid Zone Research, New York, 1968, 465 p.
- Bennett, G. D., M. J. Mundorff and S. Amjad Hussain, 1968, Electric-analog studies of brine-coning beneath fresh-water wells in the Punjab region, West Pakistan. U. S. Geological Survey, Water-Supply Paper 1608-J, 1968, 31 p.
- Blackwell, R. J., 1957, An investigation of miscible displacement processes in capillaries. Paper presented at the local section meeting of American Institute of Chemical Engineering, Galveston, Texas, 1957.
- Blair, P. M. and D. W. Peaceman, 1963, An experimental verification of a two-dimensional technique for computing performance of gas-drive reservoirs. Society of Petroleum Engineers Journal, Vol. 3, No. 1, March 1963, pp. 19-27.
- Bredehoeft, John D. and George F. Pinder, 1973, Mass-transport in flowing ground water. Water Resources Research, Vol. 9, No. 1, Feb., 1973, pp. 194-210.
- Breitenbach, E. A., D. H. Thurnau and H. K. Van Poolen, 1968, The fluid flow simulation equations. Society of Petroleum Engineers of AIME. Preprint SPE 2020, Dallas Meeting, April 1968.

- Bruch, John C. and Robert L. Street, 1967, Two-dimensional dispersion. Proceedings American Society of Civil Engineers (Sanitary Engineering Division), Vol. 93, No. SA 6, Dec. 1967, pp. 17-39.
- Chandler, Robert L., 1973, Salt water coning in anisotropic media. MS Thesis, Colorado State University, Fort Collins, December 1973, 64 p.
- Collins, R. J., 1973, Bandwidth reduction by automatic renumbering. International Journal for Numerical Methods in Engineering, Vol. 6, No. 3, 1973, pp. 345-356.
- Conte, S. D., 1965, Elementary Numerical Analysis. McGraw-Hill Book Company, New York, 1965, 278 p.
- Courant, R. and D. Hilbert, 1963, Methods of mathematical physics, Vol. 1, Interscience Publishers Inc., New York, 1963, 561 p.
- Cowper, G. R., E. Kosko, G. M. Lindberg and M. D. Olson, 1969, Static and dynamic applications of a high precision triangular plate bending moment, AIAA Journal, Vol. 7, No. 10, Oct. 1969, pp. 1957-1965.
- Crank, J. 1956, The Mathematics of diffusion. Oxford University Press, Amen House, London, E. C. 4, 1956, 347 p..
- Crank, J. and P. Nicolson, 1947, A practical method for numerical evaluation of solutions of partial differential equations of the heat conduction type. Proc. Camb. Phil. Soc., 43, 1947, pp. 50-67.
- Crandall, Stephen H., 1956, Engineering Analysis. McGraw-Hill Book Co. Inc., New York, 1956, 417 p..
- Dagan, G., 1967, Hydrodynamic dispersion in a non-homogeneous porous

- medium. *Journal of Geophysical Research*, Vol. 72, No. 16, Aug. 1967, pp. 4075-4080.
- Danel, P., 1952, The measurement of groundwater flow. *Ankara Symp. Arid Zone Hydrology, Proc. UNESCO*, No. 2, 1952, pp. 99-107.
- Davis, Stanley N. and Roger J. M. DeWiest, 1966, *Hydrogeology*. John Wiley & Sons Inc., New York, 1966, 463 p.
- de Josselin de Jong, G., 1958, Longitudinal and transverse diffusion in granular deposits. *Trans. Am. Geophysical Union*, Vol. 39, No. 1, February 1958, pp. 67-74.
- de Josselin de Jong, G., 1958a, Discussion on "Longitudinal and transverse diffusion in granular deposits". *Trans. Amer. Geophysical Union*, Vol. 39, 1958a, pp. 1160-1161.
- de Josselin de Jong, G. and M. J. Bossen, 1961, Discussion of a paper by Jacob Bear, on the tensor form of dispersion in porous media. *Journal of Geophysical Research*, Vol. 66, No. 10, Oct. 1961, pp. 3623-3624.
- Desai, Chandrakant S., 1973, Approximate solution for unconfined seepage. *Proceedings American Society of Civil Engineers (Irrigation and Drainage Division)*, Vol. 99, IR 1, March, 1973, pp. 71-87.
- Desai, Chandrakant S. and John F. Abel, 1972, *Introduction to the finite element method, a numerical method for engineering analysis*. Van Nostrand Reinhold Company, New York, 1972, 477 p.
- Douglas, J., Jr., D. W. Peaceman and H. H. Rachford, Jr., 1959, A method for calculating multi-dimensional immiscible displacement. *Transactions, AIME*, Vol. 216, 1959, pp. 297-308.
- Dunne, P., 1968, Complete Polynomial Displacement Fields for the Finite Element Method. *The Aeronautical Journal*, Vol. 72, March 1968.

- Ebach, E. A. and R. R. White, 1958, Mixing of fluids flowing through beds of packed solids. *Journal of the American Institute of Chemical Engineers*, Vol. 4, No. 2, June 1958, pp. 161-169.
- Feth, J. H., 1970, Saline groundwater resources of the Coterminous United States. *Water Resources Research*, Vol. 6, No. 5, Oct. 1970, pp. 1454-1457.
- France, P. W., C. J. Parekh, J. C. Peters and C. Taylor, 1971, Numerical analysis of free-surface seepage problems. *Proceedings American Society of Civil Engineers (Irrigation and Drainage Div.)*, Vol. 97, IR 1, March 1971, pp. 165-179.
- Fried, J. J. and M. A. Combarous, 1971, Dispersion in porous media in *Advances in Hydrosience*, Vol. 7, Ed. Ven Te Chow, Academic Press Inc., New York, 1971, pp. 170-280.
- Garder, A. O., D. W. Peaceman and A. L. Pozzi, Jr., 1964, Numerical calculation of multi-dimensional miscible displacement by the method of characteristics. *Society of Petroleum Engineers Journal*, Vol. 4, No. 1, March 1964, pp. 26-36.
- Gerald, Curtis F., 1970, *Applied numerical analysis*. Addison-Wesley Publishing Co., London, 1970, 340 p.
- Gurr, C. G., T. J. Marshall, and J. T. Hutton, 1952, Movement of water in soil due to a temperature gradient. *Soil Science*, 74, 1952, pp. 335-345.
- Guymon, L. R. Gary, 1970a, A finite element solution of the one-dimensional diffusion-convection equation, *Water Resources Research*, Vol. 6, No. 1, Feb. 1970, pp. 204-210.
- Guymon, L. R. Gary, 1970b, Mathematical modeling of movement of dissolved constituents in ground water aquifers by the finite element

- method, Ph. D. Dissertation, University of California, Davis, 1970, 99 p.
- Guymon, L. R. Gary, 1972, Note on the finite element solution of the diffusion-convection equation, *Water Resources Research*, Vol. 8, No. 5, Oct. 1972, pp. 1357-1360.
- Guymon, L. R. Gary, V. H. Scott and L. R. Herrmann, 1970, A general numerical solution of the two-dimensional diffusion-convection equation by the finite-element method. *Water Resources Research*, Vol. 6, No. 6, Dec. 1970, pp. 1611-1617.
- Habib, P. and F. Soeiro, 1957, Water movement in soil promoted by a thermal gradient. *Proc. Fourth International Conference Soil Mechanics*, London, 1, Folio TA710/F52 in French, 1957, pp. 40-43.
- Hadley, W. A. and R. Eisenstadt, 1955, Thermally actuated moisture migration in granular media. *Tran. American Geophysical Union*, 36, 1955, pp. 615-623.
- Hantush, Mahdi S., 1964, *Hydraulics of wells in Advances in Hydrosience*, Vol. I, Ed. Ven Te Chow, Academic Press Inc., New York, 1964, pp. 281-432.
- Happel, John and Howard Brenner, 1965, *Low Reynolds Number hydrodynamics with special applications to particulate media*. Prentice-Hall Inc., Englewood Cliffs, New Jersey, 1965, 553 p.
- Harleman, Donald R. F. and R. R. Rumer, 1962, Dynamics of salt-water intrusion in porous media. Technical Report No. 55, Hydrodynamics Lab., MIT, August 1962, 125 p.
- Harr, M. E., 1962, *Ground water and seepage*. McGraw-Hill Book Co., New York, 1962, 315 p.



- Hildebrand, Francis B., 1965, Methods of applied mathematics. Prentice-Hall Inc., Englewood Cliffs, New Jersey, 1965, 362 p.
- Hillel, Daniel, 1971, Soil and water, Principles and process. Academic Press, New York, 1971, 288 p.
- 
- Hoopes, John A. and Donald R. F. Harleman, 1965, Wastewater recharge and dispersion in porous media. Hydrodynamics Lab., Report No. 75, Dept. of Civil Engineering, School of Engineering, Massachusetts Institute of Technology, Cambridge 39, Massachusetts, June 1965, 166 p.
- Hoopes, John A. and D. R. F. Harleman, 1967a, Dispersion in radial flow from a recharge well. Journal of Geophysical Research, Vol. 72, No. 14, July 1967, pp. 3595-3607.
- Hoopes, John A. and D. R. F. Harleman, 1967b, Waste water recharge and dispersion in porous media. Proceedings American Society of Civil Engineers (Hydraulics Div.) Vol. 93, No. HY 5, Sept. 1967, pp. 51-71.
- Hunt, Bruce W., 1973, Dispersion in non-uniform seepage. Proceedings ASCE (Hydraulics Div.), Vol. 99, No. HY 2, Feb. 1973, pp. 293-299.
- Hurr, R. Theodore, 1971, Modelling steady-state and transient confined and unconfined groundwater flow by the finite element method, MS Thesis, Colorado School of Mines, Golden, Colorado, May 1971, 79 p.
- Jacob, C. E., 1950, Flow of ground water. Engineering Hydraulics, Ed. Hunter Rouse, Chapman and Hall, London, 1950, 1039 p.
- Javandel, Iraj and Paul A. Witherspoon, 1969, A method of analyzing transient fluid flow in multi-layered aquifers. Water Resources Research, Vol. 5, No. 4, Aug. 1969, pp. 856-869.

- Kantorovich, L. V. and V. I. Krylov, 1958, Approximate methods of higher analysis. P. Noordhoff Ltd., Groningen, The Netherlands, Interscience Publishers, Inc., New York, 1958, 681 p. (Translated by Curtis D. Benster).
- Kitagawa, K., 1934, Sur le dispersement et l'e cart moyen de l'e con-  
lement des eaux sonterraines, I. Experiences avec un modele  
le laboratoire: Kyoto Imperial Univ., Coll. Sci. Mem. Ser. A,  
v. 17, pp. 37-42.
- Kochina, Polubarinova-P. Ya., 1962, (English translation from Russian  
by DeWiest, Roger J. M.) Theory of ground-water movement.  
Princeton University Press, Princeton, New Jersey, 1962, 613 p.
- Konikov, Leonard F. and John D. Bredehoeft, 1973, Simulation of hydro-  
logic and chemical-quality variations in an irrigated stream-  
aquifer system. Colorado Water Resources Circular No. 17,  
Colorado Water Conservation Board, 1845 Sherman Street, Denver,  
Colorado 80203, 1973, 43 p.
- Kraeger, Catherine Eileen, 1972, Numerical modelling of ground-water  
contamination. MS Thesis, Colorado State University, Fort  
Collins, June 1970, 76 p.
- Kuzmak, J. M. and P. J. Serada, 1958, On the mechanism by which water  
moves through a porous material subjected to a temperature  
gradient. Natl. Res. Council Highway Res. Bd. Spec. Rpt. 40,  
1958, pp. 134-146.
- List, E. J. and N. H. Brooks, 1967, Lateral dispersion in saturated por-  
ous media. Journal of Geophysical Research, Vol. 72, No. 10,  
May 1967, pp. 2531-2541.

- Moller, C., 1972, The theory of relativity. Clarendon Press, Oxford, London, 1972, 557 p.
- Muskat, M., 1932, Potential distributions in large cylindrical disks with partially penetrating electrodes. *Physis*, Vol. 2, May 1932, pp. 329-364.
- Muskat, M., 1946, The flow of homogeneous fluids through porous media. J. W. Edwards Inc., Ann Arbor, Michigan, 1946, 763 p.
- Muskat, M., 1949, Physical Principles of oil production. McGraw-Hill Book Co., New York, 1949, 922 p.
- Nalluswami, M., R. A. Longenbaugh and D. K. Sunada, 1972, Finite element method for the hydrodynamic dispersion equation with mixed partial derivatives. *Water Resources Research*, Vol. 8, No. 5, Oct. 1972, pp. 1247-1250.
- Neuman, Shlomo P., 1973, Saturated-unsaturated-seepage by finite elements. *Proc. ASCE, Jour. of Hydraulics Div.*, Vol. 99, No. HY 12, Dec. 1973, pp. 2233-2250.
- Neuman, Shlomo P. and Paul A. Witherspoon, 1970, Finite-element method of analyzing steady seepage with a free surface. *Water Resources Research*, Vol. 6, No. 3, June 1970, pp. 889-897.
- Ogata, A., 1961, Transverse diffusion in saturated isotropic granular media. Professional Paper 411-B, 1961, U. S. Geological Survey, U. S. Gov't. Printing Office, Washington, D. C., 8 p.
- Ogata, A., 1964, Mathematics of dispersion with linear adsorption isotherm. Professional Paper 411-H, 1964, U. S. Geological Survey, U. S. Gov't. Printing Office, Washington, D. C., 7 p.
- Ogata, A., 1970, Theory of dispersion in a granular medium. U. S. Geological Survey Professional Paper 411-I, U. S. Gov't. Printing Office, Washington, D. C., 1970, 34 p.

- Ogata, A. and R. B. Banks, 1961, A solution of the differential equation of longitudinal dispersion in porous medium. Professional Paper 411-A, 1961, U. S. Geological Survey, U. S. Gov't. Printing Office, Washington, D. C., 7 p.
- Peaceman, D. W. and H. H. Rachford, Jr., 1962, Numerical calculation of multidimensional miscible displacement. Society of Petroleum Engineers Journal, Vol. 2, No. 4, Dec. 1962, pp. 327-339.
- Peter Henrici, 1965, Discrete variable methods in ordinary differential equations. John Wiley and Sons Inc., New York, 1965, 407 p.
- Pinder, George F. and Hilton H. Cooper, Jr., 1970, A numerical technique for calculating the transient position of the salt-water-front. Water Resources Research, Vol. 6, No. 3, June 1970, pp. 875-882.
- Pinder, George F. and Emil O'Frind, 1972, Application of Galerkin procedure to aquifer analysis. Water Resources Research; Vol. 8, No. 1, Feb. 1972, pp. 108-120.
- Pinder, George F., 1973, A Galerkin-finite element simulation of groundwater contamination on Long Island, New York. Water Resources Research, Vol. 9, No. 6, Dec. 1973, pp. 1657-1669.
- Poreh, Michael, 1965, The dispersivity tensor in isotropic and axi-symmetric mediums. Journal of Geophysical Research, Vol. 70, No. 16, August 1965, pp. 3909-3913.
- Price, H. S., J. C. Cavendish and R. S. Varga, 1968, Numerical methods of higher order accuracy for diffusion-convection equations, Society of Petroleum Engineers Journal, Vol. 8, No. 3, Sept. 1968, pp. 293-303.

- Rafai, M. N. E., W. J. Kaufman and D. K. Todd, 1956, Dispersion phenomena in laminar flow through porous media. California Univ., Inst. Eng. Research Ser. 93, Issue No. 2, 1956, 157 p.
- Raimondi, P., G. H. G. Gardner and C. B. Petrick, 1959, Effect of pore structure and molecular diffusion on the mixing of miscible liquids flowing in porous media, AIChE-SPE, Fundamental concepts of miscible fluid displacement, Part I, Preprint 43, San Francisco, Dec., 1959.
- Reddell, D. L. and D. K. Sunada, 1970. Numerical simulation of dispersion in groundwater aquifers. Hydrology Paper No. 41, Colorado State University, Fort Collins, June 1970, 79 p.
- Rollins, R. L., M. G. Spangler and Don Kirkham, 1954, Movement of soil moisture under a thermal gradient. Highway Res. Bd. Proc., 33, 1954, pp. 492-508.
- Saffman, P. G., 1959, A theory of dispersion in a porous medium. Journal of Fluid Mechanics, Vol. 6, Part 3, Oct. 1959, pp. 321-349.
- Saffman, P. G., 1960, Dispersion due to molecular diffusion and macroscopic mixing in flow through a network of capillaries. Journal of Fluid Mechanics, Vol. 7, Part 2, Feb. 1960, pp. 194-208.
- Sahni, Brij M., 1972, Salt water coning beneath fresh water wells. Ph. D. Dissertation, Colorado State University, Fort Collins, April 1972, 168 p.
- Scheidegger, A. E., 1954, Statistical hydrodynamics in porous media. Journal of Applied Physics, Vol. 25, No. 8, August 1954, pp. 994-1001.

- Scheidegger, A. E., 1957, On the theory of flow of miscible phases in porous media. *Compt. rend. Ass. Gen. Toronto, Assc. International Hydrology Scient.*, 2, 1957, pp. 236-242.
- Scheidegger, A. E., 1958, Statistical approach to miscible displacement in porous media. *Bull. Canda. Inst. Min. Met.*, 1958, pp. 26-30.
- Scheidegger, A. E., 1961, General theory of dispersion in porous media. *Journal of Geophysical Research*, Vol. 66, No. 10, Oct. 1961, pp. 3273-3278.
- Shamir, Uri Y. and Donald R. F. Harleman, 1966, Numerical and analytical solutions of dispersion problems in homogeneous and layered aquifers. *Hydrodynamics Lab. Report No. 89, Dept. of Civil Engineering, School of Engineering, Massachusetts Institute of Technology, Cambridge 39, Massachusetts, May 1966, 206 p.*
- Shamir, Uri Y. and Donald R. F. Harleman, 1967, Numerical solutions for dispersion in porous mediums. *Water Resources Research*, Vol. 3, No. 2, 1967, pp. 557-581.
- Slichter, C. S., 1905, Field measurement of the rate of movement of underground waters, U. S. Geological Survey, *Water Supply and Irrigation Paper No. 140, Series O, Underground Waters*, 43, 1905, 122 p.
- Smith, I. M., R. V. Farraday and B. A. O'Connor, 1973, Rayleigh-Ritz and Galerkin finite-elements for diffusion-convection problems. *Water Resources Research*, Vol. 9, No. 3, June 1973, pp. 593-606.
- Stone, Herbert L. and Brian, P. L. T., 1963, Numerical solution of convective-transport problems. *American Institute of Chemical Engineers Journal*, Vol. 9, No. 5, Sept. 1963, pp. 681-688.

- Taylor, G. I., 1953, Dispersion of soluble matter in solvent flowing slowly through a tube. Proceedings Royal Society, London, Series A, Vol. 219, No. 1137, 1953, pp. 186-203.
- Taylor, G. I., 1954, Dispersion of matter in turbulent flow through a pipe. Proceedings Royal Society, London, Series A, Vol. 223, 1954, pp. 446-468.
- Taylor, R. L. and C. B. Brown, 1967, Darcy-flow solutions with a free-surface. Proceedings American Society of Civil Engineers (Hydraulics Division), Vol. 93, No. HY 2, March 1967, pp. 25-33.
- Todd, D. K., 1959, Ground Water Hydrology. John Wiley and Sons, New York, 1959, 336 p.
- Tottenham H. and C. Brebbia, 1970, Finite element techniques in structural mechanics. Southampton University Press, Hobbs the Printers Ltd., Millbrook, Southampton, England, 1970, 348 p.
- Van Deamter, J. J., J. J. Brader and H. A. Lauweir, 1955, Fluid displacement in capillaries, Appl. Sci. Res. A., Vol. 5, No. 5, 1955, pp. 374-388.
- Volker, R. E., 1969, Non-linear flow in porous media by finite elements. Proceedings American Society of Civil Engineers (Hydraulics Div.), Vol. 95, No. HY 6, Nov. 1969, pp. 2093-2114.
- Walton, W. C., 1970, Ground Water Resources Evaluation. McGraw-Hill Book Co., New York, 1970, 664 p.
- Wang, F. C., 1965, Approximate theory for skimming well formulation in the Indus Plain of West Pakistan. Journal of Geophysical Research, Vol. 70, No. 20, Oct. 1965, pp. 5055-5063.



- Wentworth, C. K., 1948, Growth of the Ghyben-Herzberg transition zone under a rinsing hypothesis. *Tr. Am. Geophys. Union Trans.*, Vol. 29, No. 1, 1948, pp. 97-98.
- Whitaker, S., 1967, Diffusion and dispersion in porous media. *Journal American Inst. of Chemical Engineers*, Vol. 13, No. 3, 1967, pp. 420-427.
- Yih, C. S., 1961, Flow of a non-homogeneous fluid in a porous medium. *Journal of Fluid Mechanics*, Vol. 10, Part 1, Feb. 1961, pp. 133-140.
- Zienkiewicz, O. C., 1971, *The finite element method in Engineering Science*. McGraw-Hill, London, 1971, 521 p.
- Zienkiewicz, O. C., P. Meyer and Y. K. Cheung, 1966, Solution of Anisotropic seepage by finite elements. *Proceedings American Soc. Civil Engineers (Engineering Mechanics Div.)*, Vol. 92, EM 1, Feb. 1966, pp. 111-120.
- Zienkiewicz, O. C. and D. V. Phillips, 1971, An automatic mesh generation scheme for plain and curved surfaces by "isoparametric" coordinates. *International Journal for Numerical Methods in Engineering*, Vol. 3, 1971, pp. 519-528.

## LIST OF SYMBOLS

Some of the symbols have multiple definitions. Relevant definitions are given wherever such symbols are used in the text.

[A]	Reducing factor, shape function	
$A_1, A_2$	Functions of $v^2$ and the properties of the fluid, medium and tracer	
$A_i, A_j, A_k$	Components of the vector [A]	
$A_{ijk}^I$	A third rank tensor	
$A_{jilk}^{II}$	A fourth rank tensor	
$A^m, A$	Area of the $m^{\text{th}}$ triangular element	$L^2$
$a_{ijlm}$	Geometric dispersivity of the porous medium, a fourth rank tensor	$L^2T^{-1}$
$a_I$	Longitudinal constant of dispersion or longitudinal dispersivity of the medium	$L^2T^{-1}$
$a_{II}$	Lateral constant of dispersion or lateral dispersivity of the medium	$L^2T^{-1}$
$B_{jk}^I$	Tortuosity tensor	
C or c	Tracer concentration	$ML^{-3}$
$C_F$	Formation compressibility	$M^{-1}LT^2$
$C_o$	Reference value of concentration	$ML^{-3}$
$C_p$	Tracer concentration in the production or consumption fluid	$ML^{-3}$
$D_d$	Coefficient of molecular diffusion	$L^2T^{-1}$
$D_{ij}$	Dispersion coefficient (A second rank tensor)	$L^2T^{-1}$
$D_{ij}^*$	Coefficient of hydrodynamic dispersion	$L^2T^{-1}$
$D_L$	Longitudinal dispersion coefficient	$L^2T^{-1}$

$D_{rr}$	$D_{11}^* \cdot \rho/(\rho-\alpha c)$	$L^2T^{-1}$
$D_{rz}$	$D_{12}^* \cdot \rho/(\rho-\alpha c)$	$L^2T^{-1}$
$D_T$	Lateral dispersion coefficient	$L^2T^{-1}$
$D_{zz}$	$D_{22}^* \cdot \rho/(\rho-\alpha c)$	$L^2T^{-1}$
$D_{11}^*$	$D_d^T + D_T + (D_L - D_T) v_r^2/v^2$	$L^2T^{-1}$
$D_{12}^*$	$(D_L - D_T) v_r v_z/v^2$	$L^2T^{-1}$
$D_{21}^*$	$D_{12}^*$	$L^2T^{-1}$
$D_{22}^*$	$D_d^T + D_T + (D_L - D_T) v_z^2/v^2$	$L^2T^{-1}$
$D_{\alpha\beta}$	Average molecular diffusivity	$L^2T^{-1}$
$d$	Particle size of the medium	$L$
$E$	Variable representing the product $\rho_o \phi_o (\beta + C_F)$	$L^{-2}T^2$
$F$	Variable representing the product $\alpha \phi_o$	
$F_{ci}$	Convective component of the mass flux in $i$ direction	$ML^{-2}T^{-1}$
$F_d$	Diffusive component of the mass flux	$ML^{-2}T^{-1}$
$F_{ti}$	Total mass flux of the tracer in $i$ direction	$ML^{-2}T^{-1}$
$g$	Acceleration due to gravity or absolute value of the determinant of $g_{ij}$	$LT^{-2}$
$g_{ij}$	Diagonal matrix of the squares of scale factors for coordinate transformation or fundamental tensor of the Reimanian space (covariant com- ponents)	
$g^{jk}$	A second rank symmetric contravariant tensor, conjugate or reciprocal of $g_{ij}$	
$h_i$	Scale factors for coordinate transformation	
$H$	Piezometric head in energy units i.e., flow parameter $(P + \rho gz)$	$ML^{-1}T^{-2}$

$J_i$	Macroscopic tracer mass flux in $i$ direction	$ML^{-2}T^{-1}$
$J$	Variational functional	
$k$	Permeability	$L^2$
$k_r$	Relative permeability to fluid	
$k_i$	Absolute permeability in $i$ direction	$L^2$
$L$	Linear boundary over which line integral is taken	
$\ell$	Characteristic length	
$m_i$	Mass of species $i$ in the reference volume	$M$
$[N]$	Shape function	
$n$	Unit outward normal	
$p$	Pressure	$ML^{-1}T^{-2}$
$P_o$	Reference pressure	$ML^{-1}T^{-2}$
$P_e$	Peclet Number	
$Q$	Production or consumption term	$L^3T^{-1}$
$Q_w$	Well discharge	$L^3T^{-1}$
$q$	Seepage velocity along the stream line or Darcy velocity or flow velocity	$LT^{-1}$
$q_i$	Volume flux through the face perpendicular to $i$ or Darcy velocity in $i$ direction	$LT^{-1}$
$R$	Region of space, An arbitrary coefficient	$L^2$
$R_m^n$	Rate of production or consumption of constituent $n$ in the $m^{th}$ reaction	$ML^{-3}T^{-1}$
$[R]$	Symbolic representation for unknown terms in an expression	
$r$	Radial coordinates - Number of sources or sinks in the system	$L$
$\bar{r}^m$	$r$ - coordinate of the centroid of $m^{th}$ element	$L$

S	Saturation or variable representing the expression $\frac{\rho k}{\mu}$	T
T	Scalar tortuosity	
$T_{ij}$	Tortuosity tensor	$L^{-2}$
t	Time	T
u	Component of seepage velocity in x or i or r direction	$LT^{-1}$
$\bar{V}, V$	Average Darcy velocity	$LT^{-1}$
v	Average seepage velocity or seepage velocity component in z direction	$LT^{-1}$
$v_i$	Seepage velocity component in i direction	$LT^{-1}$
$v_o$	Fluctuation of seepage velocity about the mean	$LT^{-1}$
$W_p$	Weighting function	
x, $x_i$ , or $x^i$	x - coordinate	L
y	Variable representing the sum EP + FC or y - coordinate	$ML^{-3}$ L
z	Elevation of the volume element above an arbitrary datum which is normal to the direction of gravity z - coordinate	L
$z^m$	z - coordinate of the centroid of the $m^{th}$ element	L
$\alpha$	Proportionality factor relating concentration with density	
$\beta$	Fluid Compressibility or argument of the exponential in the reducing factor or experimentally determined coefficient	$M^{-1}LT^2$
$\gamma$	Unit weight of water	$ML^{-2}T^{-2}$

$\delta$	Small variation	
$\delta_{ij}$	Kronecker delta	
$\eta$	Ordinate in the transformed (local) coordinate system	L
$\lambda$	Arbitrary constant used for tensor transformation	
$\mu$	Dynamic viscosity or arbitrary constant used for tensor transformation	$ML^{-1}T^{-1}$
$\nu$	Kinematic viscosity	$L^2T^{-1}$
$\xi$	Abscissa in the transformed (local) coordinate system	L
$\rho$	Mass density of the fluid	$ML^{-3}$
$\rho_0$	Reference mass density of the fluid	$ML^{-3}$
$\rho_p$	Mass density of the fluid in the source or sink term	$ML^{-3}$
$\tau$	Dimensionless variable representing time	
$\phi$	Porosity	
$\phi_0$	Reference porosity	
$\psi$	Stream function or transformed value of the concentration C or a concentration parameter	$ML^{-3}$

## APPENDIX A

### DERIVATION OF THE FLOW EQUATION

The flow equation is obtained by combining the pertinent equation of motion with the continuity equation.

#### CONTINUITY EQUATION:

Considering mass-balance for a mixture of fluids of several chemical constituents over a control volume  $D$ , with  $\vec{n}$  as the unit outward normal to the boundary  $\partial D$  of  $D$ ,

$$\int_{\partial D} \rho^k \phi S v_i n_i d\sigma = - \left[ \int_D \rho^k \phi s dv \right]_t + \sum_{m=1}^s \int_D R_m^k dv - \int_D w^k \delta dv \quad (\text{A-1})$$

where,

$\rho^k$  = Mass of constituent  $k$  per unit volume of the mixture -  $(ML^{-3})$

$\phi$  = Porosity of the medium

$S$  = Saturation of the medium

$v_i$  = Seepage velocity component in  $i$  direction -  $(LT^{-1})$

$d\sigma$  = An element of the boundary of  $D$  -  $(L^2)$

$dv$  = An element of the volume of  $D$  -  $(L^3)$

$R_m^k$  = Rate of production or consumption of the constituent  $k$  in the  $m^{\text{th}}$  reaction -  $(ML^{-3}T^{-1})$

$s$  = Total number of reactions taking place

$w^k \delta$  = Cumulative equivalent of all the sources or sinks present in the control volume.

$$w^k \delta = \sum_{j=i}^r Q^k(x_{1j}, x_{2j}, x_{3j}) \rho_p^k \delta(x_1 - x_{1j}) \delta(x_2 - x_{2j}) \delta(x_3 - x_{3j}) - (ML^{-3}T^{-1})$$



$Q^k$  = Source or sink effect pertaining to constituent  $k$  -  
( $L^3T^{-1}$ )

$\delta$  = Dirac delta function

$r$  = Number of sources or sinks of constituent  $k$

$x_1, x_2, x_3$  = General space coordinates

$x_{1j}, x_{2j}, x_{3j}$  = Space coordinates of the location of the  $j^{\text{th}}$   
source or sink.

$\rho_p^k$  = Mass concentration of constituent  $k$  in the source or  
sink fluid - ( $L^3T^{-1}$ )

and the subscript  $t$  denotes derivative with respect to time. Using divergence theorem, equation A-1 yields,

$$\int_D \{ (\rho^k \phi_S v_i)_{,i} + (\rho^k \phi_S)_t - \sum_{m=1}^S R_m^k + Q \rho_p^k d_p \} dv = 0 \quad (\text{A-2})$$

where the comma denotes covariant derivative.  $d_p$  is a variable continuous on  $D$ , so that  $d_p \rightarrow \delta$  as  $p \rightarrow \infty$ .

Since the integrand of A-2 is continuous and the region  $D$  is arbitrary,

$$(\rho^k \phi_S v_i)_{,i} + (\rho^k \phi_S)_t - \sum_{m=1}^S R_m^k + Q \rho_p^k d_p = 0 \quad \forall p \quad (\text{A-3})$$

Therefore, as  $p \rightarrow \infty$ ,

$$(\rho^k \phi_S v_i)_{,i} + (\rho^k \phi_S)_t - \sum_{m=1}^S R_m^k + Q \rho_p^k \delta = 0 \quad (\text{A-4})$$

Assuming that,

(i) There are no reactions going on in the system,

(ii) There is only one constituent in the mixture so that the superscript  $k$  may be dropped,

(iii) There are no sources or sinks in the system,

equation A-4 reduces to,

$$\text{div}(\rho q) = - (\rho \phi S)_t \quad (\text{A-5})$$

where,

$q$  = Macroscopic flux vector with component  $q_i$  in  $i$  direction

$$q_i = v_i \phi S - (LT^{-1})$$

But in tensor notation,

$$\begin{aligned} \text{div}(\rho q) &= \nabla_i (\rho q)^i \\ &= \rho \nabla_i q^i + q^i \nabla_i \rho \\ &= \frac{\rho}{\sqrt{g}} (\sqrt{g} \cdot q_i g^{ij})_{,j} + g^{ij} q_j \rho_{,i} \\ &= \frac{\rho}{\sqrt{g}} (\sqrt{g} \frac{q_i}{h_i^2})_{,i} + \frac{q_i}{h_i^2} \rho_{,i} \end{aligned} \quad (\text{A-6})$$

where,  $g$  is the absolute value of the determinant of the metric tensor  $g_{ij}$  and  $h_i$  ( $i=1,2,3$ ) are the scale factors of coordinate transformation.

Substituting equation A-6 into A-5, collecting derivatives of  $\rho$  on one side, transferring terms and dividing out by  $\rho$ ,

$$(\phi S)_t + \frac{1}{\sqrt{g}} (\sqrt{g} \frac{q_i}{h_i^2})_{,i} = - \frac{\phi S}{\rho} \rho_t - \frac{q_i}{h_i^2} \rho_{,i} \quad (\text{A-7})$$

which is the required continuity equation.

EQUATION OF MOTION:

Assuming that,

- (i) Darcy's law holds for the flow situation under consideration,
- (ii) Axes of the coordinate system coincide with the axes of the permeability tensor,
- (iii) The system is under isothermal state,
- (iv) There is no contribution to flow due to thermodynamic gradients, due to any electrical charge carried by wet soil particles or due to adsorptive force gradients,

the appropriate equation of motion (Darcy's law) may be written as follows:

$$q_i = v_i \phi S = - \frac{k_i k_r}{\mu} \left( \frac{1}{h_i} P_{x_i} + \frac{\rho g}{h_i} z_{x_i} \right) \quad (\text{A-8})$$

where,  $h_i$  = Scale factor of coordinate transformation  
 $k_i$  = Absolute permeability in  $i$  direction at  $S=1$  - ( $L^2$ )  
 $k_r$  = Relative permeability at saturation  $S$  - ( $L^2$ )  
 $\mu$  = Dynamic viscosity of the fluid - ( $ML^{-1}T^{-1}$ )  
 $P$  = Fluid pressure - ( $ML^{-1}T^{-2}$ )  
 $g$  = Gravitational acceleration - ( $LT^{-2}$ )  
 $z$  = Elevation of the volume element above an arbitrary datum, which is normal to the direction of gravity - ( $L$ ).

It may further be assumed that the fluid density  $\rho$ , pressure  $P$  and concentration  $C$  are inter-related by a first order equation of state,

$$\rho = \rho_o + \rho_o \beta (P - P_o) + \frac{\alpha}{v_o} \sum_{i=1}^n (m_i - m_o) \quad (\text{A-9})$$

- where,
- $n$  = Number of constituents in the mixture
  - $\beta$  = Compressibility of the fluid -  $(M^{-1}LT^{-2})$
  - $P_0$  = Reference pressure -  $(ML^{-1}T^{-2})$
  - $\rho_0 = \sum_{i=1}^n \rho_{i0}$
  - $\rho_{i0}$  = Mass of constituent  $i$  per unit volume of solution at the reference pressure -  $(ML^{-3})$
  - $m_i$  = Mass of constituent  $i$  in the reference volume  $\bar{v}_0$  at the prevailing pressure -  $(M)$
  - $m_{i0}$  = Mass of constituent  $i$  in the reference volume  $\bar{v}_0$  at the reference pressure -  $(M)$
  - $\bar{v}_0$  = Reference volume of the fluid mixture  $(L^3)$
  - $\alpha$  = Proportionality factor
  - $\rho$  = Mass density of the mixture at pressure  $P$  and solute concentration  $m_i/\bar{v}_0$  -  $(ML^{-3})$  .

For solutes having only one constituent, equation A-9 reduces to,

$$\rho = \rho_0 + \rho_0 \beta (P - P_0) + \alpha (C - C_0) \quad (A-10)$$

where,  $C$  and  $C_0$  are the concentrations (mass of solute per unit volume of solution) at the prevailing state and at the reference state respectively.

Assuming that there is no change in volume upon mixing of fluids of different ionic concentrations and that the factors  $\alpha$  and  $\beta$  are independent of pressure and fluid composition,

$$\left. \begin{aligned} \rho_{x_i} &= \beta \rho_0 P_{x_i} + \alpha C_{x_i} \\ \rho_t &= \beta \rho_0 P_t + \alpha C_t \end{aligned} \right] \quad (A-11)$$

where the subscripts  $x_i$  and  $t$  denote derivatives with respect to them.

FLOW EQUATION:

The flow equation may now be obtained by assuming that  $k_i$  and  $k_r$  are independent of pressure, temperature and concentration and substituting the equation of motion (A-8) into the continuity equation (A-7),

$$(\rho\phi S)_t = \frac{\rho}{\sqrt{g}} \left[ \frac{\sqrt{g}}{h_i^2} \left\{ \frac{k_i k_r}{\mu} \left( \frac{1}{h_i} P_{x_i} + \frac{\rho g}{h_i} z_{x_i} \right) \right\} \right]_{,i} + \frac{1}{h_i^2} \rho_{,i} \left\{ \frac{k_i k_r}{\mu} \left( \frac{1}{h_i} P_{x_i} + \frac{\rho g}{h_i} z_{x_i} \right) \right\} \quad (A-12)$$

For an elastic aquifer, the aquifer compressibility is given by the relation,

$$C_F = \frac{1}{\phi_0} \phi_P$$

which may be integrated to yield,

$$\phi = \phi_0 [ 1 + C_F (P - P_0) ] \quad (A-13)$$

where,

$\phi_0$  = Reference porosity

$P_0$  = Reference pressure corresponding to the porosity  $\phi_0$  .

Therefore,

$$\phi_t = C_F \phi_0 P_t \quad (A-14)$$

Combining equations A-10, A-11 and A-14 and treating  $S$  as invariant with time,

$$(\rho\phi S)_t = \rho_o\phi_o S \left[ \beta + 2C_F\beta (P - P_o) + C_F + C_F\alpha \frac{C-C_o}{\rho_o} \right] P_t$$

$$+ \alpha\phi_o S [1 + C_F (P - P_o)] C_t$$

$C_F$  and  $\beta$  being of the same order of magnitude, the product,

$$C_F\beta (P - P_o) \ll \beta \quad \text{for small pressure changes,}$$

$$C_F\alpha \frac{C - C_o}{\rho_o} \ll C_F \quad \text{for small changes in concentration and}$$

$$C_F (P - P_o) \ll 1 \quad \text{for small pressure changes.}$$

Therefore, for small pressure and concentration changes, equation A-12 may be written as,

$$\frac{1}{\rho} [\rho_o\phi_o S (\beta + C_F) P_t + \alpha\phi_o S C_t] = \frac{1}{\sqrt{g}} \left[ \frac{\sqrt{g}}{h_i^2} \left\{ \frac{k_i k_r}{\mu} \left( \frac{1}{h_i} P_{x_i} + \frac{\rho g}{h_i} z_{x_i} \right) \right\} \right]_i$$

$$+ \frac{1}{\rho h_i} \rho_{,i} \left\{ \frac{k_i k_r}{\mu} \left( \frac{1}{h_i} P_{x_i} + \frac{\rho g}{h_i} z_{x_i} \right) \right\} \quad \text{(A-15)}$$

For axisymmetric flow towards a well (neglecting the effect of partial penetration) in a completely saturated isotropic aquifer, equation A-15 reduces to,

$$\frac{1}{r} \left\{ \frac{\rho r k}{\mu} (P_r + \rho g z_r) \right\}_r + \left\{ \frac{\rho r k}{\mu} (P_z + \rho g) \right\}_z =$$

$$\rho_o\phi_o (\beta + C_F) P_t + \alpha\phi_o C_t \quad \text{(A-16)}$$

which is the required flow equation.

Choosing  $L_o$ ,  $\rho_o$ ,  $k_o$ ,  $\mu_o$ ,  $P_o$  and  $t_o$  as the scaling factors for length, density, permeability, dynamic viscosity, pressure or compressibility and time respectively, such that,

$$P_o = g\rho_o L_o \quad \text{and} \quad t_o = \frac{\mu_o L_o}{g\rho_o k_o} = \frac{\mu_o L_o^2}{P_o k_o} ,$$

equation A-16 reduces to the following dimensionless form,

$$\begin{aligned} \phi_o (\bar{\beta} + \bar{C}_F) \bar{P}_t + \alpha\phi_o \bar{C}_t = \frac{\bar{\rho} \bar{k}}{\bar{\mu} \bar{r}} [ \bar{P}_r + \bar{\rho} \bar{z}_r ] + \\ [ \frac{\bar{\rho} \bar{k}}{\bar{\mu}} \bar{P}_r + \bar{\rho} \bar{z}_r ]_r + [ \frac{\bar{\rho} \bar{k}}{\bar{\mu}} \bar{P}_z + \bar{\rho} ]_z \end{aligned} \quad (\text{A-17})$$

where the bar denotes a dimensionless variable.



## APPENDIX B

### DERIVATION OF THE CONVECTIVE DISPERSION EQUATION

In a manner similar to the one adopted for the derivation of the flow equation, the convective-dispersion equation can be obtained by combining the mass-balance equation for the tracer with an equation that gives the mass flux of the tracer on a macroscopic scale.

#### EQUATION FOR MASS BALANCE:

Considering mass-balance for the  $k^{\text{th}}$  constituent of the tracer over a control volume  $D$ , with  $\vec{n}$  as the unit outward normal to the boundary  $\partial D$  of  $D$ ,

$$\int_{\partial D} J_i^k \phi S n_i d\sigma = - \left[ \int_D C^k \phi S dv \right]_t + \sum_{m=1}^s \int_D R_m^k dv - \int_D W^k \delta dv \quad (\text{B-1})$$

where,

$J_i^k$  = Component of the macroscopic mass-flux of tracer constituent  $k$  in  $i$  direction -  $(ML^{-2}T^{-1})$

$C^k$  = Mass concentration of the tracer constituent  $k$  -  $(ML^{-3})$

$R_m^k$  = Rate of production or consumption of the tracer constituent  $k$  in the  $m^{\text{th}}$  reaction -  $(ML^{-3}T^{-1})$

$W^k \delta$  = Cumulative equivalent of all the sources or sinks within the control volume

$$= \sum_{j=1}^r Q_j^k (x_{1j}, x_{2j}, x_{3j}) C_p^k \delta (x_1 - x_{1j}) \cdot$$

$$\delta (x_2 - x_{2j}) \delta (x_3 - x_{3j}) \quad - (ML^{-3}T^{-1})$$

$C_p^k$  = Mass concentration of tracer constituent  $k$  in the

source or sink -  $(ML^{-3})$  ,  
and other symbols are as defined in Appendix A.

Using the divergence theorem,

$$\int_D \{ (J_i^k \phi S)_{,i} + (C^k \phi S)_t - \sum_{m=1}^s R'_m{}^k + Q'^k C_p^k d_p \} dV = 0 \quad \forall p \quad (B-2)$$

where,

$$dV \rightarrow \delta \quad \text{as} \quad p \rightarrow \infty .$$

Noting that the integrand of B-2 is continuous and the region D is arbitrary and also letting  $p \rightarrow \infty$  ,

$$(J_i^k \phi S)_{,i} + (C^k \phi S)_t - \sum_{m=1}^s R'_m{}^k + Q'^k C_p^k \delta = 0 \quad . \quad (B-3)$$

Assuming that,

- (i) There are no reactions going on in the system,
- (ii) There is only one tracer constituent so that the superscript k may be dropped and,
- (iii) There are no sources or sinks in the system,

equation B-3 reduces to,

$$\text{div}(J\phi S) = - (C\phi S)_t \quad (B-4)$$

#### EQUATION FOR THE MACROSCOPIC TRACER MASS FLUX:

Assuming that Fick's law holds, it can be shown, Reddell and Sunada (1970) that on a macroscopic scale for an isotropic medium, in an orthogonal system of coordinates:

$$J_i = C v_i - D_{ij} (\text{grad } C)^j - D_d T (\text{grad } C)^j \quad (B-5)$$

where,

$Cv_i$  = Convective component of the tracer mass flux.

$D_{ij}$  = Dispersion coefficient which is a second rank covariant symmetric tensor.

$D_d$  = Coefficient of molecular diffusion.

$T$  = Reciprocal of the tortuosity tensor which is scalar for an isotropic medium.

By the rules for inner (scalar) product of a covariant and a contravariant tensor,

$$D_{ij} (\text{grad } C)^j = D_{ij} g^{jk} C_{,k} \quad . \quad (B-6)$$

It has been shown (Bachmat and Bear, 1964) that,

$$D_{ij} = a_{ij\ell m} \frac{v_\ell v_m}{V} \quad (B-7)$$

where,

$a_{ij\ell m}$  = Geometric dispersivity of the porous medium. For an isotropic medium, it is a fourth rank isotropic tensor.

$v_\ell, v_m$  = Velocity components,

$V$  = Absolute velocity.

Being an isotropic tensor of fourth rank  $a_{ij\ell m}$  may, in an orthogonal system of coordinates be expanded as follows:

$$a_{ij\ell m} = \lambda g_{ij} g_{\ell m} + B_1 g_{i\ell} g_{jm} + B_2 g_{im} g_{j\ell} \quad (B-8)$$

where,

$g_{ij}$ ,  $g_{lm}$ ,  $g_{il}$ ,  $g_{jm}$ ,  $g_{im}$  and  $g_{jl}$  are components of the metric covariant tensor.

Therefore, using the symmetry property, so that  $B_1 = B_2 = \mu$ ,

$$D_{ij} = \lambda g_{ij} V + 2\mu \frac{v_i v_j}{V} \quad . \quad (B-9)$$

Substituting B-9 and B-6 into B-5,

$$\begin{aligned} J_i &= C v_i - (\lambda g_{ij} V + 2\mu \frac{v_i v_j}{V}) g^{ik} C_{,k} - D_d T (\text{grad } C)^j \\ &= C v_i - (\lambda \delta_i^k V C_{,k} + 2\mu \frac{v_i v_j}{V} \frac{1}{(h_j)^2} C_{,j}) - D_d T (\text{grad } C)^j \\ &= C v_i - (\lambda V C_{,i} + 2\mu \frac{v_i v^k}{V} C_{,k}) - D_d T (\text{grad } C)^j \quad . \quad (B-10) \end{aligned}$$

Therefore,

$$\begin{aligned} \text{div } (J\phi S) &= \nabla_i (J^i \phi S) = \{ C \nabla_i v^i \phi S + v^i \phi S \nabla_i C \} - \\ &\quad \frac{1}{\sqrt{g}} [ \sqrt{g} \phi S g^{ij} \{ \lambda V C_{,j} + 2\mu \frac{v_j v^k}{V} C_{,k} \} ]_{,i} \\ &\quad - \text{div } \{ D_d T (\text{grad } C)^j \} \quad . \end{aligned}$$

But,

$$\text{div } \{ D_d T (\text{grad } C)^j \} = \frac{1}{\sqrt{g}} \{ \sqrt{g} g^{ij} D_d T C_{,j} \}_{,i} \quad (\text{Moller, 1972}).$$

Therefore,

$$\begin{aligned}
 \text{div } (J\phi S) &= \frac{C}{\sqrt{g}} \left( \sqrt{g} v_j \phi S g^{ij} \right)_{,i} + g^{ij} v_j \phi S C_{,i} - \\
 &\quad \frac{1}{\sqrt{g}} \left[ \sqrt{g} \phi S g^{ij} \left\{ \lambda V C_{,j} + \frac{2\mu v_j v^k}{V} C_{,k} + \right. \right. \\
 &\quad \left. \left. D_d T C_{,j} \right\} \right]_{,i} \\
 &= \frac{C}{\sqrt{g}} \left( \frac{\sqrt{g} \phi S v_i}{h_i^2} \right)_{,i} + \frac{v_i \phi S}{h_i^2} C_{,i} - \\
 &\quad \frac{1}{\sqrt{g}} \left[ \sqrt{g} \frac{\phi S}{h_i^2} \left\{ \lambda V C_{,i} + \frac{2\mu v_i v_j}{V h_j^2} C_{,j} + D_d T C_{,i} \right\} \right]_{,i} .
 \end{aligned}$$

Setting  $q_i = v_i \phi S$ ,

$$\begin{aligned}
 \text{div } (J\phi S) &= \frac{C}{\sqrt{g}} \left( \frac{\sqrt{g} q_i}{h_i^2} \right)_{,i} + \frac{q_i}{h_i^2} C_{,i} - \\
 &\quad \frac{1}{\sqrt{g}} \left[ \frac{\sqrt{g} \phi S}{h_i^2} \left\{ \lambda V C_{,i} + 2\mu \frac{v_i v_j}{V h_j^2} C_{,j} + \right. \right. \\
 &\quad \left. \left. D_d T C_{,i} \right\} \right]_{,i} . \tag{B-11}
 \end{aligned}$$

#### CONVECTIVE-DISPERSION EQUATION:

Substituting equation B-11 into B-4, separating derivatives of  $C$  and transferring terms,

$$\begin{aligned}
 (\phi S)_t + \frac{1}{\sqrt{g}} \left( \frac{\sqrt{g} q_i}{h_i^2} \right)_{,i} &= - \frac{\phi S}{C} C_t - \frac{q_i}{C h_i^2} C_{,i} + \frac{1}{C\sqrt{g}} \cdot \\
 &\quad \left[ \frac{\sqrt{g} \phi S}{h_i^2} \left\{ \lambda V C_{,i} + \frac{2\mu v_i v_j}{V h_j^2} C_{,j} + D_d T C_{,i} \right\} \right]_{,i} \tag{B-12}
 \end{aligned}$$

where the summation is performed both on  $i$  and  $j$ , except in  $h_i^2$  and  $h_j^2$ .

It is to be noted here that the L.H.S. of equations A-7 and B-12 are the same. Therefore, equating the R.H.S. of both and collecting like terms,

$$\begin{aligned} \left( \frac{\phi S}{C} C_t - \frac{\phi S}{\rho} \rho_t \right) &= -q_i \left( \frac{1}{C h_i^2} C_{,i} - \frac{1}{\rho h_i^2} \rho_{,i} \right) + \\ &\frac{1}{C \sqrt{g}} \left[ \frac{\sqrt{g} \phi S}{h_i^2} \left\{ \lambda V C_{,i} + \frac{2\mu v_i v_i}{V h_j^2} C_{,j} + D_d T C_{,i} \right\} \right]_{,i} \\ \text{or } \phi S \left[ C_t - \frac{C}{\rho} \rho_t \right] &= \frac{1}{\sqrt{g}} \left[ \frac{\sqrt{g} \phi S}{h_i^2} \left\{ \lambda V C_{,i} + \frac{2\mu v_i v_j}{V h_j^2} C_{,j} + \right. \right. \\ &\left. \left. D_d T C_{,i} \right\} \right]_{,i} - \frac{q_i}{h_i^2} \left[ C_{,i} + \frac{C}{\rho} \rho_{,i} \right] \quad . \quad (B-13) \end{aligned}$$

Substituting values of  $\rho_t$  and  $\rho_{,i}$  from equation A-11 and transferring terms,

$$\begin{aligned} \phi S \left( C_t - \frac{C}{\rho} \beta \rho_o P_t - \frac{C}{\rho} \alpha C_t \right) &= DD_i - \frac{q_i}{h_i^2} \left[ C_{,i} - \right. \\ &\left. \frac{C}{\rho} \beta \rho_o P_{,i} - \frac{C}{\rho} \alpha C_{,i} \right] \end{aligned}$$

where,

$$DD_i = \frac{1}{\sqrt{g}} \left[ \frac{\sqrt{g} \phi S}{h_i^2} \left\{ \lambda V C_{,i} + \frac{2\mu v_i v_j}{V h_j^2} C_{,j} + D_d T C_{,i} \right\} \right]_{,i}$$

Therefore,

$$C_t = \frac{\rho}{\rho - \alpha C} \frac{DD_i}{\phi S} - \frac{v_i}{h_i^2} C_{,i} + \frac{\rho_0 C \beta}{\rho - \alpha C} (P_t + \frac{v_i}{h_i^2} P_{,i}) \quad (B-14)$$

Assuming that,

- (i) Medium is completely saturated so that  $S=1$ ,
- (ii) Terms containing fluid compressibility and the derivatives of pressure are small as compared to the other terms and so may be neglected,

equation B-14 reduces to,

$$C_t = \frac{\rho}{\rho - \alpha C} \frac{1}{\phi \sqrt{g}} \left[ \frac{\sqrt{g} \phi}{h_i^2} \left\{ \lambda V C_{,i} + \frac{2\mu v_i v_j}{V h_j^2} C_{,j} + D_d T C_{,i} \right\} \right]_{,i} - \frac{v_i}{h_i^2} C_{,i} \quad (B-15)$$

This is the general convective-dispersion equation for an isotropic, saturated porous medium.

For axisymmetric flow towards a well, equation B-15 transforms as follows:

$$C_t = \frac{\rho}{\rho - \alpha C} \left[ \frac{1}{\phi r} \left\{ \phi r \left( \lambda V + 2\mu \frac{u^2}{V} \right) C_r + \frac{2\mu uv}{V} C_z + D_d T C_r \right\} \right]_r + \frac{1}{\phi} \left\{ \phi \left( \lambda V + \frac{2\mu v^2}{V} \right) C_z + \frac{2\mu uv}{V} C_r + D_d T C_z \right\}_z - u C_r - v C_z \quad (B-16)$$



where  $u$  and  $v$  are the velocity components in  $r$  and  $z$  directions respectively.

Also for an isotropic medium,

$$\lambda = a_{II} = \text{Lateral dispersivity of the medium and,}$$

$$\mu = (a_I - a_{II})/2$$

where,

$$a_I = \text{Longitudinal dispersivity of the medium,}$$

$$D_T = \lambda V = a_{II} V = \text{Coefficient of lateral dispersion,}$$

$$2\mu V = (a_I - a_{II}) V = D_L - D_T$$

$$D_L = a_I V = \text{Coefficient of longitudinal dispersion.}$$

Therefore, the expressions for the coefficients of hydrodynamic dispersion may be written as follows:

$$\left. \begin{aligned} D_{11}^* &= \lambda V + 2\mu \frac{u^2}{V^2} + D_d T \\ &= D_T + (D_L - D_T) \frac{u^2}{V^2} + D_d T \\ D_{22}^* &= \lambda V + 2\mu \frac{v^2}{V^2} + D_d T \\ &= D_T + (D_L - D_T) \frac{v^2}{V^2} + D_d T \\ D_{12}^* &= D_{21}^* = \frac{2\mu uv}{V} = (D_L - D_T) \frac{uv}{V^2} \end{aligned} \right\} \quad (B-17)$$

Using the above definitions, equation B-16 may be written as,

$$C_t = \frac{\rho}{\rho - \alpha C} \left[ \frac{1}{\phi r} \{ \phi r (D_{11}^* C_r + D_{12}^* C_z) \}_r + \frac{1}{\phi} \{ \phi (D_{22}^* C_z + D_{12}^* C_r) \}_z \right] - u C_r - v C_z \quad (B-18)$$

Choosing  $\rho_o$ ,  $V_o$  and  $D_o$  as the scaling factors for concentration, velocity and the coefficients of hydrodynamic dispersion or diffusion, in addition to those adopted for non-dimensionalizing the flow equation, such that,

$$V_o = \frac{L_o}{T_o} = \frac{g\rho_o k_o}{\mu_o}$$

and

$$D_o = \frac{L_o^2}{T_o}$$

equation B-18 reduces to the following dimensionless form,

$$\begin{aligned} \bar{C}_{\bar{t}} = \frac{\bar{\rho}}{\phi(\bar{\rho}-\alpha\bar{C})} \left[ \frac{1}{\bar{r}} \{ \phi\bar{r} (\bar{D}_{11} \bar{C}_{\bar{r}} + \bar{D}_{12} \bar{C}_{\bar{z}}) \}_{\bar{r}} + \right. \\ \left. (\bar{D}_{22} \phi \bar{C}_{\bar{z}} + \bar{D}_{12} \phi \bar{C}_{\bar{r}})_{\bar{z}} \right] - \bar{u} \bar{C}_{\bar{r}} - \bar{v} \bar{C}_{\bar{z}} \end{aligned} \quad (\text{B-19})$$

where the bar denotes dimensionless variables.

## APPENDIX C

### FINITE ELEMENT FORMULATION FOR THE FLOW EQUATION:

As shown in section 3.5, the flow equation reduces to the following form,

$$\frac{1}{r} (rSH_r)_r + (SH_z)_z - y_t = 0 \quad (C-1)$$

where the subscript denotes derivative with respect to that variable.

Following the Galerkin approach with arbitrary weighting functions  $W_p$ , ( $p = i, j, k$ ) and equating the integrated values of the weighted residuals to zero, the following equations are obtained,

$$\iiint_V W_p \left[ \frac{1}{r} (rSH_r)_r + (SH_z)_z - y_t \right] r \, dr \, d\theta \, dz = 0 \quad (C-2)$$

Using divergence theorem to reduce the order of differentials and collecting the resulting volume and surface integrals separately, equation C-2 transforms as follows:

$$\begin{aligned} \iiint_V \left[ SH_r (W_p)_r + SH_z (W_p)_z + W_p y_t \right] r \, dr \, d\theta \, dz = \\ \iint_S W_p SH_r n^1 \, dS + \iint_S W_p SH_z n^3 \, dS \end{aligned} \quad (C-3)$$

where  $n^1$  and  $n^3$  are the unit outward normals to the surface  $dS$ .

Referring to Fig. C-1 where the flow region has been shown with all its bounding surfaces and assuming that the boundaries  $c_4$  and  $c_5$  lie on the same vertical surface, the following boundary conditions will

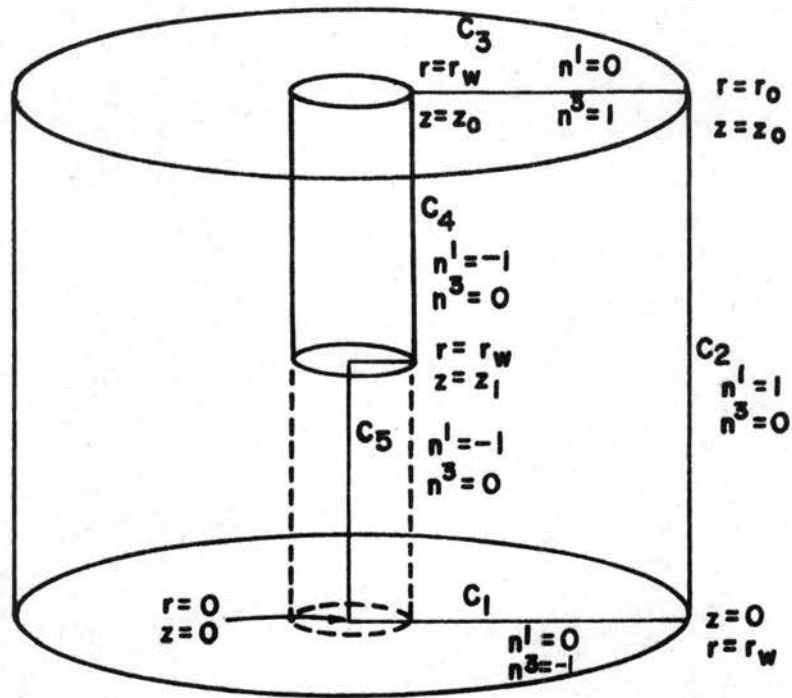


Fig. C.1 Schematic of Flow Boundaries

apply to the problem under investigation:

- (i)  $c_1$  and  $c_2$  are geometric boundaries where the values of  $H$  are specified as,

$$H = H_1(r, z) \quad \forall \quad t \geq 0 \quad .$$

As will be seen in subsequent discussion, prior knowledge of the R.H.S. of equation C-3 is not necessary for such boundaries.

- (ii)  $c_3$  and  $c_5$  are natural boundaries, the former being the upper confining layer of the flow region and the latter being a vertical stream line due to radial symmetry. Thus,

$$\begin{aligned} SH_r &= 0 \quad \forall \quad t \geq 0 \quad \text{along } c_5 \\ SH_z &= 0 \quad \forall \quad t \geq 0 \quad \text{along } c_3 \quad . \end{aligned}$$

It, therefore, follows that the R.H.S. of equation C-3 reduces to zero on both these boundaries.

- (iii)  $c_4$  is the well face so that,

$$\begin{aligned} SH_z &= 0 \quad \forall \quad t \geq 0 \\ \text{and } SH_r &= -\rho q \quad \forall \quad t \geq 0 \quad . \end{aligned}$$

In order to apply equation C-3 to all the elements in the flow region, it is better for convenience of numerical computation, to work in terms of local coordinates referred to the centroid of each element as the origin. Thus introducing the above boundary conditions for any triangular element  $m$ , whose centroid is represented by the global coordinates  $\bar{r}^m$  and  $\bar{z}^m$ , equation C-3 transforms as follows:

$$\iint_{R^m} [ SH_\xi (W_p)_\xi + SH_\eta (W_p)_\eta + W_p y_t ] (\bar{r}^m + \xi) d\xi d\eta =$$

$$\int_{S_2^m} W_p \rho q r_w d\eta + [R] \quad (C-4)$$

where,

[R] refers to the unknown value of the R.H.S. of equation C-3 for the geometric boundaries and is zero everywhere except on the surfaces  $c_1$  and  $c_2$ ,

$R^m$  refers to the area of the  $m^{\text{th}}$  element,

$S_2^m$  refers to the boundary of the  $m^{\text{th}}$  element that lies along the well face and the integral along  $S_2^m$  is zero everywhere except the well boundary  $c_4$ ,

$$\xi = r - \bar{r}^m,$$

$$\eta = z - \bar{z}^m$$

and, taking advantage of radial symmetry, the integral with respect to  $\theta$  has been omitted from both the sides.

Assuming now, that over any triangular element with local coordinates of vertices as  $(\xi_i, \eta_i)$ ,  $(\xi_j, \eta_j)$  and  $(\xi_k, \eta_k)$ , the flow parameter  $H$  may be represented by a first order polynomial,

$$H = \alpha_1 + \alpha_2 \xi + \alpha_3 \eta \quad (\text{C-5})$$

where  $\alpha_1$ ,  $\alpha_2$  and  $\alpha_3$  are unknown coefficients, sometimes referred to as generalized coordinates. Using Cramer's rule to compute the values of these coefficients in terms of the nodal point values  $H_i$ ,  $H_j$  and  $H_k$ , equation C-5 yields,

$$H = [A] \{H\}^m \quad (\text{C-6})$$

where,

$$\begin{aligned}
 [A] &= \text{shape function} \\
 &= [A_i \quad A_j \quad A_k] \\
 A_p &= (a_{1p} + a_{2p}\xi + a_{3p}\eta)/2A^m \quad p=i,j,k \\
 a_{1i} &= \xi_j\eta_k - \eta_j\xi_k \\
 a_{2i} &= \eta_j - \eta_k \\
 a_{3i} &= \xi_k - \xi_j
 \end{aligned} \quad \left. \vphantom{\begin{aligned} A_p \\ a_{1i} \\ a_{2i} \\ a_{3i} \end{aligned}} \right\} \quad (C-7)$$

and values of  $a_{1j}$ ,  $a_{2j}$ ,  $a_{3j}$ ,  $a_{1k}$ ,  $a_{2k}$  and  $a_{3k}$  follow in cyclic sequence.

$$2A^m = \begin{bmatrix} 1 & \xi_i & \eta_i \\ 1 & \xi_j & \eta_j \\ 1 & \xi_k & \eta_k \end{bmatrix}, \quad (C-8)$$

Similarly, assuming that  $y$  also varies linearly over the area of an element, it can be shown that,

$$y = [A] \{y\}^m \quad (C-9)$$

$$\text{and } y_t = [A] \{y_t\}^m \quad (C-10)$$

In view of the continuity property of the shape function  $[A]$ , it is expedient to specify that,

$$w_p = A_p \quad p=i,j,k$$

Substituting the values of  $H$ ,  $A_p$  and  $y_t$  from equations C-6, C-7 and C-10, equation C-4 yields,



$$\int_{R^m} ( [ S [A]_{\xi} (A_p)_{\xi} + S [A]_{\eta} (A_p)_{\eta} ] \{H\}^m + A_p [A] \{y_t\}^m ) \cdot (\bar{r}^m + \xi) d\xi d\eta = \int_{S_2^m} A_p \rho q r w d\eta + [R] \quad (C-11)$$

Recognizing that,

$$\left. \begin{aligned} [A]_{\xi} &= \frac{1}{2A^m} [ a_{2i} \quad a_{2j} \quad a_{2k} ] \\ [A]_{\eta} &= \frac{1}{2A^m} [ a_{3i} \quad a_{3j} \quad a_{3k} ] \\ [A_p]_{\xi} &= \frac{a_{2p}}{2A^m} \\ [A_p]_{\eta} &= \frac{a_{3p}}{2A^m} \end{aligned} \right\} \quad (C-12)$$

evaluating the integrals and writing down three separate equations with the three weighting functions  $A_i$ ,  $A_j$  and  $A_k$  in matrix form, the following system of equations is obtained,

$$\begin{aligned} & [ [SA] + [SC] ] \{H\}^m + [ [SAA] + [SALPHA] + [SBETA] + [SGAMA] \\ & + [STHETA] ] \{y_t\}^m = [Q] + [R] \end{aligned} \quad (C-13)$$

where,

$$[SA] = \frac{s \bar{r}^{-m} A}{4 A^m A^m} \cdot [A_{mn}]$$

A = Area of the element .

$$A_{mn} = a_{2m} a_{2n} \quad n=i,j,k ; m=i,j,k$$

$$[SC] = \frac{s \bar{r}^{-m} A}{4 A^m A^m} [C_{mn}]$$

$$C_{mn} = a_{3m} a_{3n}$$

$$[SAA] = \frac{\bar{r}^{-m}}{4 A^m A^m} [\phi_{mn}]$$

$$[\phi_{mn}] = a_{1m} a_{2n} A + a_{2m} a_{1n} \text{XISQ} + (a_{3m} a_{2n} + a_{2m} a_{3n}) \text{XITA} \\ + a_{3m} a_{3n} \text{TASQ}$$

$$\text{XISQ} = \iint_R \xi^2 d\xi d\eta$$

$$\text{XITA} = \iint_R \xi \eta d\xi d\eta$$

$$\text{TASQ} = \iint_R \eta^2 d\xi d\eta$$

$$[\text{SALPHA}] = \frac{1}{4 A^m A^m} [\alpha_{mn}]$$

$$\alpha_{mn} = (a_{2m} a_{1n} + a_{1m} a_{2n}) \text{XISQ} + (a_{3m} a_{1n} + a_{1m} a_{3n}) \text{XITA}$$

$$[\text{SBETA}] = \frac{\text{EXXET}}{4 A^m A^m} [\beta_{mn}]$$

$$\beta_{mn} = a_{2m} a_{3n} + a_{3m} a_{2n}$$

$$\text{EXXET} = \iint_R \xi^2 \eta d\xi d\eta$$

$$[SGAMA] = \frac{EXXX}{4 A^m A^m} [\gamma_{mn}]$$

$$\begin{aligned} \gamma_{mn} &= a_{2m} a_{2n} \\ EXXX &= \iint_{R^m} \xi^3 d\xi d\eta \end{aligned}$$

$$[STHETA] = \frac{EXETT}{4 A^m A^m} [\theta_{mn}]$$

$$\begin{aligned} \theta_{mn} &= a_{3m} a_{3n} \\ EXETT &= \iint_{R^m} \xi \eta^2 d\xi d\eta \end{aligned}$$

$$[Q] = \begin{bmatrix} q_i^* \\ q_j^* \end{bmatrix} ,$$

$i$  and  $j$  refer respectively to the lower and upper nodes of element  $m$  lying along the well face and,

$$q_i^* = \frac{r_w \rho q}{2} (\eta_j - \eta_i)$$

$$q_j^* = \frac{r_w \rho q}{2} (\eta_j - \eta_i) .$$

In a more compact symbolic form equation C-13 may be expressed as,

$$[FSL] \{H\}^m + [FPLE] \{y_t\}^m = [Q]^m + [R]^m \quad (C-14)$$

where,

$$[FSL] = [SA] + [SC] \quad \text{and}$$

$$[FPLE] = [SAA] + [SALPHA] + [SBETA] + [SGAMA] + [STHETA] .$$

In order to get the contributions pertaining to all the nodes in the system, matrix equations similar to C-14 have to be combined for all

the elements in the layout following the general assembly process of the finite element formulation. Any node common to two or more elements will have non-zero contributions from all such elements and no contribution from the remaining elements. This results in the following system of equations,

$$[SK] \{H\} + [PK] \{y_t\} - [QK] = [R] \quad . \quad (C-15)$$

Considering the solution in the time domain, it follows from the discussion in section 3.6 that equation C-15 may be written as,

$$[SK] \{H\} + E \cdot [PK] \{H_t\} - [QK] = [R] \quad . \quad (C-16)$$

Assuming a linear variation of  $H$  over a small increment of time  $\Delta t$ , the shape function  $[N]$  for the time domain formulation is given by,

$$\begin{aligned} [N] &= [N_0 \quad N_1] \\ &= \left[ \left(1 - \frac{t}{\Delta t}\right) \quad \frac{t}{\Delta t} \right] \end{aligned}$$

where the subscripts  $0$  and  $1$  refer to the time levels  $0$  and  $\Delta t$  respectively. Using the Galerkin approach with  $N_1$  as the weighting function, the following set of equations is obtained,

$$\int_0^{\Delta t} N_1 \left( [SK] \{H\} + E \cdot [PK] \{H_t\} - [QK] - [R] \right) dt = 0 \quad .$$

Recognizing that,

$$\{H_t\} = \frac{1}{\Delta t} [1 \quad -1] \begin{Bmatrix} \{H\}_0 \\ \{H\}_1 \end{Bmatrix} \quad \text{and}$$

$$\{H\} = \frac{1}{\Delta t} [(\Delta t - t) \quad t] \begin{Bmatrix} \{H\}_0 \\ \{H\}_1 \end{Bmatrix} \quad ,$$

the above integration yields,

$$\left[ \frac{2}{3} [\text{SK}] + \frac{E}{\Delta t} [\text{PK}] \right] \{H\}_1 = [R] + [QK] + \left[ \frac{E}{\Delta t} [\text{PK}] - \frac{1}{3} [\text{SK}] \right] \{H\}_0 \quad . \quad (\text{C-17})$$

As an alternative to Galerkin, sub-domain method, Crandall (1956) may be used for the time-domain solution for computational simplicity.

Thus,

$$\int_0^{\Delta t} ( [\text{SK}] \{H\} + E \cdot [\text{PK}] \{H_t\} - [QK] - [R] ) dt = 0 \quad . \quad (\text{C-18})$$

Evaluating the integral using the same interpolation function for H , results in the following:

$$\left[ \frac{1}{2} [\text{SK}] + \frac{E}{\Delta t} \cdot [\text{PK}] \right] \{H\}_1 = [R] + [QK] + \left[ \frac{E}{\Delta t} \cdot [\text{PK}] - \frac{1}{2} [\text{SK}] \right] \{H\}_0 \quad . \quad (\text{C-19})$$

APPENDIX D

FINITE ELEMENT FORMULATION FOR THE CONVECTIVE-DISPERSION EQUATION:

As shown in section 3.8, the convective-dispersion equation reduces to the following form:

$$\frac{1}{r} (r D_{rr} C_r + r D_{rz} C_z)_r + (D_{zz} C_z + D_{rz} C_r)_z - uC_r - vC_z - C_t = 0 \quad (D-1)$$

where  $D_{rr}$ ,  $D_{rz}$  and  $D_{zz}$  are the three coefficients of hydrodynamic dispersion and everywhere else the subscript denotes derivative with respect to that variable. Following the Galerkin approach with arbitrary weighting functions  $W_p$ , ( $p=i,j,k$ ) and equating the integrated values of the weighted residuals to zero, the following equations are obtained,

$$\iiint_V W_p \left[ \frac{1}{r} (r D_{rr} C_r + r D_{rz} C_z)_r + (D_{zz} C_z + D_{rz} C_r)_z - uC_r - vC_z - C_t \right] r dr d\theta dz = 0 \quad (D-2)$$

Using divergence theorem to reduce the order of differentials and collecting the resulting volume and surface integrals separately, equation D-2 transforms as follows:

$$\begin{aligned} & \iiint_V \left[ (W_p)_r (D_{rr} C_r + D_{rz} C_z) + (W_p)_z (D_{zz} C_z + D_{rz} C_r) \right. \\ & \left. + W_p (uC_r + vC_z + C_t) \right] r dr d\theta dz = \\ & \iint_S W_p (D_{rr} C_r + D_{rz} C_z) n^1 dS + \iint_S W_p (D_{zz} C_z + D_{rz} C_r) n^3 dS \end{aligned} \quad (D-3)$$

where  $n^1$  and  $n^3$  are the unit outward normals to the surface  $dS$ . Referring to Fig. C-1 and assuming that the boundaries  $c_4$  and  $c_5$  lie on the same vertical surface, the following boundary conditions will apply to the problem under investigation:

- (i)  $c_1$  and  $c_2$  are geometric boundaries where the values of  $C$  are specified as,

$$C = C_1(r, z) \quad \forall \quad t \geq 0$$

As will be seen in subsequent discussion, prior knowledge of the R.H.S. of equation D-3 is not necessary for such boundaries.

(ii)  $c_3$  and  $c_5$  are natural boundaries, the former being the upper confining layer of the flow region and the latter a vertical stream line due to radial symmetry. Thus,

$$\begin{aligned} D_{rr} C_r + D_{rz} C_z &= 0 & \forall & \quad t \geq 0 \quad \text{along } c_5 \\ D_{rz} C_r + D_{zz} C_z &= 0 & \forall & \quad t \geq 0 \quad \text{along } c_3 \end{aligned}$$

It, therefore, follows that the R.H.S. of equation D-3 reduces to zero on both these boundaries.

(iii)  $c_4$  is the well face so that,

$$\begin{aligned} D_{rz} C_r + D_{zz} C_z &= 0 & \forall & \quad t \geq 0 \\ \text{and } D_{rr} C_r + D_{rz} C_z &= qC \left( \frac{1}{\phi} - 1 \right) & \forall & \quad t \geq 0 \end{aligned}$$

For element to element application of equation D-3, it is more convenient to work in terms of local coordinates referred to the centroid of each element as the origin. Thus introducing the above boundary conditions for any triangular element  $m$ , whose centroid is represented by the global coordinates  $\bar{r}^m$  and  $\bar{z}^m$ , equation D-3 transforms as follows:



$$\begin{aligned}
& \iint_{R^m} [ (W_p)_\xi (D_{rr} C_\xi + D_{rz} C_\eta) + (W_p)_\eta (D_{zz} C_\eta + D_{rz} C_\xi) \\
& \quad + W_p (uC_\xi + vC_\eta + C_t) ] (\bar{r}^m + \xi) d\xi d\eta \\
& = - \int_{S_2^m} W_p q C \left( \frac{1}{\phi} - 1 \right) r_w d\eta + [R] \tag{D-4}
\end{aligned}$$

where,

$R^m$  refers to the area of the  $m^{\text{th}}$  element,

$S_2^m$  refers to the boundary of the  $m^{\text{th}}$  element that lies along the well face and the integral along  $S_2^m$  is non-zero only along the well boundary  $c_4$ ,

[R] refers to the unknown values of the R.H.S. of equation D-3 for the geometric boundaries. Obviously [R] is a null matrix everywhere except along the surfaces  $c_1$  and  $c_2$ ,

$$\xi = r - \bar{r}^m,$$

$$\eta = z - \bar{z}^m,$$

and, taking advantage of radial symmetry, the integral with respect to  $\theta$  has been omitted from both the sides.

Assuming now, that over any triangular element with local coordinates of vertices as  $(\xi_i, \eta_i)$ ,  $(\xi_j, \eta_j)$  and  $(\xi_k, \eta_k)$ , the concentration  $C$  may be represented by a first order polynomial,

$$C = \alpha_1 + \alpha_2 \xi + \alpha_3 \eta, \tag{D-5}$$

where,

$\alpha_1$ ,  $\alpha_2$  and  $\alpha_3$  are unknown coefficients, sometimes referred to as generalized coordinates. Using Cramer's rule to compute the values of these coefficients in terms of the nodal point values  $C_i$ ,  $C_j$  and

$C_k$ , equation D-5 yields,

$$C = [A] \{C\}^m \quad (D-6)$$

where,

[A] = shape function.

This shape function is exactly the same as was obtained for the flow equation in Appendix C. Using this shape function as the weighting function also and substituting values of  $C$ ,  $C_t$  and the derivatives of [A] in equation D-4, the following set is obtained,

$$\begin{aligned} & \iint_{R^m} \{ ((A_p)_\xi [D_{rr} [A]_\xi + D_{rz} [A]_\eta] + (A_p)_\eta [D_{zz} [A]_\eta + D_{rz} [A]_\xi] \\ & + u [A]_\xi A_p + v [A]_\eta A_p ) (\bar{r}^m + \xi) d\xi d\eta \} \{C\}^m \\ & + \iint_{R^m} \{ A_p [A] (\bar{r}^m + \xi) d\xi d\eta \} \{C_t\}^m \\ & = - \int_{S^m} A_p [A] q \left( \frac{1}{\phi} - 1 \right) r_w \{C\}^m d\eta + [R] \quad (D-7) \end{aligned}$$

Evaluating integrals and writing down three separate equations with the three weighting functions  $A_i$ ,  $A_j$  and  $A_k$  in matrix form, the following system of equations is obtained,

$$\begin{aligned} & [ [SA] + [SB] + [SC] + [SF] + [SG] + [SH] + [SI] ] \{C\}^m \\ & + [ [SAA] + [SALPHA] + [SBETA] + [SGAMA] + [STHETA] ] \{C_t\}^m \\ & = - [Q] + [R] \quad (D-8) \end{aligned}$$

where,

$$[SA] = \frac{D_{rr} \bar{r}^m A}{4 A^m A^m} [A_{mn}]$$

$A$ ,  $A^m$  and  $A_{mn}$  have the same values as defined in

## Appendix C.

$$[SB] = \frac{D_{rz} \bar{r}^m A}{4 A^m A^m} [B_{mn}]$$

$$B_{mn} = a_{3m} a_{2n} + a_{2m} a_{3n} \quad n=i,j,k \ ; \ m=i,j,k$$

$$[SC] = \frac{D_{zz} \bar{r}^m A}{4 A^m A^m} [C_{mn}]$$

$C_{mn}$  has the same values as defined in Appendix C.

$$[SF] = \frac{u}{4 A^m A^m} [F_{mn}]$$

$$F_{mn} = a_{2m} a_{2n} \text{XISQ} + a_{3m} a_{2n} \text{XITA}$$

$$[SG] = \frac{v}{4 A^m A^m} [G_{mn}]$$

$$G_{mn} = a_{2m} a_{3n} \text{XISQ} + a_{3m} a_{3n} \text{XITA}$$

$$[SH] = \frac{u \bar{r}^m A}{4 A^m A^m} [H_{mn}]$$

$$H_{mn} = a_{1m} a_{2n}$$

$$[SI] = \frac{v \bar{r}^m A}{4 A^m A^m} [I_{mn}]$$

$$I_{mn} = a_{1m} a_{3n}$$

[SAA] , [SALPHA] , [SBETA] , [SGAMA] and [STHETA] have the

same values as defined in Appendix C.

In a more compact symbolic representation, equation D-8 may be expressed as,

$$[SL] \{C\}^m + [PL] \{C_t\}^m = - [Q]^m + [R]^m \quad (D-9)$$

where,

$$[SL] = [SA] + [SB] + [SC] + [SF] + [SG] + [SH] + [SI]$$

$$[PL] = [SAA] + [SALPHA] + [SBETA] + [SGAMA] + [STHETA]$$

$$[Q]^m = \begin{bmatrix} q_i^* \\ q_j^* \end{bmatrix},$$

$i$  and  $j$  refer respectively to the lower and upper nodes of element  $m$  lying along the well face. Evaluating the integral on the R.H.S. of equation D-7 along the well boundary, yields,

$$q_i^* = r_w q \left( \frac{1}{\phi} - 1 \right) \left( \frac{C_i}{3} + \frac{C_j}{6} \right) (\eta_j - \eta_i)$$

$$q_j^* = r_w q \left( \frac{1}{\phi} - 1 \right) \left( \frac{C_i}{6} + \frac{C_j}{3} \right) (\eta_j - \eta_i) .$$

In order to get the contributions pertaining to all the nodes in the system, matrix equations similar to D-9 have to be combined for all the elements in the layout following the general assembly process of the finite element formulation. Any node common to two or more elements will have non-zero contributions from all such elements and no contribution from the remaining elements. This results in the following system of equations,

$$[SK] \{C\} + [PK] \{C_t\} + [QK] = [R] \quad (D-10)$$

For the time domain solution, following exactly the same approach as was done for the flow equation, the following expression for the weighted residual is obtained,

$$\int_0^{\Delta t} N_1 ( [SK] \{C\} + [PK] \{C_t\} + [QK] - [R] ) dt = 0 \quad . \quad (D-11)$$

Substituting value of the weighting function  $N_1$  from Appendix C, equation D-11 yields,

$$\left[ \frac{2}{3} [SK] + \frac{1}{\Delta t} [PK] \right] \{C\}_1 = [R] - [QK] + \left[ \frac{1}{\Delta t} [PK] - \frac{1}{3} [SK] \right] \{C\}_0 \quad . \quad (D-12)$$

Alternatively, the sub-domain method gives,

$$\left[ \frac{1}{2} [SK] + \frac{1}{\Delta t} [PK] \right] \{C\}_1 = [R] - [QK] + \left[ \frac{1}{\Delta t} [PK] - \frac{1}{2} [SK] \right] \{C\}_0 \quad . \quad (D-13)$$

APPENDIX E

Rayleigh-Ritz Formulation for the Convective-Dispersion Equation:

Assuming that  $\phi$ ,  $u$ ,  $v$ ,  $D_{11}^*$ ,  $D_{12}^*$  and  $D_{22}^*$  are invariant over an element and that  $C_t$  is invariant over a single time-step, the convective-dispersion equation B-18 may be derived from a variational principle, provided there exists a reducing factor  $A(r,z)$  which satisfies the following system of simultaneous first-order partial differential equations (Hildebrand, 1965),

$$\left. \begin{aligned} D_{rr} A_r + D_{rz} A_z &= \left( \frac{D_{rr}}{r} - u \right) A \\ D_{rz} A_r + D_{zz} A_z &= \left( \frac{D_{rz}}{r} - v \right) A \end{aligned} \right\} \quad (E-1)$$

It can be seen that the common solution of these equations is,

$$A(r,z) = r \exp(\beta)$$

where,

$$\begin{aligned} \beta &= \frac{v D_{rz} - u D_{zz}}{D_{zz} D_{rr} - D_{rz}^2} r + \frac{u D_{rz} - v D_{rr}}{D_{zz} D_{rr} - D_{rz}^2} z \\ &= - \frac{ur + vz}{D_L + D_d T} \cdot \frac{\rho - \alpha C}{\rho} \end{aligned} \quad (E-2)$$

The corresponding J-functional is,

$$\begin{aligned} J &= \iint_{R^m} \left[ \frac{D_{rr}}{2} (C_r)^2 + D_{rz} C_r C_z + \frac{D_{zz}}{2} (C_z)^2 + C C_t \right] r e^\beta dr dz \\ &\quad + \int_{S_2^m} r_w q \left( \frac{1}{\phi} - 1 \right) e^\beta \frac{C^2}{2} dS \end{aligned} \quad (E-3)$$

where the subscripts denote derivatives with respect to those variables,  $R^m$  represents the area of the  $m^{\text{th}}$  element,  $S_2^m$  is the well boundary, if any, included in the boundary of the  $m^{\text{th}}$  element,  $r_w$  is the well radius and,

$$q = \frac{Q_w}{2\pi r_w \text{PENETR}} ,$$

$Q_w$  being the well discharge.

To reduce the expression E-3 into a conveniently tractable minimizing problem, it is expedient to introduce a new concentration parameter  $\psi$ , such that,

$$\psi = C e^{\beta/2} . \quad (\text{E-4})$$

In terms of this parameter,  $\psi$ , equation E-3 transforms to,

$$\begin{aligned} J = \iint_{R^m} [ & \frac{D_{rr}}{2} (\psi_r)^2 + D_{rz} (\psi_r \cdot \psi_z) + \frac{D_{zz}}{2} (\psi_z)^2 + \psi ( \frac{u}{2} \psi_r + \frac{v}{2} \psi_z ) \\ & + \psi^2 f(r,z) + \psi \psi_t ] r dr dz + \int_{S_m} r_w q ( \frac{1}{\phi} - 1 ) \frac{\psi^2}{2} dS \end{aligned} \quad (\text{E-5})$$

and the convective-dispersion equation B-18 transforms to,

$$\begin{aligned} \psi_t + \{ 2 f(r,z) - \frac{u}{2r} \} \psi = & D_{rr} \psi_{rr} + 2D_{rz} \psi_{rz} + D_{zz} \psi_{zz} \\ & + \frac{D_{rr}}{r} \psi_r + \frac{D_{rz}}{r} \psi_z \end{aligned} \quad (\text{E-6})$$

where,

$$f(r,z) = \frac{D_{zz} u^2 + v^2 D_{rr} - 2 u v D_{rz}}{8 (D_{rr} D_{zz} - D_{rz}^2)} . \quad (\text{E-7})$$

That equation E-6 is the Euler equation for the variational functional E-5 may be verified by equating the first variation of J to zero. Thus,

$$\begin{aligned} \delta J = & \iint_{R^m} [ D_{rr} \psi_r \delta \psi_r + D_{rz} \psi_r \delta \psi_z + D_{rz} \psi_z \delta \psi_r + D_{zz} \psi_z \delta \psi_z \\ & + ( \frac{u}{2} \psi_r + \frac{v}{2} \psi_z ) \delta \psi + \psi \frac{u}{2} \delta \psi_r + \psi \frac{v}{2} \delta \psi_z + 2\psi f(r,z) \delta \psi \\ & + \psi_t \delta \psi ] r dr dz + \int_{S_2^m} r_w q ( \frac{1}{\phi} - 1 ) \psi \delta \psi dz = 0 \quad . \quad (E-8) \end{aligned}$$

Using the divergence theorem equation E-8 yields (Ref. Fig. C-1),

$$\begin{aligned} \delta J = & \iint_{R^m} [ - \frac{1}{r} (r D_{rr} \psi_r)_r - \frac{1}{r} (r D_{rz} \psi_r)_z - \frac{1}{r} (r D_{rz} \psi_z)_r \\ & - \frac{1}{r} (r D_{zz} \psi_z)_z + \frac{u}{2} \psi_r + \frac{v}{2} \psi_z - \frac{1}{r} (r \psi \frac{u}{2})_r - \frac{1}{r} (r \psi \frac{v}{2})_z \\ & + 2\psi f(r,z) + \psi_t ] \delta \psi r dr dz + \int_{r_w}^{r_0} - (D_{rz} \psi_r + D_{zz} \psi_z + \psi \frac{v}{2}) \\ & r dr \delta \psi \Big|_{z=0} + \int_{r_w}^{r_0} (D_{rz} \psi_r + D_{zz} \psi_z + \psi \frac{v}{2}) r dr \delta \psi \Big|_{z=z_0} \\ & + \int_0^{z_0} (D_{rr} \psi_r + D_{rz} \psi_z + \psi \frac{u}{2}) r dz \delta \psi \Big|_{r=r_0} + \int_0^{z_1} - (D_{rr} \psi_r \\ & + D_{rz} \psi_z + \psi \frac{u}{2}) r dz \delta \psi \Big|_{r=r_w} + \int_{z_1}^{z_0} - (D_{rr} \psi_r + D_{rz} \psi_z + \psi \frac{u}{2}) \\ & r dz \delta \psi \Big|_{r=r_w} + \int_{z_1}^{z_0} r_w q ( \frac{1}{\phi} - 1 ) \psi dz \delta \psi \Big|_{r=r_w} \quad . \quad (E-9) \end{aligned}$$

The boundary conditions, in terms of the variable  $\psi$  are,



$$(i) \quad D_{rr}\psi_r + D_{rz}\psi_z + u \frac{\psi}{2} = 0 \quad \text{along the natural boundary } c_5 ,$$

$$(ii) \quad D_{rz}\psi_r + D_{zz}\psi_z + v \frac{\psi}{2} = 0 \quad \text{along the natural boundary } c_3 ,$$

$$(iii) \quad D_{rr}\psi_r + D_{rz}\psi_z + \frac{u\psi}{2} - q \left( \frac{1}{\phi} - 1 \right) \psi = 0 \quad \text{along the natural boundary } c_4 ,$$

$$(iv) \quad \delta\psi \text{ is zero along the geometric boundaries } c_1 \text{ and } c_2 .$$

Substituting these boundary conditions in E-9, it is seen that all the line integrals vanish. Therefore,

$$\begin{aligned} & (r D_{rr}\psi_r)_r + (r D_{rz}\psi_r)_z + (r D_{rz}\psi_z)_r + (r D_{zz}\psi_z)_z - \frac{ur}{2} \psi_r - \frac{vr}{2} \psi_z \\ & + (r \psi \frac{u}{2})_r + (r \psi \frac{v}{2})_z - 2\psi r f(r,z) - r \psi_t = 0 \end{aligned} \quad (E-10)$$

which may be verified to be the same as the convective-dispersion equation E-6. Transforming to the local coordinate system equation E-5 becomes,

$$\begin{aligned} J = \iint_{R^m} & \left[ \frac{D_{rr}}{2} (\psi_\xi)^2 + D_{rz} \psi_\xi \psi_\eta + \frac{D_{zz}}{2} \psi_\eta^2 + \psi \left( \frac{u}{2} \psi_\xi + \frac{v}{2} \psi_\eta \right) \right. \\ & \left. + \psi^2 f(r,z) + \psi \psi_t \right] (\xi + \bar{r}^m) d\xi d\eta + \int_{S_2^m} r_w q \left( \frac{1}{\phi} - 1 \right) \frac{\psi^2}{2} d\eta \end{aligned} \quad (E-11)$$

Considering the minimization process,

$$\begin{aligned}
 J_{\psi_p} = & \iint_{R^m} [ D_{rr} \psi_\xi (\psi_\xi) \psi_p + D_{rz} \{ \psi_\xi (\psi_\eta) \psi_p + \psi_\eta (\psi_\xi) \psi_p \} \\
 p=i,j,k & + D_{zz} \psi_\eta (\psi_\eta) \psi_p + \psi \{ \frac{u}{2} (\psi_\xi) \psi_p + \frac{v}{2} (\psi_\eta) \psi_p \} \\
 & + \psi \psi_p \{ \frac{u}{2} \psi_\xi + \frac{v}{2} \psi_\eta \} + \psi \{ \frac{\rho - \alpha c}{\rho} \cdot \frac{u^2 + v^2}{4(D_L + D_d T)} \} \psi \psi_p \\
 & + \psi_t \psi \psi_p ] (\xi + \bar{r}^m) d\xi d\eta + \int_{S_2^m} r_w q \left( \frac{1}{\phi} - 1 \right) \frac{\psi^2}{2} d\eta \Big|_{r=r_w}
 \end{aligned} \tag{E-12}$$

Introducing a shape function such that,

$$\psi = [A] \{\psi\} \tag{E-13}$$

where [A] is as defined earlier and evaluating the surface and line integrals in equation E-12 separately, the following two systems of matrices are obtained:

(i) For the surface integral,

$$\begin{aligned}
 & \frac{\bar{r}^m D_{rr} A}{4 A^m A^m} [a_{2m} \ a_{2n}] + \frac{\bar{r}^m D_{rz} A}{4 A^m A^m} [a_{3m} \ a_{2n} + a_{2m} \ a_{3n}] \\
 & + \frac{\bar{r}^m D_{zz} A}{4 A^m A^m} [a_{3m} \ a_{3n}] + \frac{u}{8 A^m A^m} \{ a_{2m} [a_{2n} \text{ XISQ} + a_{3n} \text{ XITA}] \} \\
 & + \frac{v}{8 A^m A^m} \{ a_{3m} [a_{2n} \text{ XISQ} + a_{3n} \text{ XITA}] \} \\
 & + \frac{u}{8 A^m A^m} [a_{2m} \ a_{2n} \text{ XISQ} + a_{3m} \ a_{2n} \text{ XITA}] \\
 & + \frac{v}{8 A^m A^m} [a_{2m} \ a_{3n} \text{ XISQ} + a_{3m} \ a_{3n} \text{ XITA}]
 \end{aligned}$$

$$\begin{aligned}
& + \frac{u \bar{r}^{-m} A}{8 A^m A^m} [a_{1m} a_{2n} + a_{2m} a_{1n}] + \frac{v \bar{r}^{-m} A}{8 A^m A^m} [a_{1m} a_{3n} + a_{3m} a_{1n}] \\
& + \frac{\rho - \alpha c}{\rho} \cdot \frac{u^2 + v^2}{4(D_d T + D_L)} \{ [SAA] + [SALPHA] + [SBETA] + [SGAMA] \\
& + [STHETA] \} \{\psi\}^m + \{ [SAA] + [SALPHA] + [SBETA] + [SGAMA] \\
& + [STHETA] \} \{\psi_t\}^m \tag{E-14}
\end{aligned}$$

where,  $n=i,j,k$  ;  $m=i,j,k$  and the symbols are as defined in Appendix C.

The expression E-14 may be represented in the following condensed symbolic form,

$$\begin{aligned}
& \{ [SA] + [SB] + [SC] + [SD] + [SE] + [SF] + [SG] + [SH] + [SI] \\
& + \frac{\rho - \alpha c}{\rho} \frac{u^2 + v^2}{4(D_d T + D_L)} [PL] \} \cdot \{\psi\}^m + [PL] \{\psi_t\}^m
\end{aligned}$$

$$\text{or } [SL] \{\psi\}^m + [PL] \{\psi_t\}^m \tag{E-15}$$

where the matrices [SL] and [PL] are symmetric and refer to the  $m^{\text{th}}$  element.

(ii) Considering the contribution of the line integral between the two nodes  $i$  and  $j$  of the  $m^{\text{th}}$  element, which lie along the well face, the linear interpolation of  $\psi$  yields,

$$\psi = [1 \quad \eta] \begin{bmatrix} 1 & 0 \\ -1/\ell & 1/\ell \end{bmatrix} \begin{Bmatrix} \psi_i \\ \psi_j \end{Bmatrix} \tag{E-16}$$

where,  $\eta$  is the distance of the point to which the value  $\psi$  pertains, from the nodal point  $i$ , referred to as origin, and  $\ell = \eta_j - \eta_i$ ,  $\eta_i$  being treated as zero. Thus, the line integral components are,

$$\begin{aligned} [J_{\psi_i 1}^m] &= \int_0^{\ell} r_w q \left( \frac{1}{\phi} - 1 \right) \psi \psi_{\psi_i} d\eta \\ &= r_w q \left( \frac{1}{\phi} - 1 \right) \left( \frac{\psi_i}{3} + \frac{\psi_j}{6} \right) \ell \\ &= q_i^* \end{aligned}$$

and, similarly,

$$\begin{aligned} [J_{\psi_i 2}^m] &= r_w q \left( \frac{1}{\phi} - 1 \right) \left( \frac{\psi_i}{6} + \frac{\psi_j}{3} \right) \ell \\ &= q_j^* \end{aligned}$$

This could be represented by a column matrix as follows:

$$[Q]^m = \begin{Bmatrix} q_i^* \\ q_j^* \\ 0 \end{Bmatrix} \quad . \quad (E-17)$$

Combining the expressions for the surface and line integrals, the following equation in terms of elemental matrices is obtained,

$$[SL] \{\psi\}^m + [PL] \{\psi_t\}^m + [Q]^m = 0 \quad (E-18)$$

which may be assembled for all the elements in the layout to yield,

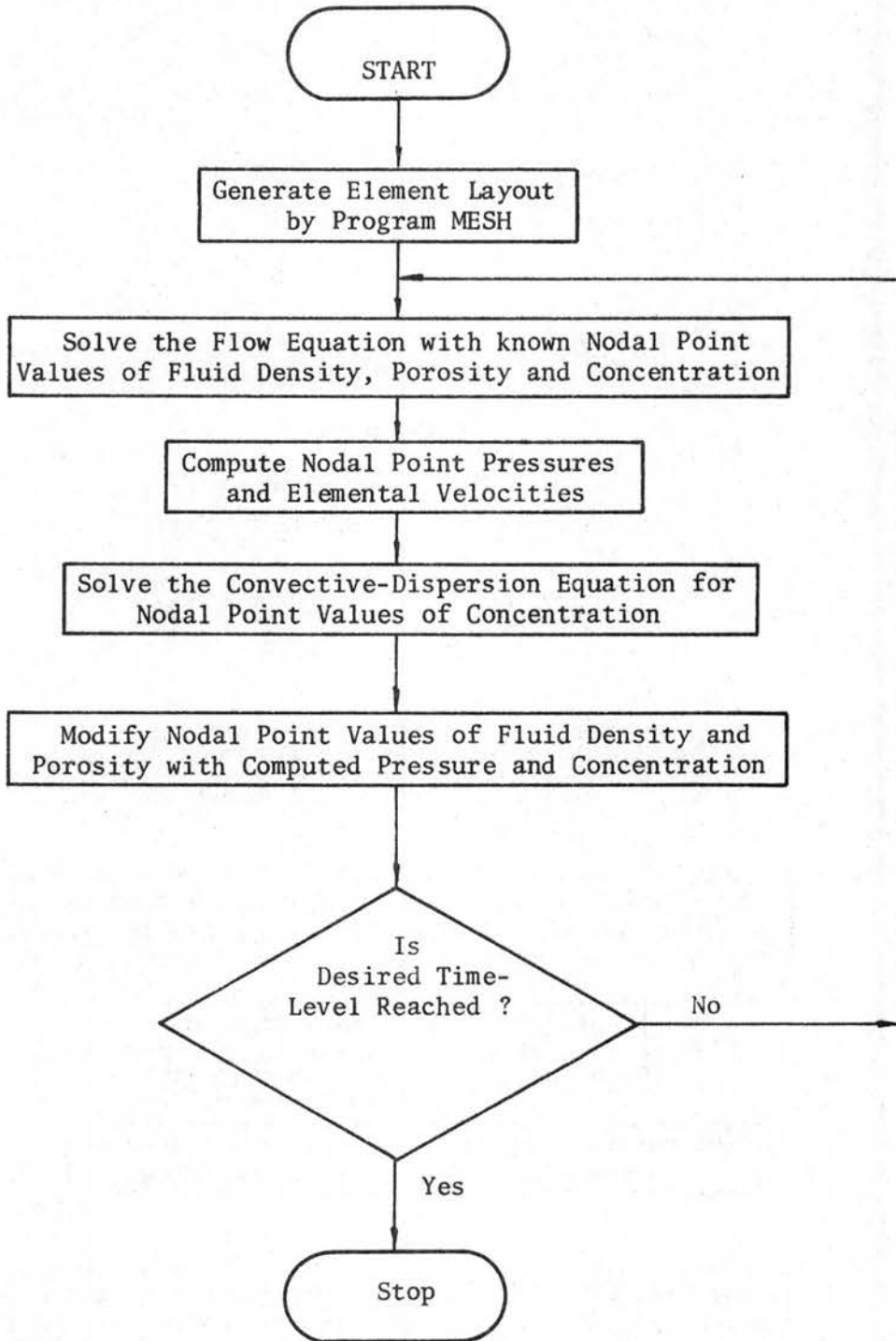
$$[SK] \{\psi\} + [PK] \{\psi_t\} + [QK] = 0 \quad (E-19)$$

where the assembled matrices  $[SK]$  and  $[PK]$  are banded and symmetric.

APPENDIX F

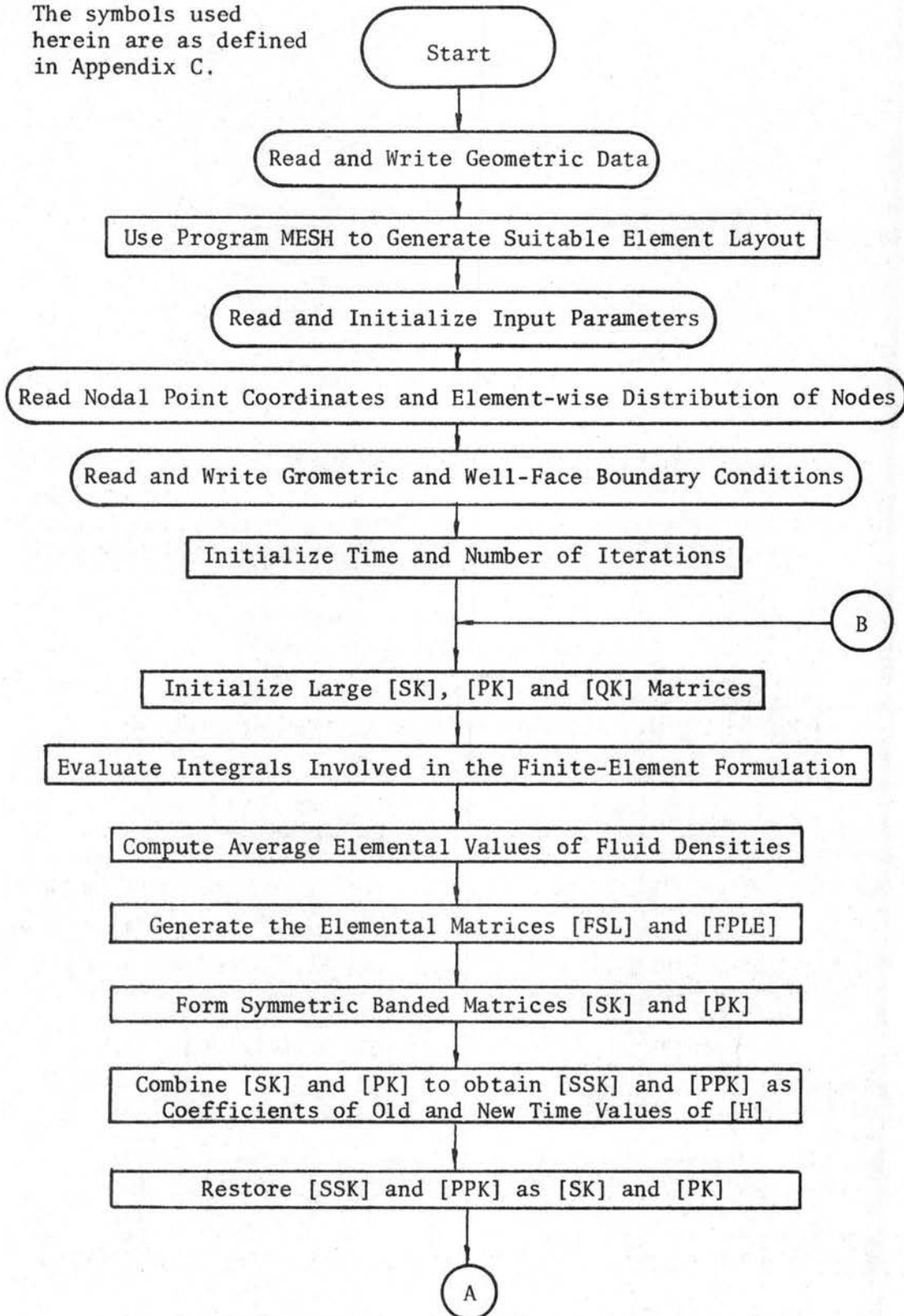
FLOW CHARTS

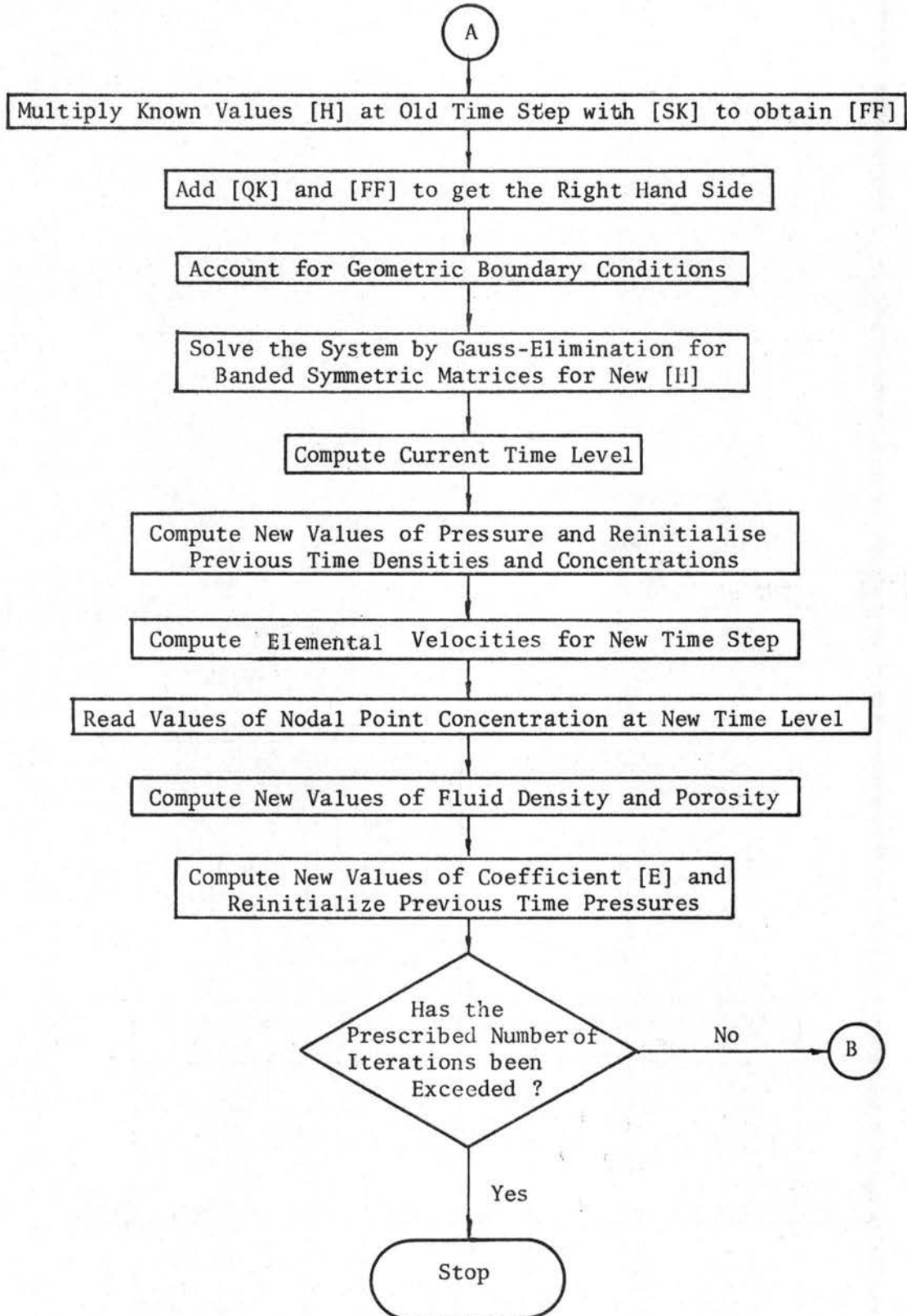
FLOW CHART FOR LEAP-FROG TECHNIQUE



## FLOW CHART FOR PROGRAM FLOW

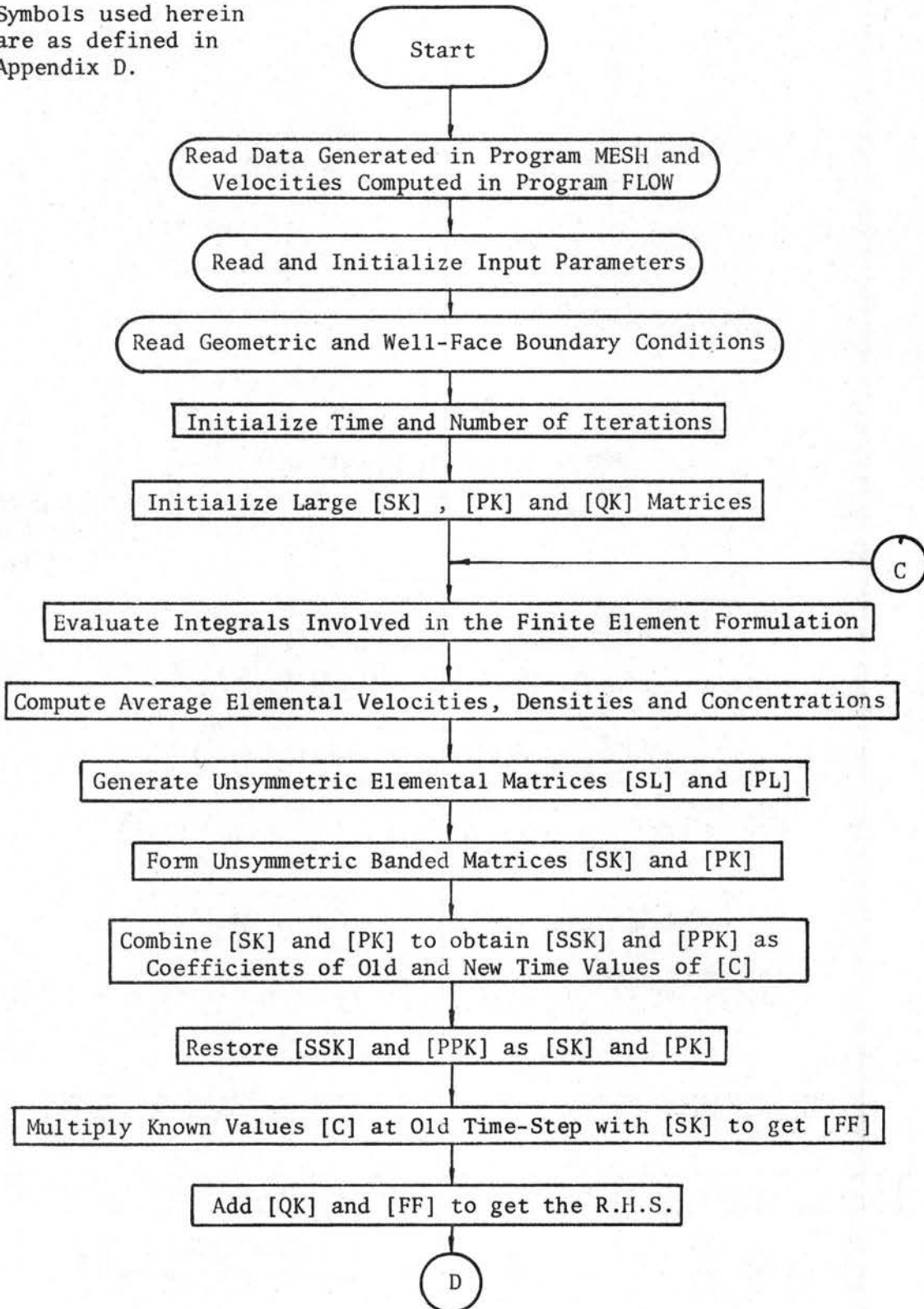
The symbols used herein are as defined in Appendix C.



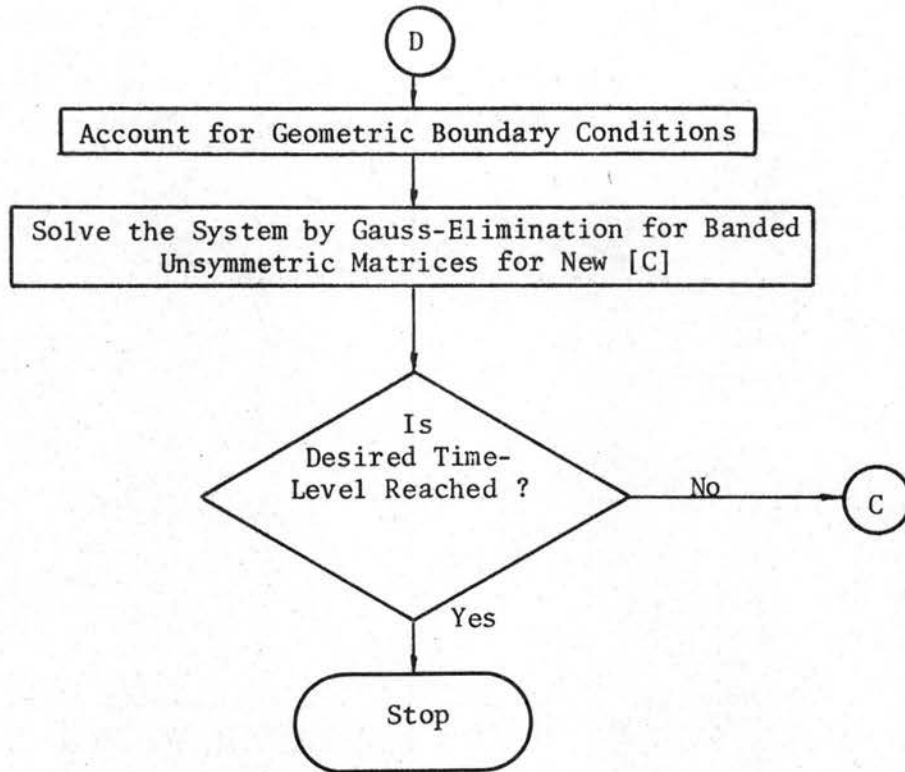


## FLOW CHART FOR PROGRAM DISPER

Symbols used herein  
are as defined in  
Appendix D.







## APPENDIX G

### Program MESH

The data requirements of the program are:

(i)  $NDIVX = N_x$  = Number of divisions of the sides along the x-axis.

(ii)  $NDIVY = N_y$  = Number of divisions of the sides along the y-axis.

(iii)  $XMIN = X_1$  = Minimum value of  $x$  in the layout.

(iv)  $YMIN = Y_1$  = Minimum value of  $y$  in the layout.

(v)  $XMAX = X_3$  = Maximum value of  $x$  in the layout.

(vi)  $YMAX = Y_3$  = Maximum value of  $y$  in the layout.

(vii) Coordinates of eight points  $a, b, c, d, e, f, g$  and  $h$  on the boundary (Fig. G-1) arranged in a counter-clockwise sense. Say,

[  $(x_1, y_1), (x_2, y_2), \dots, (x_7, y_7)$  and  $(x_8, y_8)$  ].

With the above data, the program divides the area into  $N_x \times N_y$  quadrilaterals and joins the shorter diagonal of each to produce a triangular mesh.

For a simple rectangular region, if the boundaries are oriented in such a way that the side with smaller number of divisions is treated as the side along the  $x$ -axis, the program generates a mesh with reasonably small band-width. Depending upon the relative positions of the eight boundary points, the sizes of the elements vary in an arithmetic progression as explained below.

Referring to Fig. G-1, if  $ab < bc$ , the  $x$ -dimension of the elements progressively increases from  $a$  to  $c$ . Similarly, if  $ah < gh$ , the  $y$ -dimension increases from  $a$  to  $g$ . If  $A_x$  and  $A_y$  are the shortest  $x$  and  $y$  dimensions of any element and  $dx$  and  $dy$  are the common differences for the two dimensions, then,

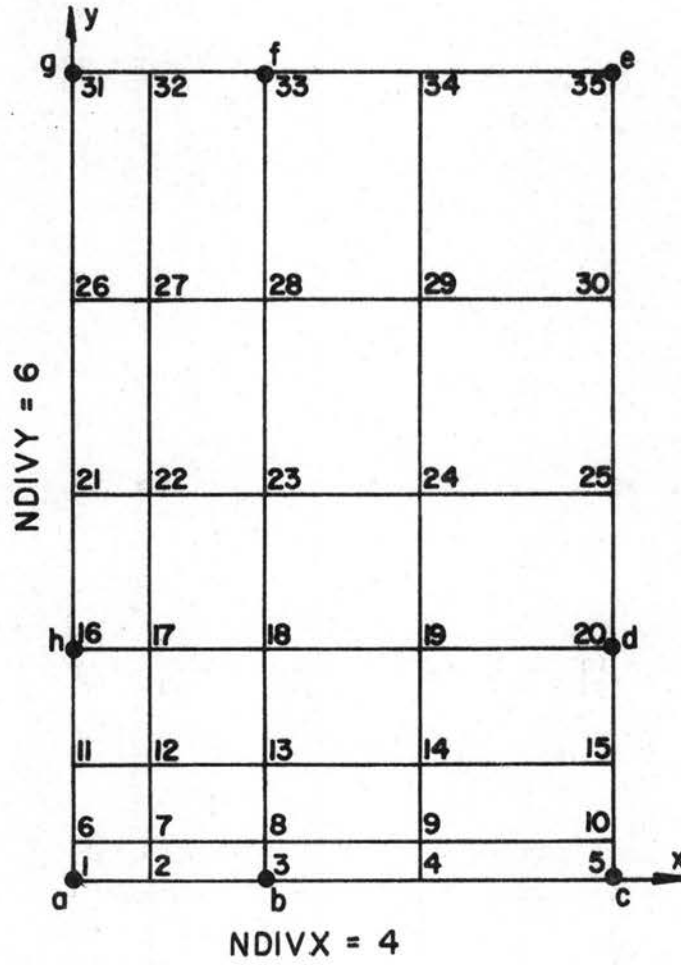


Fig. G.1 Boundary Subdivisions for Program MESH

$$A_x N_x + \frac{N_x - 1}{2} N_x dx = X_3 - X_1 \quad (G-1)$$

$$A_x \frac{N_x}{2} + \left\{ \left( \frac{N_x}{2} - 1 \right) / 2 \right\} \frac{N_x}{2} dx = X_2 - X_1 \quad (G-2)$$

and,

$$A_y N_y + \frac{N_y - 1}{2} N_y dy = Y_3 - Y_1 \quad (G-3)$$

$$A_y \frac{N_y}{2} + \left\{ \left( \frac{N_y}{2} - 1 \right) / 2 \right\} \frac{N_y}{2} dy = Y_3 - Y_1 \quad (G-4)$$

Therefore,

$$dx = 4 (X_3 - 2X_2 + X_1) / N_x^2 \quad (G-5)$$

$$dy = 4 (2Y_2 - Y_3 - Y_1) / N_y^2 \quad (G-6)$$

Knowing  $dx$  and  $dy$ ,  $A_x$  and  $A_y$  may be calculated, the  $x$  and  $y$  dimensions of the elements proceeding from  $a$  to  $c$  and from  $a$  to  $g$  respectively will be,

$$A_x, A_x + dx, A_x + 2dx, \dots, A_x + (N_x - 1) dx \quad \text{and}$$

$$A_y, A_y + dy, A_y + 2dy, \dots, A_y + (N_y - 1) dy$$

Theoretically, any sizes of  $A_x$  and  $A_y$  (as small as required) can be accommodated provided that there is no limitation to the numbers  $N_x$  and  $N_y$  for a given size of the region.

For complex regions, the area is divided into two or more loops for providing different sizes of elements in different portions as shown in Fig. 4.1. The above algorithm is then applied to each loop in succession.

Additional data required for this case are:

(i) NUMLPS = Number of loops, and

(ii) JOIN(I,J,K) array, which for the loops shown in Fig. 4.1 is

defined in the following table.

TABLE G-1

## JOIN(I,J,K) ARRAY

Loop (I) ↓	k=1 Loop No.	k=2 Side No.	k=1 Loop No.	k=2 Side No.	k=1 Loop No.	k=2 Side No.	k=1 Loop No.	k=2 Side No.
1	0	0	0	0	0	0	0	0
2	1	3	0	0	0	0	0	0
3	1	2	0	0	0	0	2	2
Side (J) →	1		2		3		4	

The above table is read as follows:

Side (J) of loop (I) is common with the side given under column k=2 of the loop number given under column k=1. This interconnection is referred only backwards with respect to the loop numbers. Thus sides of loop 1 are entered in the above table as not common (denoted by 0) with those of loops 2 and 3, and sides of loop 2 are entered as common with the sides of loop 1 but not common with those of loop 3.

For multi-loop regions, the above procedure results in a very large band-width. Therefore, two subroutines have been introduced in this program for band-width reduction. The first of these subroutines arranges the data in a form suitable for the application of the second subroutine. The latter subroutine renumbers all the nodes in the system so as to yield a minimum band-width. A listing of this program is given in Appendix H.

APPENDIX H  
PROGRAM LISTINGS

## PROGRAM FFLOW

```

PROGRAM FFLOW (INPUT=101R,PUNCH,OUTPUT=202R,TAPF5=INPUT,TAPF6=OUTP A 10
IUT,TAPER=PUNCH) A 20
COMMON /RLK3/ SK(300,20) A 30
COMMON /RLK4/ PK(300,20) A 40
COMMON /RLK5/ DK(300) A 50
COMMON /RLK6/ NP(450,3),P(300),Z(300) A 60
COMMON /RLK7/ PHI0(300) A 70
COMMON /RLK8/ VR(450),VZ(450),FK(450),RHO(300),C(300) A 80
DIMENSION RLOC(3),ZLOC(3),FPLE(3,3),FSL(3,3),H(300),NPRC(300) A 90
1, HRC(300),PP(300),AP(300),AC(300),E(300),RHOO(300),PPK(300, A 100
225),SSK(300,25),FF(300),KP(450,3),LP(450,3),PL(3,3),SL(3,3), A 110
3 CBC(300) A 120
DATA NUMNP,NUMFL,IRAND,NUMRC,ALPHA,ABETA,CF,DT,AMU,ITT,PENETR,DTV, A 130
1FQ,NRCWL,RW,AL,A11,DD,T,GG,PI/200,312,7,5,74,2,3E-R,6E-R,.1,2,4F A 140
Z=5,500,100,.4,.1,.5,5,.1,0,.0,.5,32,2,3,1415926/ A 150
C THIS PROGRAM SOLVES FLOW AND CONVECTIVE-DISPERSION EQUATIONS IN A 160
C RADIAL COORDINATES. A 170
C NUMNP=NO. OF NODAL POINTS A 180
C NUMFL=NO. OF ELEMENTS A 190
C NP(I,J)=ARRAY GIVING ASSIGNED NO. TO JTH NODE OF ELEMENT NO. I A 200
C VR(I)=VFLOCITY COMPONENT OF ELEMENT NO. I IN R-DIRECTION A 210
C VZ(I)=VFLOCITY COMPONENT OF ELEMENT NO. I IN Z-DIRECTION A 220
C NPBC(N)=0 SIGNIFIES THAT NO R.C. IS SPECIFIED AT NODE NO. N A 230
C NPBC(N)=1 SIGNIFIES THAT R.C. IS GIVEN AT NODE NO. N A 240
C NPBC(N)=2 SIGNIFIES WELL BOUNDARY A 250
C NUMRC= NUMBER OF NODES AT WHICH R.C. IS GIVEN A 260
C NRCWL=NUMBER OF NODAL POINTS ON THE WELL FACE A 270
C RW=RADIUS OF WELL A 280
C PHI0=INITIAL POROSITY A 290
C AMU=DYNAMIC VISCOSITY A 300
C A1=LONGITUDINAL DISPERSIVITY A 310
C A11=TRANSVERSE DISPERSIVITY A 320
C DD=COEFF. OF MOLECULAR DIFFUSION A 330
C T=TORTUOSITY A 340
C DIV=NO. OF DIVISIONS OF PENETRATION DEPTH A 350
C PENETR=DEPTH OF WELL PENETRATION A 360
C DT=TIME INCREMENT. A 370
C CF=AQUIFER COMPRESSIBILITY A 380
C ABETA=FLUID COMPRESSIBILITY A 390
C ALPHA=FACTOR RELATING RHO WITH C A 400
C FQ=WELL DISCHARGE A 410
C FK=INTRINSIC PERMEABILITY A 420
C RHOO=INITIAL FLUID DENSITY A 430
C AP=VALUE OF P AT PREVIOUS TIME A 440
C P=CURRENT VALUE OF PRESSURE A 450
C ITT=NO. OF TIME PERIODS OVER WHICH SOLUTION IS REQUIRED A 460
C A 470
C A 480
C A 490
C A 500
C READ AND INITIALISE DATA A 510
C READ (5,144) (FK(I),I=1,NUMFL) A 510
C READ (5,144) (RHO(I),I=1,NUMNP) A 520
C READ (5,144) (PHI0(I),I=1,NUMNP) A 530
C READ (5,144) (H(I),I=1,NUMNP) A 540
C READ (5,144) (C(I),I=1,NUMNP) A 550
C READ (5,147) (N,Z(N),N=1,NUMNP) A 560
C READ (5,146) (K,KP(K,1),KP(K,2),KP(K,3),KK=1,NUMFL) A 570
C READ (5,146) (L,LP(L,1),LP(L,2),LP(L,3),LL=1,NUMFL) A 580
C A 590
C A 600
C A 610
DZ=PFNETR/DIV
DFQ=- (FQ*DT) / (4.0*P*PENETR)

```

```

M=IRAND A 620
KBAND=(2*M)-1 A 630
DO 101 I=1,NUMNP A 640
HRC(I)=0.0 A 650
NPBC(I)=0 A 660
RHOO(I)=RHOO(I) A 670
CRC(I)=0.0 A 680
101 CONTINUE A 690
C A 700
C READ AND WRITE BOUNDARY CONDITIONS A 710
C A 720
C READ (5,143) (N,NPRC(N),HRC(N),CBC(N),NN=1,NUMRC) A 730
C READ (5,150) (N,NPRC(N),MN=1,NRCWL) A 740
C A 750
C DO 102 I=1,NUMNP A 760
C IF (NPRC(I),FQ,1) H(I)=HRC(I) A 770
C F(I)=RHOO(I)*PHI0(I)*(ABETA+CF) A 780
C AP(I)=H(I)-(RHOO(I)*GG*Z(I)) A 790
102 CONTINUE A 800
TIME=0.0 A 810
KT=0 A 820
INT=10 A 830
INTR=10 A 840
103 KT=KT+1 A 850
JK=1 A 860
104 CONTINUE A 870
JL=0 A 880
105 CONTINUE A 890
JL=JL+1 A 900
IF (JL-1) 109,106,109 A 910
106 CONTINUE A 920
DO 108 N=1,NUMFL A 930
DO 107 J=1,3 A 940
NP(N,J)=KP(N,J) A 950
107 CONTINUE A 960
108 CONTINUE A 970
GO TO 112 A 980
109 CONTINUE A 990
DO 111 N=1,NUMFL A 1000
DO 110 J=1,3 A 1010
NP(N,J)=LP(N,J) A 1020
110 CONTINUE A 1030
111 CONTINUE A 1040
112 CONTINUE A 1050
DO 114 I=1,NUMNP A 1060
IF (NPRC(I),FQ,1) C(I)=CRC(I) A 1070
IF (NPRC(I),EQ,1) H(I)=HRC(I) A 1080
RK(I)=0.0 A 1090
DO 113 J=1,IRAND A 1100
SK(I,J)=0.0 A 1110
PK(I,J)=0.0 A 1120
113 CONTINUE A 1130
114 CONTINUE A 1140
C A 1150
C A 1160
C A 1170
C DO 116 I=1,NUMFL A 1180
C CALL CENTOD (I,RRAR,ZRAR) A 1180
C CALL CLOCAL (I,RRAR,ZRAR,RLOC,ZLOC) A 1190
C CALL AREA (RLOC,ZLOC,AM) A 1200
C CALL TERPAL (RLOC,ZLOC,AM,FXRET,FXXX,FAETT,XISQ,TASO,XITA) A 1210
C CALL PHOSFL (I,PHOFL,PHOFL,RHOO,RHO) A 1220
C IF (JK,NF,1) GO TO 115 A 1230
S=RHOFL*FK(I)/AMU A 1240
CALL FSLPL (RLOC,ZLOC,RRAR,AM,FXRET,FXETT,FXXX,XISQ,XITA,TASO,F A 1250
1 SL,FPLE,S) A 1260
CALL FLSK (FSL,FPLF,I,DFQ,NPRC,RHO) A 1270
GO TO 116 A 1280
115 CONTINUE A 1290

```

```

CALL FLVFL (I,RLOC,ZLOC,H,AMU,AM) A 1300
CALL SLPL (PLOC,ZLOC,PRAR,AM,PL,SL,ALPHA,A1,ND,T,A11,EXXFT,FXX) A 1310
1 EXFTT,RHOEL,XISO,TASO,XITA,I A 1320
CALL SLSK (SL,PL,DFQ,T,NPRC,C,TRAND) A 1330
116 CONTINUE A 1340
C IF (JL,GT,1) GO TO 119 A 1350
C A 1360
DO 118 I=1,NUMNP A 1370
DO 117 J=1,TRAND A 1380
PPK(I,J)=PK(I,J) A 1390
SSK(I,J)=SK(I,J) A 1400
117 CONTINUE A 1410
118 CONTINUE A 1420
GO TO 105 A 1430
119 CONTINUE A 1440
DO 121 I=1,NUMNP A 1450
DO 120 J=1,TRAND A 1460
SK(I,J)=(SSK(I,J)+SK(I,J))/2. A 1470
PK(I,J)=(PPK(I,J)+PK(I,J))/2. A 1480
120 CONTINUE A 1490
121 CONTINUE A 1500
IF (JK,NE,1) GO TO 124 A 1510
DO 123 I=1,NUMNP A 1520
DO 122 J=1,TRAND A 1530
PPK(I,J)=(SK(I,J)/2.0)+(E(I)*PK(I,J)/DT) A 1540
SSK(I,J)=((F(I)*PK(I,J)/DT)-(SK(I,J)/2.0)) A 1550
122 CONTINUE A 1560
123 CONTINUE A 1570
GO TO 127 A 1580
124 CONTINUE A 1590
DO 126 I=1,NUMNP A 1600
DO 125 J=1,TRAND A 1610
PPK(I,J)=(SK(I,J)/2.0)+(PK(I,J)/DT) A 1620
SSK(I,J)=(PK(I,J)/DT)-(SK(I,J)/2.0) A 1630
125 CONTINUE A 1640
126 CONTINUE A 1650
127 CONTINUE A 1660
DO 129 I=1,NUMNP A 1670
DO 128 J=1,TRAND A 1680
PK(I,J)=PPK(I,J) A 1700
SK(I,J)=SSK(I,J) A 1710
128 CONTINUE A 1720
129 CONTINUE A 1730
IF (JK,NE,1) GO TO 133 A 1740
CALL SKPSI (H,NUMNP,TRAND,FF) A 1750
DO 131 I=1,NUMNP A 1760
FF(I)=OK(I)+FF(I) A 1770
C ACCOUNT FOR BOUNDARY CONDITIONS A 1780
C A 1790
IF (NPRC(T)-1) 131,130,131 A 1800
130 PK(I,1)=PK(I,1)*1.0F+50 A 1810
FF(I)=HRC(I)*PK(I,1) A 1820
131 CONTINUE A 1830
CALL GAUSS (NUMNP,IRAND,FF) A 1840
DO 132 I=1,NUMNP A 1850
H(I)=FF(I) A 1860
PP(I)=H(I)-(RHO(T)*GG*Z(I)) A 1870
RHO(I)=RHO(T) A 1880
AC(I)=C(T) A 1890
132 CONTINUE A 1900
C IF (KT,NE,INT) GO TO 137 A 1910
JK=JK+1 A 1920
IRAND=KRAND A 1930
GO TO 104 A 1940
133 CONTINUE A 1950

```

```

CALL SKPSI (C,NUMNP,TRAND,FF) A 1980
DO 135 I=1,NUMNP A 1990
FF(I)=-OK(I)+FF(I) A 2000
C ACCOUNT FOR BOUNDARY CONDITIONS A 2010
C A 2020
IF (NPRC(T)-1) 135,134,135 A 2030
134 PK(I,M)=PK(I,M)*1.0F+50 A 2040
FF(I)=CRC(I)*PK(I,M) A 2050
135 CONTINUE A 2060
CALL BSOLVE (NUMNP,IRAND,FF) A 2070
DO 136 J=1,NUMNP A 2080
C(I)=FF(I) A 2090
136 CONTINUE A 2100
137 CONTINUE A 2110
DO 138 I=1,NUMNP A 2120
RHO(I)=RHO(I)+(ARETA*RHO(I)*(PP(I)-AP(I)))+(ALPHA*(C(I)-AC(I)) A 2130
1 )) A 2140
PHIO(I)=PHIO(I)*(1.+CF*(PP(I)-AP(I))) A 2150
138 CONTINUE A 2160
DO 139 I=1,NUMNP A 2170
F(I)=PHO(I)*PHIO(I)*(ARETA+CF) A 2180
AP(I)=PP(I) A 2190
139 CONTINUE A 2200
TIME=TIME+DT A 2210
IF (KT,NE,INT) GO TO 141 A 2220
INT=INT+INTW A 2230
IRAND=M A 2240
WRITE (6,145) KT,TIME,DT A 2250
WRITE (6,148) A 2260
WRITE (6,142) (H(I),I=1,NUMNP) A 2270
WRITE (6,149) A 2280
WRITE (6,142) (C(I),I=1,NUMNP) A 2290
C CALL SFCOND (R) A 2300
A=SFCOND(R) A 2310
IF (A,LT,500.) GO TO 141 A 2320
WRITE (6,144) (H(I),I=1,NUMNP) A 2330
WRITE (6,144) (C(I),I=1,NUMNP) A 2340
141 CONTINUE A 2350
IF (KT,LT,10) GO TO 103 A 2360
DT=1. A 2370
IF (KT,LT,20) GO TO 103 A 2380
DT=10.0 A 2390
IF (KT,LT,30) GO TO 103 A 2400
DT=100.0 A 2410
IF (KT,LT,40) GO TO 103 A 2420
DT=1000. A 2430
IF (KT,LT,50) GO TO 103 A 2440
DT=10000. A 2450
IF (KT,LT,60) GO TO 103 A 2460
DT=100000. A 2470
IF (KT,LT,70) GO TO 103 A 2480
DT=1000000. A 2490
IF (KT,LT,ITT) GO TO 103 A 2500
STOP A 2510
C 142 FORMAT (5F10.8) A 2520
143 FORMAT (2I10,2F16.8) A 2530
144 FORMAT (5F10.8) A 2540
145 FORMAT (/I20,2F20.3/) A 2550
146 FORMAT (4I10) A 2560
147 FORMAT (I10,2F10.2) A 2570
148 FORMAT (/, 52H A 2580
1+,) A 2590
149 FORMAT (/, 56H A 2600
VALUES OF H A 2610
VALUES OF CONCENTRA A 2620

```



ITION,/)
 150 FORMAT (2I10)
 C
 END

A 2640
 A 2650
 A 2660
 A 2670

### SUBROUTINE CENTOD

SUBROUTINE CFNTOD (M,RRAR,ZRAR) R 10
 C R 20
 C THIS SUBROUTINE COMPUTES COORDINATES OF THE CENTROID OF THE TRIANG R 30
 C ULAR ELEMENT NO. M R 40
 C R 50
 COMMON /RLK6/ NP(450,3),R(300),Z(300) R 60
 I=NP(M,1) R 70
 J=NP(M,2) R 80
 K=NP(M,3) R 90
 RBAR=(R(I)+R(J)+R(K))/3. R 100
 ZBAR=(Z(I)+Z(J)+Z(K))/3. R 110
 RETURN R 120
 C R 130
 END R 140

### SUBROUTINE CLOCAL

SUBROUTINE CLOCAL (M,RRAR,ZBAR,RLOC,ZLOC) C 10
 C C 20
 C THIS SUBROUTINE COMPUTES LOCAL COORDINATES OF THE NODES OF THE TRI C 30
 C ANGULAR ELEMENT NO. M C 40
 C C 50
 COMMON /RLK6/ NP(450,3),R(300),Z(300) C 60
 DIMENSION RLOC(3), ZLOC(3) C 70
 DO 101 L=1,3 C 80
 I=NP(M,L) C 90
 RLOC(L)=R(I)-RRAR C 100
 101 ZLOC(L)=Z(I)-ZBAR C 110
 RETURN C 120
 C C 130
 END C 140

### SUBROUTINE AREA

SUBROUTINE AREA (RLOC,ZLOC,AM) D 10
 C D 20
 C THIS SUBROUTINE CALCULATES AREA OF THE TRIANGULAR ELEMENT NO. M D 30
 C D 40
 DIMENSION RLOC(3), ZLOC(3) D 50
 AM=(RLOC(2)\*ZLOC(3)-RLOC(3)\*ZLOC(2)-RLOC(1)\*ZLOC(3)+RLOC(3)\*ZLOC(1) D 60
 1)+RLOC(1)\*ZLOC(2)-RLOC(2)\*ZLOC(1))/2. D 70
 RETURN D 80
 C D 90
 END D 100

### SUBROUTINE TEGRAL

SUBROUTINE TEGRAL (RLOC,ZLOC,AM,EXXFT,FXXX,EXFTT,XISO,TASQ,XITA) E 10
 COMMON /RLK6/ NP(450,3),R(300),Z(300) E 20
 DIMENSION RLOC(3), ZLOC(3), AJ(3), H(3), AI(3), AS(3) E 30
 AAM=ABS(AM) E 40
 AJ(1)=.1127016654 E 50
 AJ(2)=.5 E 60
 AJ(3)=.8872983346 E 70
 H(1)=.2777777777 E 80
 H(2)=.4444444444 E 90
 H(3)=H(1) E 100
 AI(1)=.0885879595 E 110
 AI(2)=.4094668644 E 120
 AI(3)=.7876594618 E 130
 AS(1)=.2204622112 E 140
 AS(2)=.3881934688 E 150
 AS(3)=.3288443200 E 160
 XITA=0. E 170
 XISO=0. E 180
 TASQ=0. E 190
 EXXET=0. E 200
 EXXX=0. E 210
 EXFTT=0. E 220
 DO 102 I=1,3 E 230
 RL1=AI(I) E 240
 DO 101 J=1,3 E 250
 RL2=AJ(J)\*(-RL1) E 260
 PL3=1.-RL1-RL2 E 270
 W=AS(I)\*H(J)\*(-RL1)\*2.\*AAM E 280
 X=RL1\*RLOC(1)+RL2\*RLOC(2)+RL3\*RLOC(3) E 290
 Y=RL1\*ZLOC(1)+RL2\*ZLOC(2)+RL3\*ZLOC(3) E 300
 XITA=XITA+X\*Y\*W E 310
 XISO=XISO+X\*X\*W E 320
 TASQ=TASQ+Y\*Y\*W E 330
 EXXET=EXXET+X\*X\*Y\*W E 340
 EXXX=EXXX+X\*X\*X\*W E 350
 EXFTT=EXFTT+X\*Y\*Y\*W E 360
 101 CONTINUE E 370
 102 CONTINUE E 380
 RETURN E 390
 C E 400
 END E 410

### SUBROUTINE FSLPL

SUBROUTINE FSLPL (RLOC,ZLOC,RRAR,AM,EXXFT,EXFTT,FXXX,XISO,XITA,TAS F 10
 10,FSL,FPLF,S) F 20
 C F 30
 C THIS SUBROUTINE COMPUTES THE FSL,FPLF,FRHO, AND FPLF MATRICES F 40
 C F 50
 DIMENSION RLOC(3), ZLOC(3), SAA(3,3), SALPHA(3,3), SRFETA(3,3), SGA F 60
 1MA(3,3), STHETA(3,3), SA(3,3), SC(3,3), FPLF(3,3), FSL(3,3) F 70
 XII=RLOC(1) F 80
 XIJ=RLOC(2) F 90
 XIK=RLOC(3) F 100
 TAI=ZLOC(1) F 110
 TAJ=ZLOC(2) F 120
 TAK=ZLOC(3) F 130
 AII=XIJ\*TAK-TAJ\*XIK F 140

```

A2I=TAJ-TAK
A3I=XIK-XIJ
A1J=XIK-TAI-TAK*XII
A2J=TAK-TAI
A3J=XII-XIK
A1K=XII-TAJ-TAI*XIJ
A2K=TAI-TAJ
A3K=XIJ-XII
AAM=ABS(AAM)
C
C COMPUTE ELEMENTS OF SA MATRIX
C
COFSA=(RRAR*S*AM)/(4.0*AM*AM)
SA(1,1)=COFSA*A2I*A2I
SA(1,2)=COFSA*A2I*A2J
SA(1,3)=COFSA*A2I*A2K
SA(2,1)=COFSA*A2J*A2I
SA(2,2)=COFSA*A2J*A2J
SA(2,3)=COFSA*A2J*A2K
SA(3,1)=COFSA*A2K*A2I
SA(3,2)=COFSA*A2K*A2J
SA(3,3)=COFSA*A2K*A2K
C
C COMPUTE ELEMENTS OF SC MATRIX
C
COFSC=COFSA
SC(1,1)=COFSC*A3I*A3I
SC(1,2)=COFSC*A3I*A3J
SC(1,3)=COFSC*A3I*A3K
SC(2,1)=COFSC*A3J*A3I
SC(2,2)=COFSC*A3J*A3J
SC(2,3)=COFSC*A3J*A3K
SC(3,1)=COFSC*A3K*A3I
SC(3,2)=COFSC*A3K*A3J
SC(3,3)=COFSC*A3K*A3K
C
C COMPUTE ELEMENTS OF SAA MATRIX
C
CSAA=AAM
COFSAA=RRAR/(4.0*AM*AM)
SAA(1,1)=(CSAA*A1I*A1I+A2I*A2I*XISO+(A2I*A3I+A3I*A2I)*XITA+A3I*A3I
1*TSQ)*COFSAA
SAA(1,2)=(CSAA*A1J*A1I+A2J*A2I*XISO+(A2J*A3I+A3J*A2I)*XITA+A3J*A3I
1*TSQ)*COFSAA
SAA(1,3)=(CSAA*A1K*A1I+A2K*A2I*XISO+(A2K*A3I+A3K*A2I)*XITA+A3K*A3I
1*TSQ)*COFSAA
SAA(2,1)=(CSAA*A1I*A1J+A2I*A2J*XISO+(A2I*A3J+A3J*A2I)*XITA+A3J*A3J
1*TSQ)*COFSAA
SAA(2,2)=(CSAA*A1J*A1J+A2J*A2J*XISO+(A2J*A3J+A3J*A2J)*XITA+A3J*A3J
1*TSQ)*COFSAA
SAA(2,3)=(CSAA*A1K*A1J+A2K*A2J*XISO+(A2K*A3J+A3K*A2J)*XITA+A3K*A3J
1*TSQ)*COFSAA
SAA(3,1)=(CSAA*A1I*A1K+A2I*A2K*XISO+(A2I*A3K+A3K*A2I)*XITA+A3K*A3K
1*TSQ)*COFSAA
SAA(3,2)=(CSAA*A1J*A1K+A2J*A2K*XISO+(A2J*A3K+A3K*A2J)*XITA+A3K*A3K
1*TSQ)*COFSAA
SAA(3,3)=(CSAA*A1K*A1K+A2K*A2K*XISO+(A2K*A3K+A3K*A2K)*XITA+A3K*A3K
1*TSQ)*COFSAA
C
C COMPUTE ELEMENTS OF SALPHA MATRIX
C
SALPHA(1,1)=(A2I*A1I+A1I*A2I)*XISO+(A3I*A1I+A1I*A3I)*XITA
SALPHA(1,2)=(A2I*A1J+A1I*A2J)*XISO+(A3I*A1J+A1I*A3J)*XITA
SALPHA(1,3)=(A2I*A1K+A1I*A2K)*XISO+(A3I*A1K+A1I*A3K)*XITA
SALPHA(2,1)=(A2J*A1I+A1J*A2I)*XISO+(A3J*A1I+A1J*A3I)*XITA
SALPHA(2,2)=(A2J*A1J+A1J*A2J)*XISO+(A3J*A1J+A1J*A3J)*XITA
SALPHA(2,3)=(A2J*A1K+A1J*A2K)*XISO+(A3J*A1K+A1J*A3K)*XITA
SALPHA(3,1)=(A2K*A1I+A1K*A2I)*XISO+(A3K*A1I+A1K*A3I)*XITA

```

```

F 150
F 160
F 170
F 180
F 190
F 200
F 210
F 220
F 230
F 240
F 250
F 260
F 270
F 280
F 290
F 300
F 310
F 320
F 330
F 340
F 350
F 360
F 370
F 380
F 390
F 400
F 410
F 420
F 430
F 440
F 450
F 460
F 470
F 480
F 490
F 500
F 510
F 520
F 530
F 540
F 550
F 560
F 570
F 580
F 590
F 600
F 610
F 620
F 630
F 640
F 650
F 660
F 670
F 680
F 690
F 700
F 710
F 720
F 730
F 740
F 750
F 760
F 770
F 780
F 790
F 800
F 810
F 820

```

```

SALPHA(3,2)=(A2K*A1J+A1K*A2J)*XISO+(A3K*A1J+A1K*A3J)*XITA
SALPHA(3,3)=(A2K*A1K+A1K*A2K)*XISO+(A3K*A1K+A1K*A3K)*XITA
DO 102 I=1,3
  DO 101 J=1,3
    SALPHA(I,J)=SALPHA(I,J)/(4.0*AM*AM)
101 CONTINUE
102 CONTINUE
C
C COMPUTE ELEMENTS OF SRETA MATRIX
C
COFRTA=EXXET/(4.0*AM*AM)
SRETA(1,1)=COFRTA*(A2I*A3I+A3I*A2I)
SRETA(1,2)=COFRTA*(A2I*A3J+A3I*A2J)
SRETA(1,3)=COFRTA*(A2I*A3K+A3I*A2K)
SRETA(2,1)=COFRTA*(A2J*A3I+A3J*A2I)
SRETA(2,2)=COFRTA*(A2J*A3J+A3J*A2J)
SRETA(2,3)=COFRTA*(A2J*A3K+A3J*A2K)
SRETA(3,1)=COFRTA*(A2K*A3I+A3K*A2I)
SRETA(3,2)=COFRTA*(A2K*A3J+A3K*A2J)
SRETA(3,3)=COFRTA*(A2K*A3K+A3K*A2K)
C
C COMPUTE ELEMENTS OF SGAMA MATRIX
C
COFGMA=EXXX/(4.0*AM*AM)
SGAMA(1,1)=COFGMA*A2I*A2I
SGAMA(1,2)=COFGMA*A2I*A2J
SGAMA(1,3)=COFGMA*A2I*A2K
SGAMA(2,1)=COFGMA*A2J*A2I
SGAMA(2,2)=COFGMA*A2J*A2J
SGAMA(2,3)=COFGMA*A2J*A2K
SGAMA(3,1)=COFGMA*A2K*A2I
SGAMA(3,2)=COFGMA*A2K*A2J
SGAMA(3,3)=COFGMA*A2K*A2K
C
C COMPUTE ELEMENTS OF STHETA MATRIX
C
COFTTA=FXETT/(4.0*AM*AM)
STHETA(1,1)=COFTTA*A3I*A3I
STHETA(1,2)=COFTTA*A3I*A3J
STHETA(1,3)=COFTTA*A3I*A3K
STHETA(2,1)=COFTTA*A3J*A3I
STHETA(2,2)=COFTTA*A3J*A3J
STHETA(2,3)=COFTTA*A3J*A3K
STHETA(3,1)=COFTTA*A3K*A3I
STHETA(3,2)=COFTTA*A3K*A3J
STHETA(3,3)=COFTTA*A3K*A3K
DO 104 I=1,3
  DO 103 J=1,3
C
C COMPUTE ELEMENTS OF FSL MATRIX
C
FSL(I,J)=SA(I,J)+SC(I,J)
C
C COMPUTE ELEMENTS OF FPLE AND PFLF MATRICES
C
FPLE(I,J)=SAA(I,J)+SALPHA(I,J)+SRETA(I,J)+SGAMA(I,J)+STHETA(I,J)
1 CONTINUE
103 CONTINUE
104 CONTINUE
RETURN
C
END
F 830
F 840
F 850
F 860
F 870
F 880
F 890
F 900
F 910
F 920
F 930
F 940
F 950
F 960
F 970
F 980
F 990
F 1000
F 1010
F 1020
F 1030
F 1040
F 1050
F 1060
F 1070
F 1080
F 1090
F 1100
F 1110
F 1120
F 1130
F 1140
F 1150
F 1160
F 1170
F 1180
F 1190
F 1200
F 1210
F 1220
F 1230
F 1240
F 1250
F 1260
F 1270
F 1280
F 1290
F 1300
F 1310
F 1320
F 1330
F 1340
F 1350
F 1360
F 1370
F 1380
F 1390
F 1400
F 1410
F 1420
F 1430
F 1440

```

### SUBROUTINE RHOSEL

```

C
C
C
C
C
SUBROUTINE RHOSEL (M,RHOFL,RHOEL,RHO,RHO)
G 10
R 20
THIS SUBROUTINE COMPUTES THE AVERAGE RHO VALUES APPLICABLE TO THE
ELEMENT M
G 30
R 40
G 40
R 50
COMMON /RLK6/ NP(450,3),P(300),Z(300)
R 60
DIMENSION RHO0(300), RHO(300)
R 70
I=NP(M,1)
R 80
J=NP(M,2)
R 90
K=NP(M,3)
R 100
RHOEL=(RHO(I)+RHO(J)+RHO(K))/3.
G 110
RHOEL=(RHO0(I)+RHO0(J)+RHO0(K))/3.
R 120
RETURN
G 130
R 140
END
G 150

```

### SUBROUTINE FLSLK

```

C
C
C
C
C
SUBROUTINE FLSLK (FSL,FPLF,M,DFQ,NPRC,RHO)
H 10
M 20
THIS SUBROUTINE PLACES THE SL,PL AND Q MATRICES FOR DIFFERENT FIF-
ENTS INTO THE SK,PK AND Q MATRICES WHICH ARE BANDED AND SYMMETRIC
H 30
M 40
H 50
COMMON /RLK3/ SK(300,20)
H 60
COMMON /PLK4/ PK(300,20)
H 70
COMMON /PLK5/ QK(300)
H 80
COMMON /PLK6/ NP(450,3),P(300),Z(300)
H 90
DIMENSION FSL(3,3), FPL(3,3), Q(3), NPHC(300), KP(300), RHO(300)
H 100
I=NP(M,1)
H 110
LL=NP(M,2)
H 120
NN=NP(M,3)
H 130
KP(II)=0
H 140
KP(LL)=0
H 150
KP(NN)=0
H 160
IF (NPRC(II).NE.2.OR.NPRC(LL).NE.2) GO TO 101
H 170
KP(II)=1
H 180
KP(LL)=1
H 190
IF (Z(II).GT.Z(LL)) DFQ=-DFQ
H 200
101 IF (NPRC(II).NE.2.OR.NPRC(NN).NE.2) GO TO 102
H 210
KP(II)=1
H 220
KP(NN)=1
H 230
IF (Z(II).GT.Z(NN)) DFQ=-DFQ
H 240
102 IF (NPRC(LL).NE.2.OR.NPRC(NN).NE.2) GO TO 103
H 250
KP(LL)=1
H 260
KP(NN)=1
H 270
IF (Z(LL).GT.Z(NN)) DFQ=-DFQ
H 280
103 CONTINUE
H 290
DO 105 J=1,3
H 300
Q(J)=0.0
H 310
JJ=NP(M,J)
H 320
IF (KP(JJ).EQ.1) Q(J)=DFQ*RHO(JJ)
H 330
DO 104 K=1,3
H 340
KK=NP(M,K)
H 350
IF (KK.LT.JJ) GO TO 104
H 360
KK=KK-JJ+1
H 370
SK(JJ,KK)=SK(JJ,KK)+FSL(J,K)
H 380
PK(JJ,KK)=PK(JJ,KK)+FPLF(J,K)
H 390

```

```

104 CONTINUE
H 400
105 QK(JJ)=QK(JJ)+Q(J)
H 410
RETURN
H 420
C
H 430
END
H 440

```

### SUBROUTINE FSKPSI

```

C
C
C
C
C
SUBROUTINE FSKPSI (PSI,NR,NC,F)
I 10
I 20
THIS SUBROUTINE MULTIPLIES THE BANDED SYMMETRIC MATRIX SK WITH
MATRIX PSI AND STORES THE RESULT AS MATRIX F
I 30
I 40
I 50
COMMON /RLK3/ SK(300,20)
I 60
DIMENSION PSI(300), F(300)
I 70
DO 102 I=1,NP
I 80
F(I)=PSI(I)*SK(I,1)
I 90
DO 102 K=2,NC
I 100
L=I-K+1
I 110
IF (L.LT.1) GO TO 101
I 120
F(I)=F(I)+PSI(L)*SK(L,K)
I 130
N=I-K-1
I 140
IF (N.GT.NR) GO TO 102
I 150
F(I)=F(I)+PSI(N)*SK(I,K)
I 160
102 CONTINUE
I 170
RETURN
I 180
C
I 190
END
I 200

```

### SUBROUTINE GAUSS

```

C
C
C
C
C
SUBROUTINE GAUSS (NP,NC,F)
J 10
J 20
THIS SUBROUTINE SOLVES A BANDED SYMMETRIC MATRIX BY GAUSS ELIMINA.
J 30
J 40
COMMON /PLK4/ PK(300,20)
J 50
DIMENSION F(300), AF(300)
J 60
NPMI=NP-1
J 70
DO 103 I=1,NPMI
J 80
N=1./PK(I,1)
J 90
JEND=NR-I+1
J 100
IF (JEND.GT.NC) JFND=N*C
J 110
DO 102 J=2,JFND
J 120
NPN=I+J-1
J 130
FAC=PK(I,J)*D
J 140
M=0
J 150
DO 101 K=J,JFND
J 160
M=M+1
J 170
PK(NPN,M)=PK(NPN,M)-PK(I,K)*FAC
J 180
101 CONTINUE
J 190
F(NPN)=F(NPN)-F(I)*FAC
J 200
PK(I,J)=FAC
J 210
102 CONTINUE
J 220
F(I)=F(I)*D
J 230
103 CONTINUE
J 240
F(NR)=F(NR)/PK(NR,1)
J 250
C
J 260

```

```

C BACK SUBSTITUTION J 270
C AF(NR)=F(NR) J 280
DO 105 I=1,NPM J 290
  NPN=NR-I J 300
  JEND=NR-NPN+1 J 310
  IF (JFND.GT.NC) JEND=NC J 320
  RHS=F(NPN) J 330
  DO 104 J=2,JFND J 340
    M=NPN+J-1 J 350
    RHS=RHS-PK(NPN,J)*AF(M) J 360
104 CONTINUE J 370
105 AF(NPN)=RHS J 380
DO 106 I=1,NR J 390
106 F(I)=AF(I) J 400
RETURN J 410
C END J 420
      J 430
      J 440

```

### SUBROUTINE ELVEL

```

SUBROUTINE FLVEL (M,RLOC,ZLOC,H,AMU,AM) K 10
COMMON /RLK6/ NP(450,3),P(300),Z(300) K 20
COMMON /RLKR/ VP(450),VZ(450),FK(450),RHO(300),C(300) K 30
DIMENSION RLOC(3), ZLOC(3), H(300) K 40
I=NP(M,1) K 50
J=NP(M,2) K 60
K=NP(M,3) K 70
XII=RLOC(1) K 80
XIJ=RLOC(2) K 90
XIK=RLOC(3) K 100
TAI=ZLOC(1) K 110
TAJ=ZLOC(2) K 120
TAK=ZLOC(3) K 130
AII=XIJ*TAK-TAJ*XIK K 140
A2I=TAJ-TAK K 150
A3I=XIK-XIJ K 160
A1J=XIK*TAI-TAK*XII K 170
A2J=TAK-TAI K 180
A3J=XII-XIK K 190
A1K=XII*TAJ-TAI*XIJ K 200
A2K=TAI-TAJ K 210
A3K=XIJ-XII K 220
VR(M)=-FK(M)/AMU*((A2I*H(I))+(A2J*H(J))+(A2K*H(K)))/(2.*AM) K 230
VZ(M)=-FK(M)/AMU*((A3I*H(I))+(A3J*H(J))+(A3K*H(K)))/(2.*AM) K 240
RETURN K 250
C END K 260
      K 270

```

### SUBROUTINE SLPL

```

SUBROUTINE SLPL (RLOC,ZLOC,RBAR,AM,PL,SL,ALPHA,A1,DD,T,A11,FXFY,F L 10
IXXX,EXFTT,RHOEL,XISO,TASO,XITA,M) L 20
COMMON /RLKR/ VP(450),VZ(450),FK(450),RHO(300),C(300) L 30
L 40
C THIS SUBROUTINE COMPUTES THE SL AND PL MATRICES L 50
C L 60

```

```

DIMENSION RLOC(3), ZLOC(3), PL(3,3), SL(3,3), SA(3,3), SH(3,3), SC L 70
I(3,3), SF(3,3), SG(3,3), SH(3,3), SI(3,3), SAA(3,3), SALPHA(3,3), L 80
PSRETA(3,3), SGAMA(3,3), STHETA(3,3) L 90
XII=RLOC(1) L 100
XIJ=RLOC(2) L 110
XIK=RLOC(3) L 120
TAI=ZLOC(1) L 130
TAJ=ZLOC(2) L 140
TAK=ZLOC(3) L 150
AII=XIJ*TAK-TAJ*XIK L 160
A2I=TAJ-TAK L 170
A3I=XIK-XIJ L 180
A1J=XIK*TAI-TAK*XII L 190
A2J=TAK-TAI L 200
A3J=XII-XIK L 210
A1K=XII*TAJ-TAI*XIJ L 220
A2K=TAI-TAJ L 230
A3K=XIJ-XII L 240
AAM=ABS(AM) L 250
VV=SQRT(VR(M)*VR(M)+VZ(M)*VZ(M)) L 260
DRR=A1*VV L 270
DRZ=0.0 L 280
DZZ=0.0 L 290

```

C  
C  
C

### COMPUTE ELEMENTS OF SA MATRIX

```

COFSA=(RRAP*AAM*DRR)/(4.0*AAM*AM) L 300
SA(1,1)=COFSA*A2I*A2I L 310
SA(1,2)=COFSA*A2I*A2J L 320
SA(1,3)=COFSA*A2I*A2K L 330
SA(2,1)=COFSA*A2J*A2I L 340
SA(2,2)=COFSA*A2J*A2J L 350
SA(2,3)=COFSA*A2J*A2K L 360
SA(3,1)=COFSA*A2K*A2I L 370
SA(3,2)=COFSA*A2K*A2J L 380
SA(3,3)=COFSA*A2K*A2K L 390

```

C  
C  
C

### COMPUTE ELEMENTS OF SH MATRIX

```

COFSH=(RRAP*AAM*DRZ)/(4.0*AAM*AM) L 400
SR(1,1)=COFSH*((A3I*A2I)+(A2I*A3I)) L 410
SR(1,2)=COFSH*((A3I*A2J)+(A2I*A3J)) L 420
SR(1,3)=COFSH*((A3I*A2K)+(A2I*A3K)) L 430
SR(2,1)=COFSH*((A3J*A2I)+(A2J*A3I)) L 440
SR(2,2)=COFSH*((A3J*A2J)+(A2J*A3J)) L 450
SR(2,3)=COFSH*((A3J*A2K)+(A2J*A3K)) L 460
SR(3,1)=COFSH*((A3K*A2I)+(A2K*A3I)) L 470
SR(3,2)=COFSH*((A3K*A2J)+(A2K*A3J)) L 480
SR(3,3)=COFSH*((A3K*A2K)+(A2K*A3K)) L 490

```

C  
C  
C

### COMPUTE ELEMENTS OF SC MATRIX

```

COFSC=(RRAP*AAM*DZZ)/(4.0*AAM*AM) L 500
SC(1,1)=COFSC*A3I*A3I L 510
SC(1,2)=COFSC*A3I*A3J L 520
SC(1,3)=COFSC*A3I*A3K L 530
SC(2,1)=COFSC*A3J*A3I L 540
SC(2,2)=COFSC*A3J*A3J L 550
SC(2,3)=COFSC*A3J*A3K L 560
SC(3,1)=COFSC*A3K*A3I L 570
SC(3,2)=COFSC*A3K*A3J L 580
SC(3,3)=COFSC*A3K*A3K L 590

```

C  
C  
C

### COMPUTE ELEMENTS OF SF MATRIX

```

COFSF=VR(M)/(4.0*AAM*AM) L 700
SF(1,1)=COFSF*(A2I*A2I*XISO+A2I*A3I*XITA) L 710
SF(1,2)=COFSF*(A2J*A2I*XISO+A2J*A3I*XITA) L 720
L 730
L 740

```

```

SF(1,3)=COFSF*(A2K*A2I*XISO+A2K*A3I*XITA)
SF(2,1)=COFSF*(A2I*A2J*XISO+A2I*A3J*XITA)
SF(2,2)=COFSF*(A2J*A2J*XISO+A2J*A3J*XITA)
SF(2,3)=COFSF*(A2K*A2J*XISO+A2K*A3J*XITA)
SF(3,1)=COFSF*(A2I*A2K*XISO+A2I*A3K*XITA)
SF(3,2)=COFSF*(A2J*A2K*XISO+A2J*A3K*XITA)
SF(3,3)=COFSF*(A2K*A2K*XISO+A2K*A3K*XITA)
C
C
C
COMPUTE ELEMENTS OF SG MATRIX
COFSG=(V7(M)/(4.0*AM*AM)
SG(1,1)=COFSG*(A3I*A2I*XISO+A3I*A3I*XITA)
SG(1,2)=COFSG*(A3J*A2I*XISO+A3J*A3I*XITA)
SG(1,3)=COFSG*(A3K*A2I*XISO+A3K*A3I*XITA)
SG(2,1)=COFSG*(A3I*A2J*XISO+A3I*A3J*XITA)
SG(2,2)=COFSG*(A3J*A2J*XISO+A3J*A3J*XITA)
SG(2,3)=COFSG*(A3K*A2J*XISO+A3K*A3J*XITA)
SG(3,1)=COFSG*(A3I*A2K*XISO+A3I*A3K*XITA)
SG(3,2)=COFSG*(A3J*A2K*XISO+A3J*A3K*XITA)
SG(3,3)=COFSG*(A3K*A2K*XISO+A3K*A3K*XITA)
C
C
C
COMPUTE ELEMENTS OF SH MATRIX
COFSH=(VR(M)*RRBAR*AM)/(4.0*AM*AM)
SH(1,1)=A1I*A2I*COFSH
SH(1,2)=A1I*A2J*COFSH
SH(1,3)=A1I*A2K*COFSH
SH(2,1)=A1J*A2I*COFSH
SH(2,2)=A1J*A2J*COFSH
SH(2,3)=A1J*A2K*COFSH
SH(3,1)=A1K*A2I*COFSH
SH(3,2)=A1K*A2J*COFSH
SH(3,3)=A1K*A2K*COFSH
C
C
C
COMPUTE ELEMENTS OF SI MATRIX
COFSI=(VZ(M)*RRAR*AM)/(4.0*AM*AM)
SI(1,1)=A1I*A3I*COFSI
SI(1,2)=A1I*A3J*COFSI
SI(1,3)=A1I*A3K*COFSI
SI(2,1)=A1J*A3I*COFSI
SI(2,2)=A1J*A3J*COFSI
SI(2,3)=A1J*A3K*COFSI
SI(3,1)=A1K*A3I*COFSI
SI(3,2)=A1K*A3J*COFSI
SI(3,3)=A1K*A3K*COFSI
C
C
C
COMPUTE ELEMENTS OF SAA MATRIX
COFSAA=PRAR/(4.0*AM*AM)
SAA(1,1)=(AAM*A1I*A1I+A2I*A2I*XISO+(A2I*A3I+A3I*A2I)*XITA+A3I*A3I*
ITASQ)*COFSAA
SAA(1,2)=(AAM*A1J*A1I+A2J*A2I*XISO+(A2J*A3I+A3J*A2I)*XITA+A3J*A3I*
ITASQ)*COFSAA
SAA(1,3)=(AAM*A1K*A1I+A2K*A2I*XISO+(A2K*A3I+A3K*A2I)*XITA+A3K*A3I*
ITASQ)*COFSAA
SAA(2,1)=(AAM*A1I*A1J+A2I*A2J*XISO+(A2I*A3J+A3I*A2J)*XITA+A3I*A3J*
ITASQ)*COFSAA
SAA(2,2)=(AAM*A1J*A1J+A2J*A2J*XISO+(A2J*A3J+A3J*A2J)*XITA+A3J*A3J*
ITASQ)*COFSAA
SAA(2,3)=(AAM*A1K*A1J+A2K*A2J*XISO+(A2K*A3J+A3K*A2J)*XITA+A3K*A3J*
ITASQ)*COFSAA
SAA(3,1)=(AAM*A1I*A1K+A2I*A2K*XISO+(A2I*A3K+A3I*A2K)*XITA+A3I*A3K*
ITASQ)*COFSAA
SAA(3,2)=(AAM*A1J*A1K+A2J*A2K*XISO+(A2J*A3K+A3J*A2K)*XITA+A3J*A3K*
ITASQ)*COFSAA
SAA(3,3)=(AAM*A1K*A1K+A2K*A2K*XISO+(A2K*A3K+A3K*A2K)*XITA+A3K*A3K*

```

```

ITASQ)*COFSAA
C
C
C
COMPUTE ELEMENTS OF SALPHA MATRIX
SALPHA(1,1)=(A2I*A1I+A1I*A2I)*XISO+(A3I*A1I+A1I*A3I)*XITA
SALPHA(1,2)=(A2I*A1J+A1I*A2J)*XISO+(A3I*A1J+A1I*A3J)*XITA
SALPHA(1,3)=(A2I*A1K+A1I*A2K)*XISO+(A3I*A1K+A1I*A3K)*XITA
SALPHA(2,1)=(A2J*A1I+A1J*A2I)*XISO+(A3J*A1I+A1J*A3I)*XITA
SALPHA(2,2)=(A2J*A1J+A1J*A2J)*XISO+(A3J*A1J+A1J*A3J)*XITA
SALPHA(2,3)=(A2J*A1K+A1J*A2K)*XISO+(A3J*A1K+A1J*A3K)*XITA
SALPHA(3,1)=(A2K*A1I+A1K*A2I)*XISO+(A3K*A1I+A1K*A3I)*XITA
SALPHA(3,2)=(A2K*A1J+A1K*A2J)*XISO+(A3K*A1J+A1K*A3J)*XITA
SALPHA(3,3)=(A2K*A1K+A1K*A2K)*XISO+(A3K*A1K+A1K*A3K)*XITA
DO 102 I=1,3
DO 101 J=1,3
SALPHA(I,J)=SALPHA(I,J)/(4.0*AM*AM)
101 CONTINUE
102 CONTINUE
C
C
C
COMPUTE ELEMENTS OF SRETA MATRIX
COFRTA=EXXET/(4.0*AM*AM)
SRETA(1,1)=COFRTA*(A2I*A3I+A3I*A2I)
SRETA(1,2)=COFRTA*(A2I*A3J+A3I*A2J)
SRETA(1,3)=COFRTA*(A2I*A3K+A3I*A2K)
SRETA(2,1)=COFRTA*(A2J*A3I+A3J*A2I)
SRETA(2,2)=COFRTA*(A2J*A3J+A3J*A2J)
SRETA(2,3)=COFRTA*(A2J*A3K+A3J*A2K)
SRETA(3,1)=COFRTA*(A2K*A3I+A3K*A2I)
SRETA(3,2)=COFRTA*(A2K*A3J+A3K*A2J)
SRETA(3,3)=COFRTA*(A2K*A3K+A3K*A2K)
C
C
C
COMPUTE ELEMENTS OF SGAMA MATRIX
COFGMA=FXXX/(4.0*AM*AM)
SGAMA(1,1)=COFGMA*A2I*A2I
SGAMA(1,2)=COFGMA*A2I*A2J
SGAMA(1,3)=COFGMA*A2I*A2K
SGAMA(2,1)=COFGMA*A2J*A2I
SGAMA(2,2)=COFGMA*A2J*A2J
SGAMA(2,3)=COFGMA*A2J*A2K
SGAMA(3,1)=COFGMA*A2K*A2I
SGAMA(3,2)=COFGMA*A2K*A2J
SGAMA(3,3)=COFGMA*A2K*A2K
C
C
C
COMPUTE ELEMENTS OF STHETA MATRIX
COFTTA=FXETT/(4.0*AM*AM)
STHETA(1,1)=COFTTA*A3I*A3I
STHETA(1,2)=COFTTA*A3I*A3J
STHETA(1,3)=COFTTA*A3I*A3K
STHETA(2,1)=COFTTA*A3J*A3I
STHETA(2,2)=COFTTA*A3J*A3J
STHETA(2,3)=COFTTA*A3J*A3K
STHETA(3,1)=COFTTA*A3K*A3I
STHETA(3,2)=COFTTA*A3K*A3J
STHETA(3,3)=COFTTA*A3K*A3K
C
C
C
COMBINE THESE MATRICES TO GET SL AND PL MATRICES

```



```

DO 104 I=1,3          L 2020
  DO 103 J=1,3        L 2030
    PL(I,J)=SAA(I,J)+SALPHA(I,J)+SRETA(I,J)+SGAMA(I,J)+STHETA(I,
1      J)             L 2040
    SL(I,J)=SA(I,J)+SR(I,J)+SC(I,J)+SF(I,J)+SG(I,J)+SH(I,J)+SI(I
1      +J)            L 2050
103 CONTINUE          L 2060
104 CONTINUE          L 2070
RETURN                L 2080
END                    L 2090
                      L 2100
                      L 2110
                      L 2120

```

### SUBROUTINE SLSK

```

SUBROUTINE SLSK (SL,PL,DFQ,M,NPBC,PSI,IRAND) M 10
C THIS SUBROUTINE PLACES THE SL,PL AND Q MATRICES FOR DIFFERENT ELEM M 20
C ENTS INTO THE SK,PK AND Q MATRICES WHICH ARE Banded AND SYMMETRIC M 30
C M 40
COMMON /RLK3/ SK(300,20) M 50
COMMON /RLK4/ PK(300,20) M 60
COMMON /RLK5/ QK(300) M 70
COMMON /RLK6/ NP(450,3),R(300),Z(300) M 80
COMMON /RLK7/ PHI0(300) M 90
DIMENSION SL(3,3), PL(3,3), Q(3), NPROC(300), KP(300), PSIR(300), P
1SI(300) M 100
II=NP(M+1) M 110
LL=NP(M+2) M 120
NN=NP(M+3) M 130
KP(II)=0 M 140
KP(LL)=0 M 150
KP(NN)=0 M 160
IF (NPROC(II).NE.2.OR.NPROC(LL).NE.2) GO TO 101 M 170
KP(II)=1 M 180
KP(LL)=1 M 190
IF (Z(II).GT.Z(LL)) DFQ=-DFQ M 200
PSIR(II)=(PSI(II)/3.0)+(PSI(LL)/6.0) M 210
PSIR(LL)=(PSI(II)/6.0)+(PSI(LL)/3.0) M 220
101 IF (NPROC(II).NE.2.OR.NPROC(NN).NE.2) GO TO 102 M 230
KP(II)=1 M 240
KP(NN)=1 M 250
IF (Z(II).GT.Z(NN)) DFQ=-DFQ M 260
PSIR(II)=(PSI(II)/3.0)+(PSI(NN)/6.0) M 270
PSIR(NN)=(PSI(II)/6.0)+(PSI(NN)/3.0) M 280
102 IF (NPROC(LL).NE.2.OR.NPROC(NN).NE.2) GO TO 103 M 290
KP(LL)=1 M 300
KP(NN)=1 M 310
IF (Z(LL).GT.Z(NN)) DFQ=-DFQ M 320
PSIR(LL)=(PSI(LL)/3.0)+(PSI(NN)/6.0) M 330
PSIR(NN)=(PSI(LL)/6.0)+(PSI(NN)/3.0) M 340
103 CONTINUE M 350
DO 105 J=1,3 M 360
  Q(J)=0.0 M 370
  JJ=NP(M+J) M 380
  IF (KP(JJ).EQ.1) Q(J)=DFQ*PSIR(JJ)*((1./PHI0(JJ))-1.)*2. M 390
  DO 104 K=1,3 M 400
    KK=NP(M+K) M 410
    KK=KK-JJ+((IRAND+1)/2) M 420
    SK(JJ+KK)=SK(JJ+KK)+SL(J,K) M 430
    PK(JJ+KK)=PK(JJ+KK)+PL(J,K) M 440

```

```

104 CONTINUE M 470
105 QK(JJ)=QK(JJ)+Q(J) M 480
RETURN M 490
C M 500
END M 510

```

### SUBROUTINE BSOLVE

```

SUBROUTINE BSOLVE (N,M,V) N 10
COMMON /RLK4/ PK(300,20) N 20
DIMENSION V(300) N 30
C N 40
C BSOLVE WORKS FOR FOR UNSYMMETRIC Banded MATRICES. N 50
C BSOLVE IS EFFECTIVE IN SOLVING THE MATRIX EQUATION AX = R WHEN THE N 60
C MATRIX A IS LARGE AND SPARSE SUCH THAT A NARROW UNSYMMETRIC BAND N 70
C CENTERED ON THE MAIN DIAGONAL INCLUDES ALL THE NON-ZERO ELEMENTS. N 80
C ARGUMENT N IS THE ORDER OF A, AND M IS THE WIDTH OF THE BAND. N 90
C NECESSARILY AN ODD NUMBER OF ELEMENTS. BSOLVE IS VERY EFFICIENT N 100
C BECAUSE IT OPERATES ONLY ON THE BAND PORTION OF MATRIX A, GIVEN N 110
C IN THE N BY M ARRAY PK. THE BAND ELEMENTS OF A GIVEN ROW OF A N 120
C APPEAR IN THE SAME ROW OF PK BUT SHIFTED SUCH THAT ELEMENT A(I,J) N 130
C BECOMES PK(I,J-I*(M+1)/2). ALL BAND ELEMENTS WHETHER ZERO OR NON- N 140
C ZERO MUST BE GIVEN. THE VALUES OF UNDEFINED ELEMENTS OF PK, SUCH N 150
C AS PK(I+1) AND PK(N+M) ETC. ARE IRRELEVANT. THE ARRAY V INITIALLY N 160
C CONTAINS THE VECTOR R. AFTER SOLUTION, THE ARRAY V CONTAINS THE N 170
C ANSWER VECTOR X. THE CONTENTS OF PK ARE DESTROYED DURING SOLUTION N 180
C WHICH IS DONE BY GAUSS ELIMINATION WITH ROW INTERCHANGES, FOLLOWED N 190
C BY RACK SUBSTITUTION. N 200
C THE ROW DIMENSION OF PK AS WELL AS THE DIMENSION OF V MUST BE NO N 210
C LESS THAN N. THE COLUMN DIMENSION OF PK MUST BE NO LESS THAN M. N 220
C SHIFT TOP (M-1)/2 ROWS AND PLACE NEEDED ZEROES N 230
C N 240
C N 250
LR=(M-1)/2 N 260
DO 102 L=1,LR N 270
  IM=LR-L+1 N 280
  DO 102 I=1,IM N 290
    DO 101 J=2,M N 300
      PK(L+J-1)=PK(L,J) N 310
      KN=N-L N 320
      KM=M-J N 330
      PK(L,M)=0.0 N 340
102 PK(KN+1,KM+1)=0.0 N 350
C GAUSS FLIMINATION WITH ROW INTERCHANGES N 360
C N 370
LR=LR+1 N 380
IM=N-1 N 390
DO 112 I=1,IM N 400
  NPIV=I N 410
  LS=I+1 N 420
  DO 104 L=LS,LR N 430
    IF (ABS(PK(L,1))-ABS(PK(NPIV,1))) 104,104,103 N 440
103 CONTINUE N 450
IF (NPIV=I) 107,107,105 N 460
DO 106 J=1,M N 470
  TEMP=PK(I,J) N 480
  PK(I,J)=PK(NPIV,J) N 490
106 PK(NPIV,J)=TEMP N 500
  TEMP=V(I) N 510
  V(I)=V(NPIV) N 520

```

	V(NP1V)=TEMP	N	550
107	V(I)=V(I)/PK(I+1)	N	560
	DO 108 J=2,M	N	570
108	PK(I+J)=PK(I+J)/PK(I+1)	N	580
	DO 110 L=LS,LR	N	590
	TEMP=PK(L+1)	N	600
	V(L)=V(L)-TEMP*V(I)	N	610
	DO 109 J=2,M	N	620
109	PK(L+J-1)=PK(L+J)-TEMP*PK(I+J)	N	630
110	PK(L+M)=0.0	N	640
	IF (LP-N) 111,112,112	N	650
111	LR=LR+1	N	660
112	CONTINUE	N	670
	V(N)=V(N)/PK(N+1)	N	680
C		N	690
C	BACK SUBSTITUTION	N	700
C		N	710
	JM=2	N	720
	DO 115 I=1,IM	N	730
	L=N-I	N	740
	DO 113 J=2,JM	N	750
	KM=L+J	N	760
113	V(L)=V(L)-PK(L+J)*V(KM-1)	N	770
	IF (JM-M) 114,115,115	N	780
114	JM=JM+1	N	790
115	CONTINUE	N	800
	RETURN	N	810
C		N	820
	END	N	830

### SUBROUTINE SKPSI

	SUBROUTINE SKPSI (PSI,NR,NC,F)	0	10
C		0	20
C	THIS SUBROUTINE MULTIPLIES THE BANDED SYMMETRIC MATRIX SK WITH	0	30
C	MATRIX PSI AND STORES THE RESULT AS MATRIX F	0	40
C		0	50
	COMMON /RLK3/ SK(300,20)	0	60
	DIMENSION PSI(300), F(300)	0	70
	M=(NC+1)/2	0	80
	DO 102 I=1,NR	0	90
	F(I)=PSI(I)*SK(I,M)	0	100
C		0	110
	DO 102 K=2,M	0	120
	L=I-K+1	0	130
	IF (L.LT.1) GO TO 101	0	140
	LL=M-K+1	0	150
	F(I)=F(I)+PSI(L)*SK(I,LL)	0	160
101	N=I+K-1	0	170
	IF (N.GT.NR) GO TO 102	0	180
	NN=K+M-1	0	190
	F(I)=F(I)+PSI(N)*SK(I,NN)	0	200
102	CONTINUE	0	210
	RETURN	0	220
C		0	230
	END	0	240

## PROGRAM MESH

```

PROGRAM MESH7 (INPUT,OUTPUT,PUNCH,F(LMPL,TAPE5=INPUT,TAPE6=OUTPUT,
1TAPE8=PUNCH,DERUG=OUTPUT)
C
C C
C S DFRUG
C S ARRAYS
C
COMMON /PLK1/ JMEN(300),MEWJT(2000),JNT(300)
DIMENSION JT(2000)
C
C READ AND INITIALIZATION OF DATA
C
C READ (5,139) NCON
C WRITE (6,161)
C WRITE (6,139) NCON
C READ (5,139) NUMLPS
C WRITE (6,140)
C WRITE (6,139) NUMLPS
C
C WRITE (6,142)
C READ (5,141) XMIN,XMAX,YMIN,YMAX
C WRITE (6,141) XMIN,XMAX,YMIN,YMAX
C
C WRITE (6,156)
C READ (5,157) IPUNCH
C WRITE (6,157) IPUNCH
C
C DO 101 I=1,NUMLPS
C WRITE (6,143) I
C WRITE (6,145)
C READ (5,144) NDIV(I,1),NDIV(I,2)
C WRITE (6,144) NDIV(I,1),NDIV(I,2)
C
C WRITE (6,146)
C READ (5,147) ((JOIN(I,J,K)+K=1,2),J=1,4)
C WRITE (6,147) ((JOIN(I,J,K)+K=1,2),J=1,4)
C
C WRITE (6,148)
C READ (5,149) (XCOR(I,J),YCOR(I,J),J=1,8)
C WRITE (6,149) (XCOR(I,J),YCOR(I,J),J=1,8)
C
101 CONTINUE
C
102 CONTINUE
C
C DO 103 I=1,NUMLPS
C NDIV(I,3)=NDIV(I,1)
C NDIV(I,4)=NDIV(I,2)
103 CONTINUE
DUM=CHFK(4)
C
C CALCULATE NUMBER OF NODAL POINTS
C
C NUMNP=0
C
C DO 106 I=1,NUMLPS
C NUMNP=NUMNP+(NDIV(I,1)+1)*(NDIV(I,2)+1)
C
C J1=4
C

```

```

DO 105 J=1,4
IF (JOIN(I,J+1),EQ,0) GO TO 104
NUMNP=NUMNP+(NDIV(I,J)+1)
IF (JOIN(I,J1),NE,0) NUMNP=NUMNP+1
104 CONTINUE
J1=J
C
105 CONTINUE
106 CONTINUE
C
KT=1
107 CONTINUE
C
INP=0
C
IEL=0
C
DO 125 I=1,NUMLPS
C
I1=NDIV(I,1)
I2=I1+1
C
I4=NDIV(I,2)
I5=I4+1
C
I7=I2*I5
IA=I1*I4
C
CALCULATE SIDE ARRAYS
C
JRGN=1
JEND=I2
C
J2=I7-I2
J4=I2+1
C
DO 108 J=JRGN,JEND
J4=J4-1
LNR(I,1,J)=J
LNR(I,3,J4)=J2+J
108 CONTINUE
C
C
JRGN=1
JEND=I5
C
J4=I5+1
C
DO 109 J=JRGN,JEND
J4=J4-1
LNR(I,2,J)=J*I2
LNR(I,4,J4)=(J-1)*I2+1
109 CONTINUE
C
C
CALCULATE NPN ARRAY
C
JRGN=1
JEND=I7
C
DO 110 J=JRGN,JEND
NPN(J)=0
110 CONTINUE
C
DO 112 J=1,4
IF (JOIN(I,J+1),EQ,0) GO TO 112

```



```

      J1=JOIN(I,J+1)
      J2=JOIN(I,J+2)
C
      KRGN=1
      KEND=NDIV(I,J)+1
      K2=KEND+1
C
      DO 111 K=KRGN,KEND
        K1=LNP(I,J,K)
        K2=K2-1
        NPN(K1)=LNP(J1,J2,K2)
111      CONTINUE
C
112      CONTINUE
C
      JRGN=1
      JEND=I7
      DO 113 J=JRGN,JEND
        IF (NPN(J),NE,0) GO TO 113
        INP=INP+1
        NPN(J)=INP
113      CONTINUE
C
      WRITE (6,159)
      WRITE (6,158) (NPN(J),J=1,I7)
C
      FORM LNP ARRAY
C
      JRGN=1
      JEND=I2
C
      DO 114 J=JRGN,JEND
        J1=LNP(I+1,J)
        J3=LNP(I+3,J)
C
        LNP(I+1,J)=NPN(J1)
        LNP(I+3,J)=NPN(J3)
114      CONTINUE
C
      JRGN=1
      JFND=I5
C
      DO 115 J=JRGN,JFND
        J2=LNP(I+2,J)
        J4=LNP(I+4,J)
C
        LNP(I+2,J)=NPN(J2)
        LNP(I+4,J)=NPN(J4)
115      CONTINUE
      WRITE (6,159)
      WRITE (6,158) (LNP(I+1,J),J=1,I2)
      WRITE (6,158) (LNP(I+2,J),J=1,I5)
      WRITE (6,158) (LNP(I+3,J),J=1,I2)
      WRITE (6,158) (LNP(I+4,J),J=1,I5)
      WRITE (6,159)
C
      CALCULATE NODAL POINT COORDINATES
C
      O=I1
      DX=1.0/R
      O=I4
      OY=1.0/R

```

```

A 1240
A 1290
A 1300
A 1310
A 1320
A 1330
A 1340
A 1350
A 1360
A 1370
A 1380
A 1390
A 1400
A 1410
A 1420
A 1430
A 1440
A 1450
A 1460
A 1470
A 1480
A 1490
A 1500
A 1510
A 1520
A 1530
A 1540
A 1550
A 1560
A 1570
A 1580
A 1590
A 1600
A 1610
A 1620
A 1630
A 1640
A 1650
A 1660
A 1670
A 1680
A 1690
A 1700
A 1710
A 1720
A 1730
A 1740
A 1750
A 1760
A 1770
A 1780
A 1790
A 1800
A 1810
A 1820
A 1830
A 1840
A 1850
A 1860
A 1870
A 1880
A 1890
A 1900
A 1910

```

```

C
      JRGN=1
      JEND=I5
C
      KRGN=1
      KEND=I2
C
      K1=0
C
      DO 118 J=JRGN,JEND
        P=J-1
        RY=R*DY
C
        DO 117 K=KRGN,KEND
          R=K-1
          RX=R*DX
          RN(1)=+1.0*(1.0-RX)*(1.0-RY)*(1.0-2.0*RX-2.0*RY)
          RN(2)=+4.0*(RX)*(1.0-RX)*(1.0-RY)
          RN(3)=-1.0*(RX)*(1.0-RY)*(1.0-2.0*RX+2.0*RY)
          RN(4)=+4.0*(RX)*(RY)*(1.0-RY)
          RN(5)=-1.0*(RX)*(RY)*(3.0-2.0*RX-2.0*RY)
          RN(6)=+4.0*(RX)*(1.0-RX)*(RY)
          RN(7)=-1.0*(1.0-RX)*(RY)*(1.0+2.0*RX-2.0*RY)
          RN(8)=+4.0*(1.0-RX)*(RY)*(1.0-RY)
          K1=K1+1
          K2=NPN(K1)
          XORD(K2)=0.0
          YORD(K2)=0.0
          DO 116 L=1+R
            XORD(K2)=XORD(K2)+RN(L)*XCOR(I,L)
            YORD(K2)=YORD(K2)+RN(L)*YCOR(I,L)
116          CONTINUE
C
117          CONTINUE
118          CONTINUE
C
      CALCULATION OF NP ARRAY
C
      JRGN=1
      JFND=I4
      KRGN=1
      KEND=I1
C
      DO 124 J=JRGN,JFND
        DO 123 K=KRGN,KEND
C
          IEL=IEL+2
          N1=IEL-1
          N2=IEL
C
          K1=(J-1)*I2+(K-1)+1
          K2=K1+1
          K3=K1+I2
          K4=K3+1
C
          K1=NPN(K1)
          K2=NPN(K2)
          K3=NPN(K3)
          K4=NPN(K4)
C
          O1=(XORD(K4)-XORD(K1))*2+(YORD(K4)-YORD(K1))*2
          O1=O1+0.000001
          O2=(XORD(K3)-XORD(K2))*2+(YORD(K3)-YORD(K2))*2
C
          IF (KT-1) 119,119,120
          CONTINUE
          IF (D2,LT,0) GO TO 122
119

```

```

A 1950
A 1960
A 1970
A 1980
A 1990
A 2000
A 2010
A 2020
A 2030
A 2040
A 2050
A 2060
A 2070
A 2080
A 2090
A 2100
A 2110
A 2120
A 2130
A 2140
A 2150
A 2160
A 2170
A 2180
A 2190
A 2200
A 2210
A 2220
A 2230
A 2240
A 2250
A 2260
A 2270
A 2280
A 2290
A 2300
A 2310
A 2320
A 2330
A 2340
A 2350
A 2360
A 2370
A 2380
A 2390
A 2400
A 2410
A 2420
A 2430
A 2440
A 2450
A 2460
A 2470
A 2480
A 2490
A 2500
A 2510
A 2520
A 2530
A 2540
A 2550
A 2560
A 2570
A 2580
A 2590
A 2600
A 2610

```

```

120      GO TO 121
        CONTINUE
        IF (D2.GE.D1) GO TO 122
121      CONTINUE
C
        NP(N1,1)=K1
        NP(N1,2)=K4
        NP(N1,3)=K3
C
        NP(N2,1)=K1
        NP(N2,2)=K2
        NP(N2,3)=K4
C
        GO TO 123
        CONTINUE
122      CONTINUE
C
        NP(N1,1)=K1
        NP(N1,2)=K2
        NP(N1,3)=K3
C
        NP(N2,1)=K2
        NP(N2,2)=K4
        NP(N2,3)=K3
C
123      CONTINUE
124      CONTINUE
C
125      CONTINUE
        NUMEL=IFL
C
        OUTPUT OF DATA
C
        IF (KT.GT.1) GO TO 130
        DO 126 I=1,NUMEL
          NP(I,4)=0
126      CONTINUE
        K=0
        DO 128 J=1,4
          DO 127 I=1,NUMEL
            K=K+1
            JT(K)=NP(I,J)
127      CONTINUE
128      CONTINUE
        CALL SETUP (NUMNP,NUMEL,NCON,JT,IDIFF)
        CALL OPTNUM (NUMNP,NUMEL,NCON,IDIFF)
        WRITE (6,154)
        WRITE (6,155) NUMNP,NUMEL
        WRITE (6,163)
        WRITE (6,162) (J,JNT(J),J=1,NUMNP)
        WRITE (8,162) (J,JNT(J),J=1,NUMNP)
        WRITE (6,150)
        DO 129 I=1,NUMNP
          WRITE (6,151) JNT(I),XORD(I),YORD(I)
129      CONTINUE
C
130      CONTINUE
        WRITE (6,152)
        DO 131 I=1,NUMEL
          WRITE (6,153) I,(JNT(NP(I,J)),J=1,3)
131      CONTINUE
C
        IF (IPUNCH.NE.R) GO TO 135
        IF (KT.GT.1) GO TO 133
        WRITE (8,155) NUMNP,NUMEL

```

```

A 2620
A 2630
A 2640
A 2650
A 2660
A 2670
A 2680
A 2690
A 2700
A 2710
A 2720
A 2730
A 2740
A 2750
A 2760
A 2770
A 2780
A 2790
A 2800
A 2810
A 2820
A 2830
A 2840
A 2850
A 2860
A 2870
A 2880
A 2890
A 2900
A 2910
A 2920
A 2930
A 2940
A 2950
A 2960
A 2970
A 2980
A 2990
A 3000
A 3010
A 3020
A 3030
A 3040
A 3050
A 3060
A 3070
A 3080
A 3090
A 3100
A 3110
A 3120
A 3130
A 3140
A 3150
A 3160
A 3170
A 3180
A 3190
A 3200
A 3210
A 3220
A 3230
A 3240
A 3250
A 3260
A 3270
A 3280

```

```

        DO 132 I=1,NUMNP
          WRITE (8,151) JNT(I),XORD(I),YORD(I)
132      CONTINUE
133      CONTINUE
        DO 134 I=1,NUMEL
          WRITE (8,153) I,(JNT(NP(I,J)),J=1,3)
134      CONTINUE
135      CONTINUE
        CALL SET (0.0,1.0,0.0,0.0,1.0,XMIN,XMAX,YMIN,YMAX,1)
C
        DO 136 I=1,NUMEL
          I1=NP(I,1)
          I2=NP(I,2)
          I3=NP(I,3)
C
          CALL POINT (XORD(I1),YORD(I1))
          CALL VECTOR (XORD(I2),YORD(I2))
          CALL VECTOR (XORD(I3),YORD(I3))
          CALL VECTOR (XORD(I1),YORD(I1))
136      CONTINUE
C
        CALL FRAME
C
        KT=KT+1
        IF (KT.LE.2) GO TO 107
C
        READ (5,160) IFND
        IF (IFND.EQ.0) GO TO 138
C
        WRITE (6,145)
        DO 137 I=1,NUMLPS
          READ (5,144) NDIV(I,1),NDIV(I,2)
          WRITE (6,144) NDIV(I,1),NDIV(I,2)
137      CONTINUE
C
        GO TO 102
C
138      CONTINUE
C
        STOP
C
        FORMAT STATEMENTS
C
139      FORMAT (I10)
140      FORMAT (10H1 NUMLPS)
141      FORMAT (4F10,3)
142      FORMAT (40H0 XMIN XMAX YMIN YMAX)
143      FORMAT (///1PH LOOP NUMHFR,I5)
144      FORMAT (2I10)
145      FORMAT (20H0NDIV(I,1) NDIV(I,2))
146      FORMAT (20H0 JNT(I,J,K) ARRAY)
147      FORMAT (4(I7,13))
148      FORMAT (20H0 XCOR YCOR)
149      FORMAT (2F10,3)
150      FORMAT (30H0 NP XORD YORD)
151      FORMAT (I10,2F10,3)
152      FORMAT (40H0 FLEM NP )
153      FORMAT (4I9)
154      FORMAT (20H1 NUMNP NUMEL)
155      FORMAT (2I10)
156      FORMAT (10H0 IPUNCH)
157      FORMAT (I10)
158      FORMAT (20I5)
159      FORMAT (1H0)
160      FORMAT (I10)

```

```

A 3290
A 3300
A 3310
A 3320
A 3330
A 3340
A 3350
A 3360
A 3370
A 3380
A 3390
A 3400
A 3410
A 3420
A 3430
A 3440
A 3450
A 3460
A 3470
A 3480
A 3490
A 3500
A 3510
A 3520
A 3530
A 3540
A 3550
A 3560
A 3570
A 3580
A 3590
A 3600
A 3610
A 3620
A 3630
A 3640
A 3650
A 3660
A 3670
A 3680
A 3690
A 3700
A 3710
A 3720
A 3730
A 3740
A 3750
A 3760
A 3770
A 3780
A 3790
A 3800
A 3810
A 3820
A 3830
A 3840
A 3850
A 3860
A 3870
A 3880
A 3890
A 3900
A 3910
A 3920
A 3930
A 3940
A 3950

```

```

161 FORMAT (10H1      NCON)
162 FORMAT (2I10)
163 FORMAT (/, 22H OLD NUMBER NEW NUMBER,/)
C
END

```

```

A 3460
A 3470
A 3480
A 3490
A 4000

```

### SUBROUTINE SETUP

```

SUBROUTINE SETUP (NUMNP,NUMEL,NCON,JT,DIFF)
COMMON /PLK1/ JMEM(300),MEMJT(2000),JNT(300)
DIMENSION JT(2000)
C
C
C
IDIFF=NUMNP
C
DO 101 J=1,NUMNP
101 JMEM(J)=0
DO 106 J=1,NUMFL
DO 105 I=1,4
JNTI=JT(MUMEL*(I-1)+J)
IF (JNTI.EQ.0) GO TO 104
JSUR=(JNTI-1)*NCON
C
DO 104 II=1,4
IF (II.EQ.1) GO TO 104
JJT=JT(NUMFL*(II-1)+J)
IF (JJT.EQ.0) GO TO 105
MEM1=JMEM(JNTI)
IF (MEM1.EQ.0) GO TO 103
C
DO 102 III=1,MEM1
IF (MEMJT(JSUR+III).EQ.JJT) GO TO 104
102 CONTINUE
103 JMEM(JNTI)=JMEM(JNTI)+1
MEMJT(JSUR+JMEM(JNTI))=JJT
IF (IARS(JNTI-JJT).GT.IDIFF) IDIFF=IARS(JNTI-JJT)
104 CONTINUE
105 CONTINUE
106 CONTINUE
RETURN
C
END

```

```

R 10
R 20
R 30
P 40
R 50
R 60
R 70
R 80
R 90
R 100
R 110
R 120
R 130
R 140
R 150
R 160
R 170
R 180
R 190
R 200
R 210
R 220
R 230
R 240
R 250
R 260
R 270
R 280
R 290
R 300
R 310
R 320
R 330
R 340

```

### SUBROUTINE OPTNUM

```

SUBROUTINE OPTNUM (NUMNP,NUMEL,NCON,DIFF)
COMMON /BLK1/ JMEM(300),MEMJT(2000),JNT(300)
DIMENSION JOINT(300), NEWJT(300)
C
C
MINMAX=DIFF
DO 107 IK=1,NUMNP
DO 101 J=1,NUMNP
JOINT(J)=0
101 NEWJT(J)=0
MAX=0
I=1
NEWJT(I)=IK
JOINT(IK)=1
K=1
102 K4=JMEM(NEWJT(I))
IF (K4.EQ.0) GO TO 104
JSUR=(NEWJT(I)-1)*NCON
C
DO 103 JJ=1,K4
K5=MEMJT(JSUR+JJ)
IF (JOINT(K5).GT.0) GO TO 103
K=K4
NEWJT(K)=K5
JOINT(K5)=K
NDIFF=IARS(I-K)
IF (NDIFF.GE.MINMAX) GO TO 107
IF (NDIFF.GT.MAX) MAX=NDIFF
103 CONTINUE
C
IF (K.EQ.NUMNP) GO TO 105
104 I=I+1
GO TO 102
105 MINMAX=MAX
DO 106 J=1,NUMNP
106 JNT(J)=JOINT(J)
107 CONTINUE
C
WRITE (6,108) MINMAX
C
RETURN
C
108 FORMAT (//10X,20HREDUCED BAND-WIDTH =.I4//)
C
END

```

```

C 10
C 20
C 30
C 40
C 50
C 60
C 70
C 80
C 90
C 100
C 110
C 120
C 130
C 140
C 150
C 160
C 170
C 180
C 190
C 200
C 210
C 220
C 230
C 240
C 250
C 260
C 270
C 280
C 290
C 300
C 310
C 320
C 330
C 340
C 350
C 360
C 370
C 380
C 390
C 400
C 410
C 420
C 430
C 440
C 450
C 460

```